The Influence of Different Types of Water on the Water Distribution and the Swelling Behavior of Polyelectrolyte Multilayers

vorgelegt von

Diplom-Chemiker Maximilian Zerball

geb. in Berlin

von der Fakultät II - Mathematik und Naturwissenschaften

der Technischen Universität Berlin

zur Erlangung des akademischen Grades

Doktor der Naturwissenschaften

Dr. rer. nat.

genehmigte Dissertation

Promotionsausschuss

Vorsitzender: Prof. Dr. Reinhard Schomäcker
1. Gutachter: Prof. Dr. Regine von Klitzing
2. Gutachter: Prof. Dr. Andreas Taubert

Tag der wissenschaftlichen Aussprache: 19.07.2016

Berlin 2016

This work is dedicated to the previous and the next generation.
My parents Albert and Gisela Zerball and "unser kleines wir"
You are not born yet, but you already changed our life.

Acknowledgements

First of all, I thank Prof. Regine von Klitzing for the opportunity to doing the research for my Ph.D. in her group, for all guidance, advises and helpful discussions.

Further, I want to thank the colleagues who thought me neutron reflectometry: Chloé Chivigny, Stefan Wellert and Ralf Köhler. I would neither have been able to carry out the most of my experiments nor to interpret the data without their help.

In addition, I would like to thank my lab and office mates, especially Stephanie Christau, Samantha Micciulla, Johannes Hellwig for your support and your friendship. Also all the other former and actual colleges have to be mentioned, you always create a comfortable climate to work.

Then, I thank the whole technical stuff. The CTAs, without you, probably the labs would be a mess. The precision mechanical workshop produces all the small (and sometimes big) gizmos, which improve several work procedures.

Then, I want to thank the Technical University Berlin and the DFG for financial support via the SPP 1369 "Interphases and Interfaces". Further, the HZB and FRM II granted financial support during beam time.

Special thanks to my family, my sisters Stephanie Zerball and Daniela De Marco and my parents Albert and Gisela Zerball. Thank you for your support and your love.

Finally, I want to thank my wife Patricia Zerball-van Baar for her love, support and patience.

Table of Contents

Abstract

Polyelectrolyte Multilayers (PEM) are organic films built up via subsequent adsorption of oppositely charged polyanions. Because of their sensitivity to external stimuli they are interesting candidates for applications in the field of sensing and biosensing, drug delivery, food industries, catalysis, energy storage and energy conversion.

For all these applications the swelling behavior is from crucial importance. The response of PEMs to changes in relative humidity (RH) can be exploited especially for sensor devices. In the past, three main contributions to the swelling behavior were identified: The uniformity of the swelling, the dependence to the chemical nature of the outermost layer (odd-even effect) and the existence of void water inside the PEM. Even if these three contributions were investigated separately, the interaction between each contribution is still unknown.

In order to better understand the interaction between void water, odd-even effect and water distribution several experiments were carried out. First, the amount of void water was investigated in dependence of the number of deposited layers and the chemical nature of the outermost layer. In order to allow measuring samples over a larger thickness regime the investigation of a larger amount of samples was required. Therefore, the concept of separating void water from swelling water using neutron reflectometry was transferred to ellipsometry. The amount of void water is independent of the terminated layer and the thickness of PEMs. Further, the voids are completely filled if the relative humidity is higher than 30% RH. Therefore, the RH region between 1% and 30% was investigated more in detail. In this context measuring the amount of void water in dependence of the RH can be considered as an adsorption isotherm. The qualitative analysis of this adsorption isotherm indicates that, if the voids are considered as holes or pores, the void size should be about 0.3-0.9 nm.

In the second part of the thesis the water distribution inside PEMs was investigated in dependence of the outermost layer. In order to get insight into the internal structure, PEMs with a deuterated inner block close to the substrate and a non-deuterated outer block were prepared and investigated by neutron reflectometry (NR). The PEMs

were measured in dried state, at 30% RH (D_2O vapor), 70% RH (D_2O vapor) and in liquid D_2O. PEMs swollen in humid air show a homogenous water distribution. Inside PEMs swollen in liquid water the water distribution is non-uniform; the most water is located in the middle of the PEM. Further, also the odd-even effect only appears in liquid water. The odd-even effect and the non-uniform water distribution inside PEMs swollen in liquid water are related to the amount and distribution of extrinsic binding sites inside the PEM. The extrinsic binding sites cause in liquid water an osmotic pressure which forces the PEM to uptake more water. This does not happen in humid air.

In the last part of the thesis the influence of thermal treatment on the swelling behavior of PEMs was investigated. The analysis of the temperature treated PEMs showed that polyelectrolytes of the inner part of the PEM are mainly intrinsically bound, while polyelectrolytes inside the outermost part are mainly extrinsically bound. The temperature treatment causes a densification of the inner part and a degeneration of the outermost part. The densification can be explained by reorganization to a more dense conformation. The degeneration only appears where the polyelectrolytes inside the PEM are mainly extrinsically bound, because the PEM is less stable, in this region.

In summary, the water distribution and the odd-even effect are strongly connected and related to the amount and distribution of extrinsic binding sites inside the PEM. The amount of void water is independent of water distribution and chemical nature of the outermost layer. In addition was shown, that the swelling of PEMs completely differs in humid air and in liquid water.

Abbreviations

ϕ_{swell}	swelling water
ϕ_{void}	void water
Đ	polydispersity index
$\overline{M}_{\mathrm{n}}$	number average molar mass
$\overline{M}_{\mathrm{w}}$	mass average molar mass
λ	wavelength
n	refractive index
k	absorption constant
Q_z	momentum transfer
d	thickness
Ψ	amplitude ratio
Δ	phase shift
x	polymer fraction
SLD	scattering length density
RH	relative humidity
AFM	atomic force microscopy
XRR	x-ray reflectometry
NR	neutron reflectometry
NMR	nuclear magnetic resonanz spectroscopy
PE	polyelectrolyte
PEM	polyelectrolyte multilayer
PEI	Poly(ethyleneimine)
PDADMAC	Poly(diallyldimethylammonium chloride)
PSS	Poly(sodium 4-styrenesulfonate)
d-PSS	completely deuterated Poly(sodium 4-styrenesulfonate)
PAH	Poly(allylamine)

Chapter 1

Introduction

The layer-by-layer technique introduced by Decher[1] enables the preparation of thin polymer films, so-called polyelectrolyte multilayers (PEM). The high tunability of film thickness, ranging from a few angstroms up to several micrometers, and the ability to control the chemical and physical properties of these PEMs to create hierarchical systems is of greatest interest for fundamental science and applied use.[2,3,4] Thus, PEMs are suitable candidates for applications in sensing and biosensing[5,6], drug delivery[7,8], food industries[9,10], catalysis[11,12,13], energy storage and conversion[14,15,16].

The properties of PEMs are influenced either by the preparation conditions, such as preparation time[17,18], number of layers, temperature[19,20], type[21,22,23] and concentration[24,25] of salt added to the polyelectrolyte solution and the chemical nature of the polyelectrolyte itself or can be affected by external stress such as changes in temperature[26,27,28], humidity in air[29,30] or ion concentration[31] and pH[32] in liquid.

At the first glance, the preparation conditions of PEMs and the resulting properties are most important for the construction of PEM containing devices. However, during operation of a device, the influence of the environment is most important, especially, how variations in temperature and relative humidity affect the PEM's physicochemical properties, both reversibly and irreversibly. The thickness, roughness, permeability, etc. change due to the uptake of water from the environment. This can constrain the functionality of a device. However, the swelling properties can also be exploited for applicable uses, e.g. for humidity sensors. Further, swelling and deswelling can be coupled with the ability to uptake and release small molecules, which is of importance for micro-containers, and drug delivery systems.[7,8] These applications need the ability to control the swelling behavior, and such control is not possible without understanding the fundamental process.

Previous work about the swelling behavior of PEMs revealed that three main contributions influence PEM swelling. The swelling behavior depends on the chemical nature of the outermost layer[29,33,34,35], the existence of void water (ϕ_{void}) inside the PEM[22] and the water distribution inside the PEM.[36,37] The water distribution inside a PEM is mainly affected by the preparation conditions, the effect of the substrate and the balance between intrinsic and extrinsic charge compensation.[38] The existence of voids is connected with the density of the PEM.[22] Denser PEMs show usually a higher amount of voids. The odd-even effect is connected with the amount of extrinsic binding sites inside the PEMs.[35] In the past, these three contributions were investigated individually, but how water distribution, odd-even effect and the amount of void water are connected was not known before.

In this thesis, the mutual effects between odd-even effect, water distribution and amount of void water are investigated. First, the amount of void water and swelling water (ϕ_{swell}) over a larger thickness regime is studied. To be capable to investigate a high number of samples, the concept of separating void water from swelling water using neutron reflectometry (NR) is transferred to ellipsometry. Then the water distribution is investigated. In order to probe the internal properties of PEMs, NR is used. PEMs with a deuterated inner block and a non-deuterated outer block are measured in dry state, in air with relative humidity (RH) of 30% and 70% and in liquid D_2O. Further, the absorption of void water inside PEMs with increasing RH and the resulting adsorbtion isotherm is investigated. Finally, to probe how swelling behavior in general and odd-even effect, water distribution and amount of void water in particular are influenced by external stress, PEMs are temperature treated.

Chapter 2

Scientific Background

2.1 Polyelectrolyte Multilayer

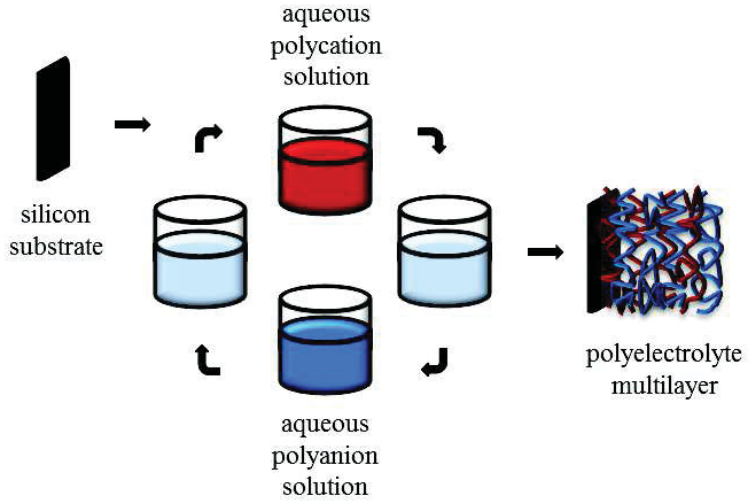

Figure 2.1: Scheme of the layer-by-layer preparation process. The substrate is immersed into an aqueous solution containing the polycation. After rinsing with water, the substrate covered with one polyelectrolyte layer is immersed into the second aqueous solution, which contains the polyanion. After the second rinsing step, the first preparation cycle is accomplished and can be repeated until the desired number of layers is reached.[39]

A polyelectrolyte multilayer is a thin polymer film, consisting of at least two different alternatively adsorbed polyelectrolytes (PEs). PEs are macromolecules with charged functional groups.[40] PEMs are prepared by the layer-by-layer technique.[1,39] During the preparation of a PEM a charged substrate is consecutively coated by two oppositely charged polyelectrolytes. Figure 2.1 shows a scheme of the PEM pre-

paration.[39] In the first step, the substrate is immersed into a solution of oppositely charged polyelectrolytes. As substrate various materials[41] (e.g. different modifications of silica[42], gold[43], latex[44] etc.) and various shapes (fibers[45], particle[46], membranes[47]) of the material[48,49] can be used. After the first adsorption step, the substrate is rinsed with water. The rinsing removes not completely adsorbed polyelectrolyte. Thus, the contamination of the following dipping solution is avoided.[50] The adsorption of the first layer of polyelectrolyte reverses the surface charge, which has been proved by zeta potential measurements of coated particles.[33] Thus, the second oppositely charged polyelectrolyte can be adsorbed. After the adsorption of the second polyelectrolyte the PEM is rinsed again. This presents a dipping cycle. This procedure can be repeated until the desired number of layers is reached. It is also possible to prepare PEMs with more complex structure by adding additional polyelectrolyte solutions into the adsorption sequence.[39] The adsorption of the polyelectrolytes on the substrate can be achieved also by various other methods[4] like spray-coating[51,52], or spin-coating[53,54,55]. The combination of different polyelectrolytes on various materials and the possibility to incorporate further nano-materials (e.g. nanoparticles) enables the creation of complex nanostructures.[2,3,4] Furthermore, due to the repetitive character of the layer-by-layer process it can be easily automated.[56,57,58]

2.1.1 Formation of PEMs

The formation of a PEMs is driven by a complex interplay of different interactions, e.g. the interaction between both polyelectrolytes, the interaction between polyions and small counter ions, the interaction between polyelectrolytes and the solvent and the interaction between polyelectrolytes and the substrate. In general, the formation of PEMs can be considered as the controlled complexation of polyelectrolytes on a substrate. Therefore, the stability of the corresponding polyelectrolyte complex serves as a good indicator for the stability of a PEM system.[59] The probability to form a complex between two oppositely charged polyelectrolytes depends on the free energy of the complexation process. The free energy consists of the enthalpic and the entropic contribution. Changes in enthalpy are driven mainly by Coulomb interactions between the charged functional groups of the polyelectrolytes, while changes in entropy are driven by the release of counter ions and the accompanied generation of a hydration shell around the ion.[60]

For a long time Coulomb interactions were considered as the main driving force for PEM formation.[17] However, several studies published the last decade, showed

that the gain of entropy due to the release of small counter ions is much more important for the formation of PEMs, while electrostatic interactions have only a minor effect.[38,59,60,61,62] There are at least three reasons for entropy as main driving force for PEM formation: 1) PEMs are formed also at high ionic strength where electrostatic forces are screened.[63,64] 2) A charge reversion needs a lot of energy and a process only driven by electrostatic forces should stop at zero charge. 3) From an electrostatic point of view there should be no difference between a polyelectrolyte compensated by small counter ions or another polyelectrolyte.[38,61]

Although, the gain of entropy is identified as the main driving force the enthalpic contribution (Coulomb interaction) of the complexation reaction can influence the properties of the PEM. Laugel et al.[59] investigated the complexation energy of different PE combinations suitable for PEM fabrication. They showed, if the complexation reaction of a certain PEM system is strongly exothermic, then the resulting PEMs are more thin and compact. A strong exothermic reaction indicates a strong negative enthalpy during the complexation. If the complexation reaction of a polyelectrolyte is endothermic than the resulting PEM is thicker and more fluffy. An endothermic reaction indicates that the enthalpy is positive, i.e. the Coulomb interaction counteract a complexation but the gain in entropy is still stronger.

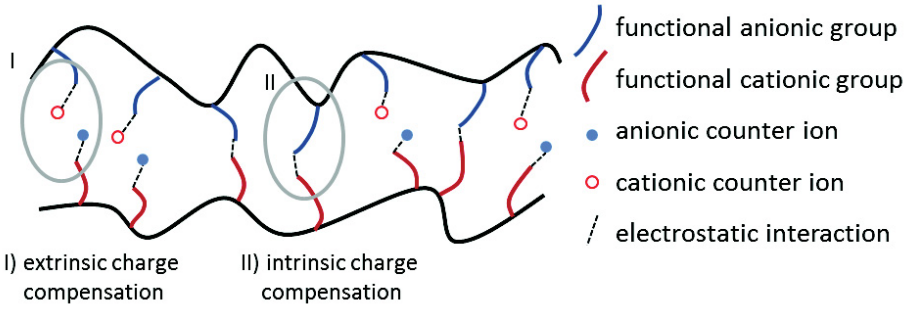

Figure 2.2: Scheme of charge compensation inside PEMs. 1) Example for extrinsic charge compensation. The functional groups of the PEM are compensated by small counterions (salt ions). 2) Example for intrinsic charge compensation the functional groups of the oppositely charged polyelectrolyte compensate each other.

The compactness and stability of the PEM depends on how the charges inside the PEM are compensated. In generally, the type of charge compensation is distinguished between intrinsic and extrinsic charge compensation.[65] Intrinsic charge compensation describes that the functional groups of polyanion and polycation are compensated by direct interaction between both PEs. Extrinsic charge compensation occurs if the charge compensation due to a small counter ion is more favored as the intrinsic charge

compensation. Figure 2.2 shows schematically the difference between extrinsic and intrinsic charge compensation. Mainly intrinsically compensated PEMs are usually tightly packed and therefore thin and smooth. For PEMs with a high number of extrinsic binding sites the opposite is true. In addition a high amount of extrinsically compensated binding sites increases the amount of ions inside PEMs, which increases the capability of the PEM to uptake water due to an osmotic pressure inside the PEM.[35]

In summary, PEMs with an exothermic complexation process form thin, compact and stable PEMs which are mainly intrinsically compensated, while PEMs with an endothermic reaction enthalpy form fluffy and less stable PEMs with a high amount of extrinsic charge compensation.

2.1.2 Type of Growth

The mechanism of PEM growth is still not completely understood. The evolution of thickness with increasing number of layers of PEMs can be distinguish between linear and non-linear.[61,66,67,68,69] During linear growing the thickness increment stays constant with increasing number of layers, while during non-linear growing the thickness increment increases with increasing number of layers. Usually a PEM system first grows non-linearly and switches to a linear growth after a certain number of layers.[20,68]

The most common model to describe the non-linear growth is the diffusion model.[68] The diffusion model assumes that as long as one of the PEs are capable to diffuse in and out of the PEM during the adsorption process the PEM grows non-linearly. If no diffusion is possible the PE grows linearly.

PEs diffused into the PEM remains inside the PEM until the next preparation step. During the adsorption of the oppositely charged PE the remained PE diffuses back to the surface, where it forms complexes with the oppositely charged PE. The additional complexes lead to an increase of the thickness increment per layer. The amount of PE that is capable to diffuse into the PEM is dependent on the PEM thickness. Therefore, with increasing thickness the thickness increment per layer increases.

So far, non-linear growth can be explained by the diffusion model. Anyway, the often observed transition from non-linear to linear is still not completely understood. Indeed, one explanation to explain the transition from non-linear to linear growth might be the diffusion depth. The diffusion depth is dependent on the time of the polyelectrolyte in the dipping solution and the diffusion constant of the respective

polyelectrolyte. The diffusion constant depends on the molecular weight. Thus, how depth a polyelectrolyte can diffuse in and out of the PEM should depend on dipping time and molecular weight. However, the opposite was found. The transition point is independent of dipping and molecular weight.[68,70] Thus, diffusion cannot be the only explanation for the linear to non-linear transition.

An extension of the diffusion model is the "3-zone model". The 3-zone model subdivides the PEM into the outer diffusion zone and the inner restructured zone. Additionally, it considers a small substrate zone which is dominated by the properties of the used substrate. Only the diffusion zone is penetrable for polyelectrolytes. As long as the diffusion zone grows the PEM grows non-linearly. After a certain thickness the inner part of the PEM begins to restructure and form the restructured zone, which is not penetrable for polyelectrolytes. When the restructuring begins the diffusion zone does not grow anymore, the PEM switches to a linear growing behavior. The restructuring is based on the fact that the PEM matrix is kinetically, not thermodynamically, stabilized. With every additional preparation cycle the deeper buried polyelectrolytes are able to change their conformation into a thermodynamically more favorable conformation.[68,70]

Volodkin et al.[38] suggested a correlation between the charge compensation and the type of growth. They assumed that the restructured zone close to the substrate is mainly intrinsically compensated, while the outermost part, where polyelectrolytes are able to diffuse into are mainly extrinsically compensated. As described in section 2.1.1 intrinsic charge compensated PEMs are more compact as mainly extrinsically compensated PEMs. Therefore, the polyelectroyltes are only able to diffuse through the mainly extrinsically compensated diffusion zone. Such a correlation is in accordance to the findings of calorimetry measurements of PECs. If the corresponding PEC of a PEM system shows an exothermic complexation reaction the PEM grows linearly. An exothermic complexation reaction indicates a high enthalpic contribution which is typical for mainly intrinsically compensated PEM, i.e. linear growing PEMs are mainly intrinsic charge compensated. On the other hand, the corresponding PECs of non-linear growing PEMs shows endothermic reaction which indicates a high amount of extrinsic charge compensation. Fig. 2.3 illustrates the described 3-zone model under the assumption that the differences between diffusion and restructured zone are caused by extrinsic and intrinsic charge compensation.

Next to the 3-zone model there are other discussed models like the roughness model[71] and the dendrimeric model[72]. The roughness model assumes the formation of islands during the adsorption of the initial layers, i.e. the substrate is not com-

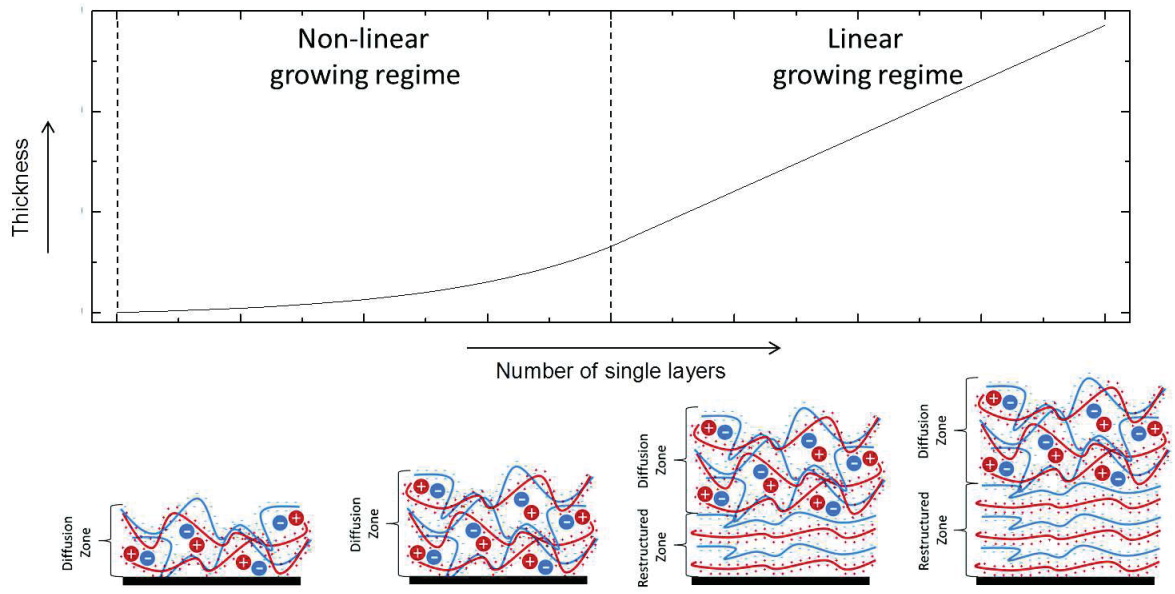

Figure 2.3: Theoretical evolution of thickness for PEM systems who initially grows non-linearly and switch to a linear growing behavior after a certain number of layers. The sketch shows the PEM structure during the respective growing phase. 1) The diffusion zone is as thick as the entire PEM. The PEM is less compact and polyelectrolytes can diffuse through the entire PEM. The diffusion zone shows a high number of extrinsic binding sites. 2) With increasing number of layers the PEM and the diffusion zone increases. The diffusion zone is still as large as the PEM, the PEM still grows non-linearly. 3) The grow changes to a linear one. The diffusion zone does not grow anymore. The restructured zone is forming from the deep buried polyelectrolytes, whose are mainly intrinsically compensated. 4) The diffusion zone stays constant while the restructured zone grows due to further restructuring of polyelectrolytes. The PEM grows linearly as fast as the restructured zone grows. The scheme is based on ref. 38.

pletely covered by a complete polyelectrolyte layer but by a high number of small PEM islands. These islands grow with increasing layer number until the islands begin to conglomerate.[71] The dendritic model assumes the adsorption of PE chains at the substrate and the formation of branch-like structures in following adsorption steps, which increases the number of possible binding sites with every additional adsorption step. The maximum number of binding sites is limited by the covered area. If the maximum is reached the PEM begins to grow linearly.[72] The reasons for the transition from non-linear to linear growth regime are extensively discussed in ref. 38.

2.2 Tuning the Properties of PEMs

The properties of PEMs can be affected by a large number of parameters during the preparation or afterwards. The most parameters influence the balance between enthalpic and entropic contribution, which in turn affects the stability, density and type of growth of the PEM. The parameters with the strongest impact are the type of polyelectrolyte (especially their charge density[30,73,74]), the temperature during preparation[19,20], the amount of salt added to the PE solution[24,25] as well as the type of salt[21,22,23] and the preparation time[17,18].

2.2.1 Type of Polyelectrolyte

The type of polyelectrolyte is defined by their functional group, which mainly defines the chemical properties of the PEM; i.e. the ability for crosslinking[75,76,77] after preparation or the possibility to interact with specific molecules or particles[78]. Important for the preparation is primarily the charge density, i.e. the amount and available charged binding sites, which is primarily determined by the acid dissociation constant (pK_a) of the respective PE. Like all electrolytes also polyelectrolytes are distinguished between strong and weak electrolytes. Strong PEs completely dissociate in water and provide a high number of binding sites. Usually they form rather stable PEMs. The charge density of strong polyelectrolytes can be varied by introducing a non-charged co-polymer.[30,73] A well investigated example is the PEM system PSS/PDADMAC$_{1-x}$NMVA$_x$ (whereby x is NMVA/PDADMAC ratio). This system does not build up PEMs if the charge density of PDADMAC-NMVA is less than 70%. Beyond this critical charge density the thickness and roughness of the PEMs decreases with increasing charge density. Apparently, higher charge densities favor intrinsic charge compensation, leading to a transition from a coiled conformation at lower charge densities to a flat chain conformation at high charge densities.

Weak polyelectrolytes show a rather high acidity constant and consequently dissociate only partially in water. The rate of dissociation defines the amount of binding sites, which in turn affects the charge density, i.e. the charge density of PEM systems consisting of weak polyelectrolytes can be varied due to the pH of the solution.[74] This makes these PEM systems very flexible. Anyway, PEM systems consistent of weak polyelectrolytes are usually only stable at intermediate pH.[61] The pH at which the polycation is strongly charged, usually causes high protonation at the polyanion and vice versa. Therefore, if the pH of the polyion in the dipping solution is high, it is low in the oppositely charged solution. For this reason PEM systems consisting of weak

polyelectrolytes only build up stable PEM within a concrete pH range, in which both PEs are proper charged.

Next to the functional group, the rigidity of the polymer backbone is important for the properties of the PEMs. The rigidity of the backbone reduces the flexibility of the polyelectrolytes and constrict the formation of complexes.[79]

PEMs can consist of numerous different polyelectrolytes. Anyway, some PEM systems have been established as standard systems for fundamental research. The most investigated PEM systems are the systems PSS/PAH, PSS/PDADMAC and PLL/HA. PSS/PAH is the typical representative for a linear growing PEM system, as only for high temperatures and high salt concentration a pronounced non-linear growing phase is detectable.[20,80]

PSS/PDADMAC PEMs consists of two strong polyelectrolytes. This system shows linear grow at low salt concentrations and non-linear grow at high salt concentrations.[25] PSS/PAH and PSS/PDADMAC are the typical representatives for synthetic PEM systems. For medical applications like drug delivery systems, biological systems are more reasonable. PLL/HA is the most investigated biological PEM systems. PLL/HA consists of two weak polyelectrolytes. In addition to these standard systems there were published dozens of variation especially for application related use. The combination of different polyelectrolytes enables chemical cross linking[81,82] after the preparation, affinity to certain molecules[83,84] and hierarchically structures.[85,86]

2.2.2 Type and Concentration of Salt

Adding salt to the dipping solution provides the possibility to fine tune thickness and roughness of PEMs.[25,87] On the one hand, the salt ions screen the charges of the functional groups of the polyelectrolyte. On the other hand, the presence of salt ions decreases the gain in entropy, as due to the release of counterions depends on the ionic strength of the surrounding solution. Therefore, the amount of extrinsic binding sites increases, i.e. the polyelectrolyte complexes become less stable. PEMs with a high number of extrinsic binding sites show more coiled and consequently less dense, rougher and thicker structure. The effect of the ionic strength of the solution on the resulting PEM thickness is specific for the respective PEM system but mainly depends on the charge density of the system.

Added salt also changes the non-linear to linear transition point.[25,87] The added salt increases the amount of extrinsic binding sites[35], i.e. the number of connections between polyelectrolyte chains decreases, the mesh size of the polymer matrix

increases. Therefore, the mobility of polyelectrolytes increases[79] and with it the probability of polyelectrolytes to diffuse in and out of the PEM during the preparation.

Not only the amount of added salt but also the type of salt added to the dipping solution influences the thickness and roughness of PEMs.[21,23] Small, less polarizable ions (cosmotropic ions) which form a big well-ordered hydration shell form thinner and smother PEMs than large well polarizable ions (chaotropic ions).[88] Because of the weak hydration shell chaotropic ions can easier interact with the oppositely charged polyelectrolyte. The stronger interaction results in a higher screening potential for chaotropic ions, causing thicker and rougher PEMs. The effect of the type of ion agrees with the Hoffmeister series.[89] Thus, thickness and roughness of PEMs increases in the order F^-<Cl^-<Br^- for anions and Li^+<Na^+<K^+ for cations.[21,23]

2.2.3 Effect of Preparation Time

The adsorption kinetics depends on the used polyelectrolyte, the molecular mass, ionic strength and temperature. However, it was found, that at a concentration of 10^{-2} monomol/L the most material is adsorbed after 10 minutes, complete saturation is reached after 20 minutes. Obviously, the adsorption process is a two-step process. First, the polyelectroylte chains are anchored at the surface, which increases the adsorbed mass fastly. Afterwards, the polyelectrolyte chains relax to a more compact structure.[17]

2.2.4 Effect of Temperature

In general, an increase in temperature during PEM preparation increases the thickness increment per PE layer and extends the non-linear growing phase of non-linearly growing PEMs.[20,80] The increase in temperature changes the balance between polyion-polyion and polyion-counterion interaction. Thus, the amount of extrinsic binding sites increases. The PEM become less compact and thicker. In addition, linear growing PEM systems can be forced to a non-linear growth. The probability of polymer transport to the surface is increased because of the less compact structure of the PEM.

In summary, thickness roughness and density of a PEM can be fine-tuned mainly by the ionic strength, the type of ions and the temperature. The effect of these different parameters on the thickness results from a change in the balance between polyion-polyion and polyion-counterion interaction. As more preferred a strong polyion-counterion interaction is, as more extrinsic binding sites are present and as more coiled the PEM structure becomes. Figure 2.4 summarizes the most important parameters

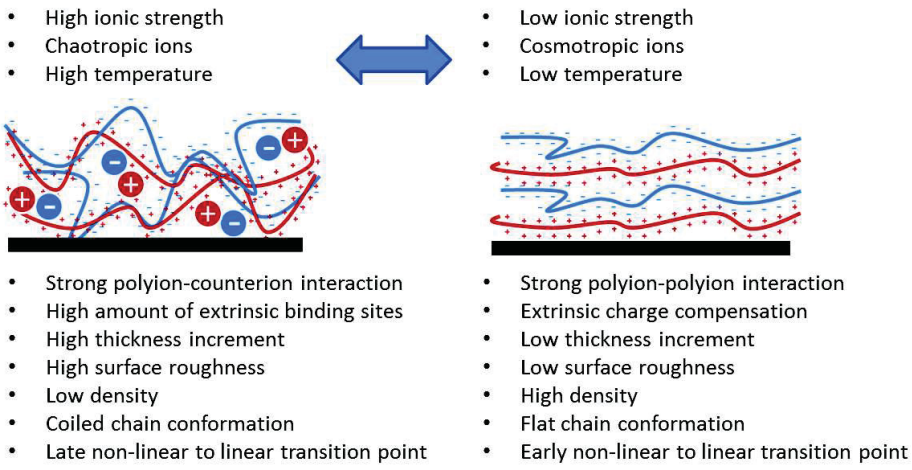

Figure 2.4: Properties of mainly extrinsically compensated PEMs (left) versus mainly intrinsically compensated PEM (right). The upper part shows preparation conditions which promote extrinsic charge compensation in opposite to intrinsic charge compensation. The middle part shows schematically the structure of extrinsic charge compensated PEM and intrinsic charge compensated PEM. The bottom part shows the resulting properties of the PEMs.

and how they affect the amount of extrinsic binding sites of a PEM and consequently the resulting thickness and roughness.

2.3 Interaction of PEMs with the Environment

With the preparation conditions the physical and chemical properties of the PEM is controlled. The physical and chemical properties define how the PEM interact with the environment. The interaction with the environment is from greatest interest for application, like sensing and biosenssing[6], drug delivery[90], tissue engineering[91], catalysis[13] or energy storage and conversation[92]. Many applications are based on the incorporation of materials into the PEM; as for biosensors.[6] Thereby the PEM serves as the detector element and transforms a signal into a measurable and quantifiable physical value. Thus, it is possible to incorporate a redox enzyme into a PEM with an electroactive polyelectrolyte. The reaction of the enzyme with a specific molecule induces an electrochemical reaction of the polymer which can be detected as an electrical signal.

For the incorporation of molecules into the PEM the swelling behavior is from greatest interest. Either if the material is incorporated after the preparation the

structural changes of the PEM during swelling influences amount and distribution of the material incorporated into the film or if the material is incorporated during the film preparation, the swelling of the PEM can change the amount and the distribution of the material afterwards.

Therefore it is important to understand the swelling behavior of PEMs. During swelling the PEM takes up water and responds with an increase in thickness and density, the least also influences optical constants (scattering length density (SLD), refractive index (n)) due to the diluting of the polymer matrix with water.[93] Furthermore, the topology of the surface and the elasticity of the PEM can change.[94]

The swelling behavior of PEMs differs significantly from the swelling behavior of pure polymer films. Three main effects were identified, which causes these differences in the swelling behavior: 1) the distribution of water inside the PEMs[36,37], 2) the chemical nature of the outermost layer (odd-even effect) and 3) the existence of voids inside the PEM[93].

2.3.1 Water Distribution

Little is known about the water distribution inside PEMs. PEMs consisting of two weak polyelectrolytes show non uniform water distribution as detected by Tanchak et al.[36]. De Vos et al.[37] found differences in the water distributions inside PSS/PAH PEM under confining pressure. Further, Ghostine et al.[35] found hints for non-uniform contributions of extrinsic binding sites inside PSS/PDADMAC PEMs. The amount of extrinsic binding sites strongly influences the amount of absorbed water. Extrinsic binding sites induce an osmotic pressure which forces the PEM to take up additional amounts of water.

According to the three zone model (see section 2.1.2) PEMs have a non-uniform structure. Consequently, a non-uniform water distribution is very likely. PEMs consist of an inner mainly intrinsically compensated restructured zone and an outermost diffusion zone characterized by a high amount of extrinsic binding sites. The restructured zone is denser, which could influence the swelling behavior. Additionally, the influence of the substrate itself on the PEM is obvious but not understood yet and could influence the swelling behavior.

2.3.2 Probing Internal Properties

The water distribution inside a PEM is difficult to probe. Therefore, little is known about the water distribution inside PEMs. The amount of water inside a PEM is usu-

ally determined by the change in thickness or optical properties, which is for the most methods an average variation of the entire PEM. While investigations of the average structure of PEMs are well established with a high variety of methods (ellipsometry, quartz crystal microbalance (QCM), x-ray reflectometry (XRR), etc.), the access to internal properties is rather challenging.

For micrometer thick PEMs the labeling of polymer chains with dyes and afterwards investigating the labeled polymers with optical methods such as confocal microscopy is suitable.[68,70] However, for nanometer thick PEMs optical methods still show a too low resolution to distinguish between different areas inside the PEM. Indeed, smaller wave lengths increase the resolution of spectroscopic methods. Thus, x-ray photoelectron spectroscopy is a suitable method of probing internal properties. Hence, it is possible to measure depth depending atomic distribution.[95] Unfortunately, the method is not suitable for measurements in aqueous environment because of the strong scattering of x-rays in waters. In water swollen PEMs were also investigated by nuclear magnetic resonance spectroscopy (NMR).[33,96] NMR is capable to distinguish between water in different chemical environment, i.e. if water is tightly bound to the PEM (immobile water) or is water capable to move through the PEM (mobile water). Hence, it is known that different kinds of water inside PEMs exist, but a localization of this water is not possible with NMR.

A powerful technique to probe internal properties of swollen nanometer thin PEMs is Neutron Reflectometry.[36,97] NR determines the scattering length density profile across the PEM. In order to get information about the internal structure of the film, one can change the contrast by controlled deuteration of specific regions. In general there are two approaches to use deuteration. First, the creation of a super structure due to selective substitution of non-deuterated polyelectrolyte by deuterated polyelectrolyte.[37,97] If the distance between particular deuterated layers is constant an bragg peak is detectable. Position and width of the peak give information about the uniformity of the PEM. The second method is the deuteration of an entire PEM block.[98,99] Especially, the properties of the interface between deuterated and non-deuterated block is of interest, but also changes in block sizes during swelling.

2.3.3 Odd-Even Effect

The odd-even effect describes the phenomenon that the amount of absorbed water depends on the chemical nature of outermost layer of the PEM. The differences in water uptake are usually detected by the change in thickness. However, also other

properties are influenced by the odd-even effect as the optical properties, the roughness of the PEM and the elasticity.

The occurrence of the odd-even effect strongly depends on the investigated PEM system. For example for the system PSS/PAH, PSS-terminated PEMs take up more water than PAH-terminated PEMs. This is detectable at high RH[29] and in liquid water[33]. Furthermore, the odd-even effect is strongly pronounced for small layer numbers and decreases with increasing number of layers and is not detectable anymore at layer number higher than 28 single layers. NMR[33] and NR measurements[100] show higher water content in PSS-terminated PEMs. Apparently, the decay of the odd-even effect is related to the chemical properties of PSS. PSS-terminated PEMs have a lower contact angle than PAH-terminated PEMs, i.e. the PSS surface is more hydrophilic. Of course the chemical structure of PSS indicates the opposite, the backbone with the benzene ring should be hydrophobic. However, the higher charge density of PSS (strong PE) in opposite to PAH (weak PE) provides a more hydrophilic surface. Therefore, the PEM take up more water. With increasing number of layers the effect of PSS decreases because the effect of an additional layer becomes smaller in comparison to the PEM size. Another explanation considers the PSS-layer as a barrier between the water and the rest of the PEM. The surface potential of the PSS-layer influences the counter ion concentration inside the film, which increases the amount of absorbed water. A potential from the PEM surface towards the substrate was measured for PSS-terminated PEMs but not for PAH-terminated PEMs.[101] Both theories could not be verified yet.

The odd-even effect of PSS/PDADMAC PEMs is completely different. PDADMAC-terminated PEMs take up more water than PSS-terminated PEMs.[34,35] Furthermore, the odd-even effect is increasing with increasing number of layers. Therefore, the explanations concerning PSS/PAH PEM are not valid for PSS/PDADMAC PEMs. Instead, the odd-even effect in PSS/PDADMAC is related to the high amount of extrinsic binding sites. Ghostine et al.[35] detected a much higher amount of extrinsic binding sites inside PDADMAC-terminated PEMs. More extrinsic binding sites indicate a higher amount of counter ions inside PDADMAC-terminated PEMs. The counter ions induce an osmotic pressure in water, which is compensated by an increased water uptake. The finding of extrinsic binding sites inside PSS/PDADMAC terminated PEMs arises again the question about water distribution inside the PEMs. Figure 2.5 illustrates the odd-even effect of PSS/PDADMAC PEMs.

The odd-even effect describes only the dependence between amount of swelling water and the composition of the outermost layer. It has to be strictly distinguish

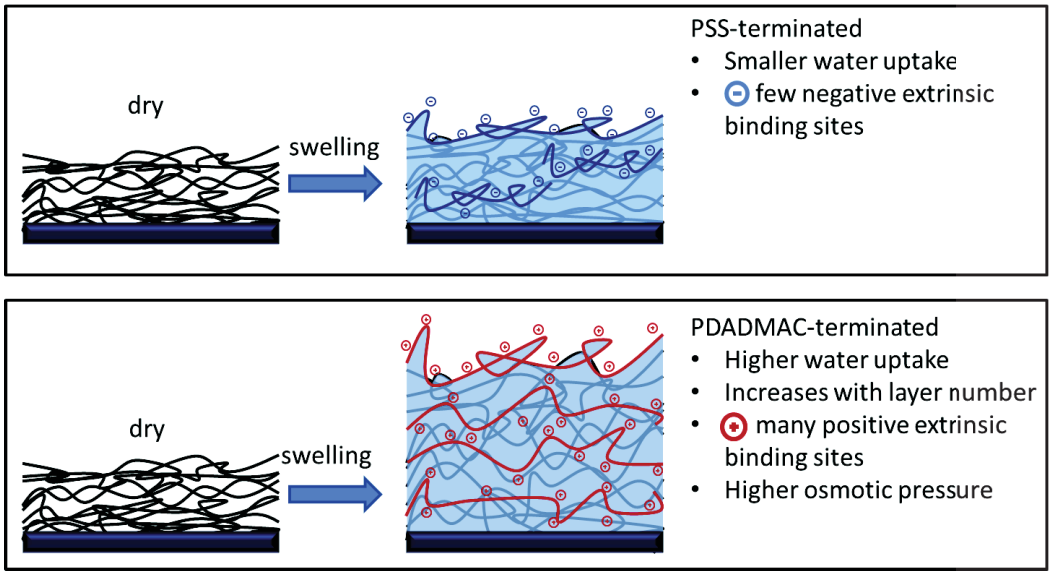

Figure 2.5: The odd-even effect of PSS/PDADMAC PEMs. The dried PEMs do not differ. In swollen state, the PSS-terminated PEM take up less water than the PDADMAC-terminated PEM. The reason is a higher amount of extrinsic binding sites inside PDADMAC-terminated PEMs.

from the "zig-zag" growing shape of some unstable PEM systems.[23,102]

2.3.4 Void Water

To compare the swelling behavior of PEMs it is important to calculate the amount of swelling water correctly.[22,93] In general there are two methods to calculate the amount of absorbed water. Firstly, under the assumption that the incorporated water leads to a change in thickness, the amount of absorbed water can be calculated by

$$\phi_{swell} = \frac{d_{swollen} - d_{dry}}{d_{swollen}} \tag{2.1}$$

where ϕ_{swell} is the amount of absorbed water, d_{dry} is the dry PEM thickness and $d_{swollen}$ the thickness in swollen state. With this method the amount of absorbed water is accessible due to the PEM thickness. Thus, the absorbed water can be obtained by a lot of lab methods like ellipsometry and atomic force microscopy (AFM).

NR provides an additional way to calculate the amount of absorbed water, as water incorporation changes the scattering length density of the PEM. Thus, the amount of absorbed water can be calculated by:

$$\phi'_{swell} = \frac{SLD_{swollen} - SLD_{dry}}{SLD_{water} - SLD_{dry}} \tag{2.2}$$

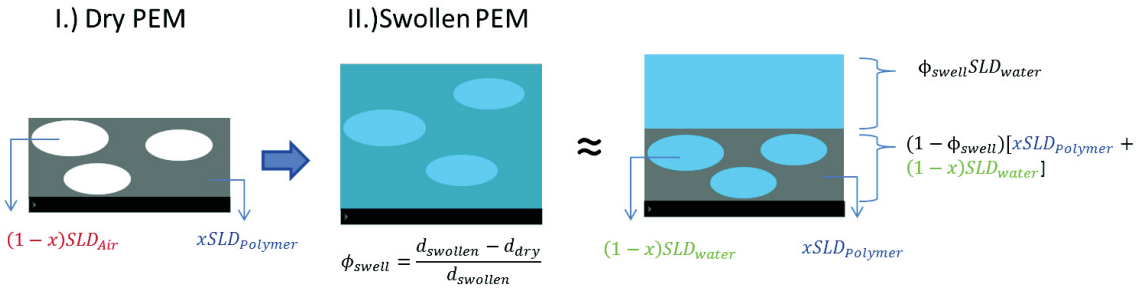

Figure 2.6: 1. For a PEM in dry state the SLD is a combination of the Polymer SLD diluted by air. 2. For a PEM in swollen state the polymer is now diluted by water and the air inside the voids are substituted by water.

where ϕ'_{swell} is the the amount of absorbed water, SLD_{dry} is the SLD of the dry PEM, $SLD_{swollen}$ is the SLD of the swollen PEM. SLD_{water} is the SLD of either D_2O or H_2O.

The comparison between water content calculated by SLD (eq. 2.2) and from the thickness (eq. 2.1) shows a discrepancy between both values. The reason is the existence of voids inside the PEM.[22,93] Due to the voids, an additional volume fraction inside the PEM have to be considered. Figure 2.6 shows the considerations which are necessary to separate the total amount of absorbed water into swelling water and void water. The amount of swelling water is already defined by equation 2.1. The SLD of the PEM in dried state can be described as:

$$SLD_{Dry} = SLD_{Polymer} + (1-x)SLD_{Air}(SLD_{Air} = 0 SLD_{Dry} = xSLD_{Polymer} \quad (2.3)$$

where x is the polymer fraction and $SLD_{Polymer}$ the SLD of the PEM without voids. In water the PEM swells and the voids were filled. This state can be described as followed:

$$SLD_{swollen} = \phi_{swell}SLD_{water} + (1-\phi_{swell})[xSLD_{Polymer} + (1-x)SLD_{water}] \quad (2.4)$$

The polymer fraction is unknown but can be calculated by inserting eq. 2.3 into eq. 2.4.

$$x = \frac{SLD_{dry}}{SLD_{D_2O}} - \frac{SLD_{swollen} - \phi_{swell}SLD_{D_2O}}{(1-\phi_{swell})(SLD_{D_2O})} + 1 \quad (2.5)$$

The amount of void water is calculated by:

$$\phi_{void} = (1 - \phi_{swell})(1 - x) \tag{2.6}$$

The role of void water inside PEMs was recently reviewed.[93] Furthermore, a method to calculate the amount of void water from ellipsometry data is shows in this thesis.

2.3.5 Influence of Salt

Salt can also influence PEMs after the preparation. Immersing a PEM in solutions with low ionic strength (< 1mol/L; depends on PEM system) leads to an annealing[103], i.e. the PEM becomes smoother and denser. Due to the salt the PEM chains become more mobile and can move into a better conformation. High salt concentrations lead to dissolving of the PEM.[104] A more specific way to change the properties of PEMs due to a salt treatment was recently investigated by Ghoussoub et al.[105]. They showed a way to balance out all extrinsic binding sites inside a PSS/PDADMAC PEM due to a cyclic salt treatment, where the PEM is alternatively immersed into salt solutions with and without PSS.

2.3.6 Temperature Treatment

The effect of temperature on PEMs was intensively investigated for microcapsules.[26,27,28] During the heating of PSS/PDADMAC microcapsules to temperatures over $65°C$ PSS-terminated capsules shrink, while PDADMAC-terminated capsules swell until they rupture. The different behavior of PSS-terminated and PDADMAC-terminated capsules was attributed to the different ratio of positive and negative charges inside the PEM capsules. The PDADMAC-terminated PEM capsules take up more water during heating to increase the distance between charges, while the more charge balanced PSS-terminated PEM capsules minimize the polymer water surface. Unfortunately, the behavior of PEM microcapsules cannot be transferred easily to PEMs attached to a solid substrate. Due to the fixation on the substrate, the PEMs are less flexible, provide a smaller surface and are sterically hindered. Microcapsules can respond with changes in wall thickness and changes in capsule diameter, while a PEM attached on a solid substrate can only react by changes in thickness. Further, the influence of the substrate itself on the PEM is obvious but not understood yet. Moreover, QCM-D measurements show an increasing swelling of PEMs with in-

creasing temperature, but a rupturing was not reported.[106] For non-linear growing PSS/PDADMAC PEMs (prepared at ionic strength >0.1 mol/L) a glass transition temperature at about $50°C$ was determined. Linear growing PSS/PDADMAC PEMs (prepared without salt) did not show any transition up to $110°C$.[106] Neutron reflectometry measurements after a thermal treatment revealed annealing effects related to a loss in swelling, which was detectable by a decrease in roughness and SLD.[107]

Chapter 3

Experimental Section

3.1 Chemicals

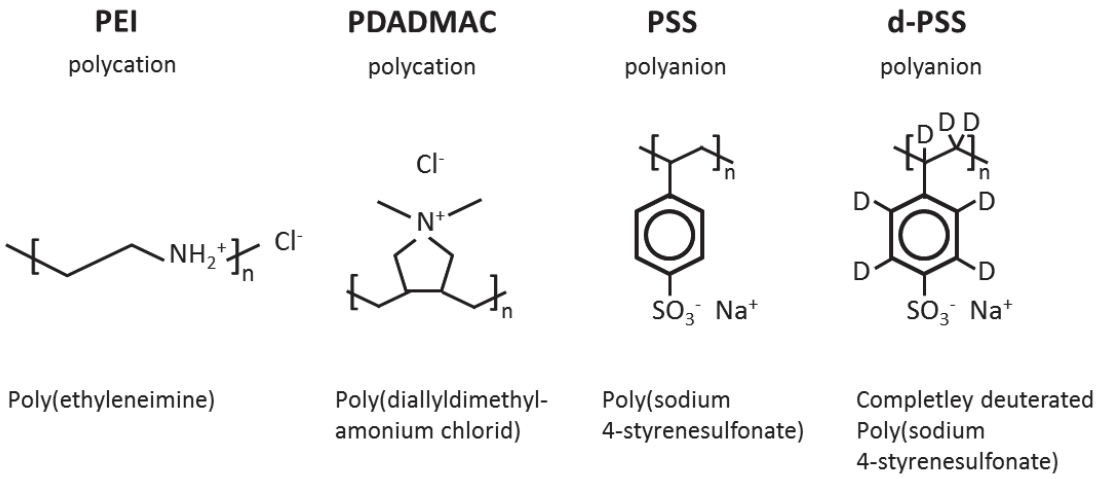

Figure 3.1: Chemical structure of a) Poly(ethyleneimine) (PEI), b) Poly(diallyldimethylammonium chloride) (PDADMAC), c) Poly(sodium 4-styrenesulfonate) (PSS) and d) completely deuterated Poly(sodium 4-styrenesulfonate) (d-PSS).

Poly(ethyleneimine) (PEI, $\overline{M}_{\mathrm{n}} \approx 60$ kDa determined by GPC $\overline{M}_{\mathrm{w}} \approx 750$ kDa determined by LS) and Poly(sodium 4-styrenesulfonate) (PSS, $\overline{M}_{\mathrm{w}} = 70$ kDa), were purchased from Sigma-Aldrich (Steinheim, Germany) and were used without further purification. Fully deuterated PSS (dPSS $\overline{M}_{\mathrm{w}} = 78.3$ kDa $Đ_M < 1.2$ by GPC) was purchased from Polymer Standard Service GmbH (Mainz, Germany). Poly-(diallyldimethylammonium chloride) (PDADMAC, $\overline{M}_{\mathrm{w}} = 135$ kDa $Đ_M = 1.8$ determined by GPC and H^1-NMR) was synthesized by free radical polymerization of diallyl-dimethyl-ammonium chloride in aqueous solution, as described in a previous

work.[108]. The chemical structure of all used polymers is summarized in figure 3.1 The silicon wafers were a gift from Wacker Chemie AG (München, Germany). The silicon blocks were purchased by Silizium Bearbeitung A. Holm (Tann, Germany).

3.2 Layer-by-Layer Deposition

For the ellipsometry, AFM and XRR measurements, the multilayers were built on silicon wafers via the layer-by-layer method introduced by Decher.[39] All preparation steps were done by an automatic dipping device (Riegler & Kirstein, Berlin, Germany). The silicon wafers were cleaned for 30 min in a 1:1 mixture of 98% H_2SO_4/ 35% H_2O_2 and then rinsed with Milli-Q water. Also after etching a thin SiO_x layer is preserved. The thickness of the SiO_x layer does not influence the PEM preparation but is important for the determination of PEM thickness. The average thickness and roughness of the SiO_x layer was determined by measuring five individual silicon wafers with ellipsometry and x-ray reflectometry after the etching. Afterwards, the wafers were covered by a precursor layer of PEI. PEI was deposited to the surface by immersing the wafers for 30 min into an aqueous solution containing 10^{-2} monomol/L (concentration based on monomer unit) PEI. The branched PEI precursor provides a lot of binding sites for consecutive layers, which results in more homogenous and less rough PEMs.[109] Then the wafer is alternately immersed into aqueous (Milli-Q water) polyelectrolyte solutions containing 10^{-2} monomol/L of the respective polyelectrolyte and 0.1 mol/L NaCl. Every polyelectrolyte layer was adsorbed for 20 min. After every adsorbed layer, the samples were rinsed three times for 1 min in Milli-Q water. After completion of the multilayer assembly the wafers were dried in air. The preparation started with a PSS layer followed by a PDADMAC layer.

For neutron reflectivity measurements the samples were prepared on a silicon block (80 x 50 x 15 mm^3). Further, for some samples the PSS of the first 6 bilayers were substituted by dPSS. Otherwise the preparation was the same as for samples intended for ellipsometry, AFM or XRR. In the following the neutron reflectivity samples are named by the number of deuterated bilayer (Dx) and protonated bilayer (Hy), while half numbers indicate an additional layer of PSS on top. For example the sample PEI/ $(\text{dPSS/PDADMAC})_6$/ $(\text{PSS/PDADMAC})_4$/ PSS is named as D6H4.5.

The layer numbers for deuterated PEMs were chosen in consideration of the limits of internal structure and of the NR measurements. The lower limit for the preparation of PEMs with a block structure is the creation of a complete block structure. Polyelectrolytes within PEMs strongly interdigitate. Too thin deuterated blocks are

completely mixed with non-deuterated material. Soltwedel et al.[99] showed that the inner block should have at least 5 double layers and the outermost block at least 3 double layers. To be sure to prepare a block structure PEMs with at least 6 deuterated bilayer and 4 non-deuterated bilayers were prepared. The upper limit for the preparation of PEMs is the specifications of the neutron reflectometer. The V6 can resolve depth profiles of about 200 nm depth. Therefore, the thickest samples were prepared 10-20% thinner than 200 nm.

3.3 Ellipsometry

3.3.1 Theoretical Background

Ellipsometry is an optical method that allows precise and accurate determination of PEMs thickness and refractive index. Ellipsometry measures the change of polarization state after the reflection of a laser beam at a surface.[110] The change in state of polarization can be transferred in the PEMs thickness and refractive index. The state of polarization of an electromagnetic wave, describes the oscillation of the electric field vector perpendicular to the propagation of the wave. In general, the state of polarization is categorized into three kind of polarization; linearly polarized light, circularly polarized light and elliptically polarized light. For linearly polarization light the field vector oscillates up and down in an x-y plane perpendicular to the propagation of the electromagnetic wave. The more general case of polarization is elliptically polarized light, than the maximum of the electric field vector rotates in an elliptically way around the center of the x-y plane perpendicular to the propagation of the electric wave. The third state of polarization, the circularly polarization, is a special case of elliptically polarized light. The maximum of the electric field vector oscillates around the center of the x-y plane but perfect circular.

All states of polarization can be described as a superposition of two orthogonal linearly polarized waves.[111] These waves are defined as parallel (p-polarized) and perpendicular (s-polarized) to the plane of incident. The different states of polarization result from different ratios in amplitude (E) and phase shift (δ) between p- and s-polarized wave. Linearly polarized light is not shifted in phase; the ratio of amplitude defines the direction of the oscillation. Circularly polarized light occurs if the phase is shifted by $\pi/2$ and the amplitudes are equal. Elliptically polarized light results from all other cases. During the reflection at an interface the electromagnetic wave interacts with the sample. Therefore, the s-polarized (r_s) and p-polarized (r_p) component of

the wave reflects differently giving a complex reflectance ratio (ρ) :

$$\rho = \frac{r_p}{r_s} = tan\Psi \times e^{i\Delta} \tag{3.1}$$

where Δ and Ψ are the so called ellipsometric angles. Δ describes the change of phase shift due to the reflection

$$\Delta = (\delta_p^r - \delta_s^r) - (\delta_p^i - \delta_s^i) \tag{3.2}$$

where the indices r and i denote the reflected and the incidental beam, respectively. Ψ describes the change in amplitude ratio:

$$tan\Psi = \frac{|E_p^r|/|E_p^i|}{|E_s^r|/|E_s^i|} \tag{3.3}$$

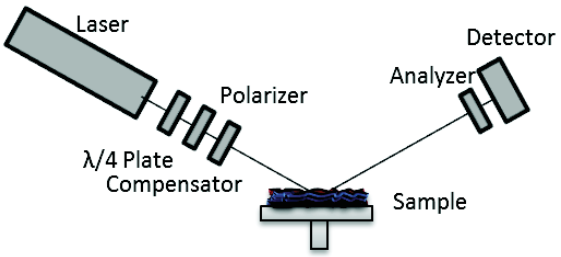

Figure 3.2: Schematic of an ellipsometer with PCSA setup. First, the laser beam passes a linear polarizer (P) followed by a quarter wave plate called compensator (C). After the reflection at the sample (S) it passes a second polarizer the so called analyzer (A) and incidents the detector.

The typical setup for ellipsometry is the PCSA setup consisting of a light source an linear polarizer (P), a compensator(C), the sample (S), a second linear polarizer (A) (also called analyzer) and the detector. A schematic of the setup is shown in figure 3.2. Usually, the components before the samples provide a known state of polarization, while the components after the sample measure the new state of polarization. A more accurate but slower way to determine the change of polarization is null ellipsometry. In order to obtain information about the change of polarization, the polarizer and analyzer are varied until the reflected light is extinguished ("nulling").[110] For the PCSA setup, and if a quarter wave plate is used as compensator set in an angle of 45°, there exist only two positions of polarizer and analyzer where the wave is extinguished: A_1, P_1 and A_3, P_3 which are related by $P_1 = \pm P_3$, $A_1 = -A_3$. These positions are related to the measured ellipsometric angles Ψ and Δ:

$$\Psi = A_1, \Delta = 2P_1 + \pi/2 \tag{3.4}$$

For a detailed mathematically examination of ellipsometry and especially null ellipsometry the reader is referred to the handbook of ellipsometry.[110]

The complex reflection ratio depends on the optical structure of the sample, i.e. it contains optical parameters of the sample, including thickness refractive index and adsorption constant (at the measured wavelength λ) of every single layer.[112] To solve the complex reflection ratio an analytical layer model is used. Because two parameters are obtained by the measurements (Δ and Ψ) the layer model has to contain the correct values for all but two parameters. Usually the thickness and refractive index of the sample is chosen as free parameter.

3.3.2 Experimental Setup

Setup for Ambient Conditions The measurements were performed with a PCSA (polarizer- compensator- sample- analyzer) ellipsometer (Optrel GbR, Sinzing, Germany). The laser is a NeHe-Laser with a fixed wavelength of $\lambda = 632.8$ nm. The linear polarizers (polarizer and analyzer) are Glan-Thompson-Prisms inserted into a rotary state. A Glan-Thompson-Prism polarizes the incoming beam due to total reflection of the perpendicular to the prisma polarized component of the beam. The compensator consists of a quartz retardation plate cut to a $\lambda/4$ retardation, leading to a phase shift of $\pi/2$. The detector is a four quadrant photo diode, able to locate the position of the laser beam at the detector, to simplify sample alignment. The experiments were carried out at a constant wavelength of 632.8 nm and a fixed angle of incidence of 70° (close to the Brewster angle of the Si/air interface). The samples were measured at least at five different positions on the sample.

Setup for measurements in liquid water Ellipsometric measurements in water are complicated by refraction at the air water interface. At an angle of incident different from 90° a laser beam is refracted at the air water interface. The refraction results in a different angle of incident onto the sample. To avoid that problem, the ellipsometer is equipped with two light guides.[113] The light guides are cylindrically metal tubes with a thin glass slide at the end. The light guides are attached to the ellipsometer. The laser beam incidents the glass slide at 90° (no refraction) and afterwards the water interface at 90°. To be sure that the sample was fully equilibrated in water, Δ and Ψ were observed at one position of the sample until a constant value of the ellipsometric

angles was reached. Then the samples were measured at five different positions. The angle of incidence was fixed at 60°.

Setup for Measurements in Controlled Relative Humidity For measurements with controlled relative humidity a special measurement cell was constructed. The humidity cell was made of stainless steel. To ensure hermetic sealing, light guides are attached to the cell sealed by a rubber gasket. The light guides are connected with the detector and laser arm. This setup allows a movement of laser and detector arm about 10°. Sensors for temperature and humidity can be inserted from the top of the cell and can be placed right above the sample. The sensors are connected with the computer and are read out by the ellipsometer control software. The front of the cell is closed by a Plexiglas window. At the rear of the cell, the in- and outtake for gas with controlled humidity are located. The humidity can be adjusted between 1% RH and 95% RH by the mixing of two streams of nitrogen. The first stream is dried (1% RH) the second stream is saturated by water vapor, due to injection of nitrogen into water. Inside the cell a round sample table is attached which height can be adjusted. To measure PEMs in controlled humidity, the samples were equilibrated for 20 min at the respective relative humidity. The relative humidity was measured and recorded by a Testo 6681 Humidity measuring transducer with testo 6614 sensor (Testo Ag, Lenzkirch, Germany).

Temperature Treatment In chapter 7 the effect of temperature treatment on the structure of PEMs is investigated. For the temperature treatment, the following procedure was carried out. Initially, the sample was measured in dry N_2 (1% RH) followed by a measurement in water. Then the sample was kept for 2 h at 65°C in water. During the temperature treatment Δ and Ψ were monitored. After the temperature treatment the PEM was first measured in water and then in dry N_2 (1% RH). During the temperature treatment, the ellipsometric angles were monitored over time at one spot.

Data treatment The software "Ellipsometry: simulation and data evaluation" (Optrel, v. 3.1) was used for calculating the thickness and refractive index. A one-box model for the PEM was assumed. Table 3.1 shows the used model. The continuum media were air (n = 1.000) and silicon (n = 3.885; k = -0.180).[114] The thin SiO_x layer at the surface of the Si wafer was fixed with n = 1.459[114] and d = 1.5 nm. As fitting parameters the thickness and the refractive index of the PEMs were chosen.

Layer	d [nm]	n	k
Air	infinite	1.000	0.000
PEM	fit	fit	0.000
SiOx	1.5	1.4598	0.000
Si	infinite	3.885	-0.018

Table 3.1: The layer model for ellipsometry; Air and silicon are the surrounding media (infinite thickness). Thickness (d) and refractive index (n) of the PEM are the fitting parameters. Thickness of the SiO_x layer is determined by XRR. Optical constant of air, SiO_x and Si are from literature.[114]

The average thickness d = 1.5 nm of the SiO_x layer was determined by measuring five individual Si wafers with ellipsometry and x-ray reflectometry after the etching in H_2O_2/H_2SO_4. For samples measured in water the above described model was used but with water (n = 1.332) instead of air as continuum.

The change of the ellipsometric angle Ψ in dependence of the refractive index of the sample depends on the thickness of the sample. For a thickness d < 20 nm the change of the ellipsometric angles Ψ are small. Thus, the refractive index and the thickness cannot be simultaneously determined with sufficient accuracy. Therefore, thickness and refractive index were simultaneously determined only for PEMs with thickness d > 20 nm. For PEMs with thickness d < 20 nm the average refractive index of the PEMs with thickness d > 20 nm and the same terminating layer were taken under the assumption that the refractive index is independent of the PEM thickness.

3.4 Atomic Force Microscopy

3.4.1 Theoretical Background

The Atomic Force Microscopy (also called scanning force microscopy) was invented in the late 1980s by Binning et al.[115] as an enhancement of the scanning tunneling microscopy (STM). STM is only able to measure the topography of *conducting* materials, while AFM can also obtain topographic images of *insulating* materials like PEMs. An AFM "senses" the surface of the sample, by measuring the interaction between the probed surface and the tip of the scanning AFM-probe. Although the basic principle is very simple, the technical implementation is rather complex, at least if surfaces with features of nano meter scale are measured.

The central part of the AFM is the AFM probe, which scans over the surface. The probe measures several micrometers in length and a few nanometers in diameter

at the tip. The lateral resolution of an AFM is limited by the diameter of the tip; it is not possible to detect objects that are smaller than the diameter of the tip. In principle, lateral resolutions of atomic scale can be obtained by using fictionalized tips for scanning samples at temperatures close to 0 K.[116] More typical are lateral resolutions of 2-10 nm. The vertical resolution is about 0.1 nm and only depends on thermal noise.[117] The probe itself is mounted on a cantilever, on one hand the cantilever serves as the attachment point for the probe. Thus, the cantilever defines the force which applies on the surface. Cantilever with a high spring constant are suitable to measure hard surfaces while for soft surface it is necessary to use a weak spring constant otherwise the samples can be damaged. Further, the cantilever is an important part of the detection system which measures the forces between probe and sample. The cantilever moves in dependence on the force between surface and probe. The movement of the cantilever is detected by a laser beam reflected on the backside of the cantilever. Due to the relatively long optical path of the laser beam before it reaches the detector, a small change in angle results in a strong change of laser spot position at the detector. Thus, it is possible to detect even smallest changes of cantilever deflection. The cantilever itself is fixed to a silicon chip of a few mm in dimensions, thus allowing the use of tweezers to handle it. The whole ensemble of tip, cantilever and chip is fixed to a system of piezoelectric crystals, which use the piezo-mechanical effect to enables movement with nanometer precision. Figure 3.3 shows the typical setup for imaging AFM.

The movement of cantilevers and with it the tip of the AFM is controlled by a feedback system which excites the cantilever in different ways according to the operation mode. These modes are typically the contact, non-contact and intermediate contact mode. All modes have their advantages and disadvantages. For contact mode the tip is in direct contact with the sample. The force of the tip applied at the surface is defined by the bend of the cantilever. Since the feedback systems regulates the distance between probe and surface to a fixed value, the applied force does not change during the measurement. The advantage of this method is its high resolution, the downside is the high risk of both; damaging the sample as well as the probe. Therefore, it is only suitable for samples with high mechanical resistance, e.g. metallic surfaces.

On the other side of the spectrum is the non-contact mode. Here, the cantilever oscillates at a defined distance away from the surface. This oscillation is interfered by attracting and repelling forces between surface and probe. This mode is completely non-destructive, but the lateral resolution is much worse than in contact mode.

For the investigation of PEMs, which are pretty soft in comparison to metallic

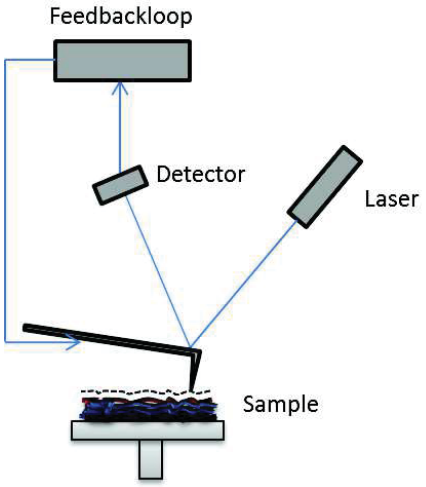

Figure 3.3: Scheme of a typical AFM setup. The tip scans over the sample. A change of the samples topography results in a change of the interaction with the tip. The cantilever bends. The reflection angle of the laser reflected at the cantilever back side changes and the laser spot incidents the detector in another position. The feedback system reacts with either an increase or decrease of the cantilevers height.

surfaces, the intermediate contact mode is the most convenient mode. In intermediate contact mode, the cantilever oscillates close to the surface and taps with every oscillation on the surface. This allows lateral resolutions similar to contact mode, but with less danger for the sample. The tapping avoids friction of the tip on the sample. Further the short contact times avoid deformation of the surface (especially for rather soft samples).[117]

3.4.2 Experimental Setup

The AFM images were performed on a commercial instrument, Cypher AFM (Asylum Research, Santa Barbara, USA). All measurements were done with a scanning rate of 1 Hz. The investigation of PEMs in air was done in intermittent contact mode, with silicon cantilevers (Olympus, Tokyo, Japan). The used cantilever of rectangular shape had an Al coating, it was 160 μm in length with a resonance frequency of 320 kHz and a force constant of 42 N/m. For measurements in water, the images were recorded in intermittent contact mode with silicon nitride cantilevers (Olympus, Tokyo Japan). The used cantilever of triangular shape had a Cr/Au coating, it was 100 μm in length with a resonance frequency of 8 kHz and a force constant of 0.02 N/m. The roughness was calculated by the imaging software of the Cypher instrument (based on Igor Pro (WaveMetrics, Inc.)), which performs the calculation of the roughness.

All AFM images had a size of 2 μm $\times$ 2 μm and were corrected for tilt using a line fit. The errors reported here were calculated from the standard deviation for all the measurements, which included at least three areas on the samples. For the comparison with the x-ray reflectometry measurements, the roughness was calculated as the average of the roughness of four 1 μm $\times$ 1 μm boxes inside of the 2 μm $\times$ 2 μm images. The choice is motivated by the coherence length of x-rays of about 1 μm.[118]

3.5 Reflectometry

3.5.1 Theoretical Background

Reflectometry techniques measure the specular reflection of x-ray or neutron radiation. They are non-destructive methods to determine thickness roughness and composition of thin films. In surface science x-ray reflectometry is a complementary method to ellipsometry. Both measure the thickness and the optical constant, namely the refractive index and the scattering length density, of the system. While the refractive index usually correlates with the density of the system[119], the scattering length density obtained by XRR correlates with the electron density of the sample.[120] One advantage of XRR is that the thickness of a film can be determined without knowledge about the properties of the surrounding media. Neutron NR is equal to XRR but uses a beam of neutrons as source of radiation. X-rays interact with the electron shell of an atom, while neutrons interact with the nucleus. Therefore, x-rays are only sensitive to quite big differences in atomic order. Thus, it is not possible to distinguish between material consistent of light elements like carbon and hydrogen. The interaction between neutrons and the nucleus depends on the strong interaction, which depends on number of protons and neutrons and their symmetry inside the nucleus.[121] The strong interaction varies strongly between different nuclides. Additional to the higher contrast between light elements, the sensitivity to different isotopes is a great advantage compared to XRR. Especially the high sensitivity to hydrogenated and deuterated materials allows deep insight into internal properties of PEMs.

For the specular reflection of x-rays and neutrons on a surface the same considerations apply as for visible light, i.e. the refractive index of the material is the most important parameter. The refractive index for x-rays and neutrons can be described as:

$$n = 1 - \delta - i\beta \tag{3.5}$$

where δ is the scattering length density and β is the adsorption constant. For x-rays δ and β are defined as:

$$\delta = \frac{\lambda^2}{2\pi}\rho_e r_e \tag{3.6}$$

where r_e is the radius of the free electron ($2.82\times10^{-}5$ Å) and ρ_e is the electron density. Because δ depends on the electron density the scattering length density increases with the atomic number. For neutrons the formula for δ is similar

$$\delta = \frac{\lambda^2}{2\pi_e}Nb \tag{3.7}$$

where N is the number density and b is the coherent neutron scattering length.

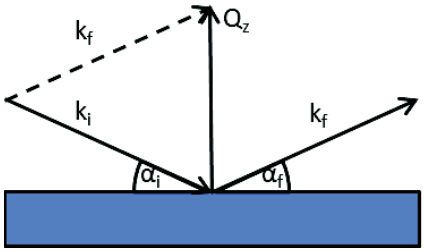

Figure 3.4: Elastic scattering on a planar surface.

When a particle (photon or neutron) is specular reflected on a surface the momentum of the particle changes. The momentum transfer can be described as the sum of the wave vectors of the incident beam (k_i)and the reflected beam (k_f) (see figure 3.4):

$$\vec{Q} = \vec{k_f} - \vec{k_i} \tag{3.8}$$

For a given wavelength the momentum transfer in z-direction is described as:

$$Q_z = \frac{4\pi}{\lambda}sin(\alpha_i) \tag{3.9}$$

Similar to optics, for an ideal reflecting flat surface the reflectivity depends on the complex reflection coefficient (r):

$$r = \frac{k_z - k'_z}{k_z + k'_z} \tag{3.10}$$

k_z and k'_z are the vertical component of the respective wave vector. r describes the reflection on one interface. For multilayer systems all interface have to be considered for the reflection coefficient:

$$r_{j,j+1} = \frac{k_{z,j} - k_{z,j+1}}{k_{z,j} + k_{z,j+1}} \tag{3.11}$$

Additionally, the investigated interface is not perfectly flat. The roughness can be described as:

$$r_{rough} = r_{ideal} e^{-2k_z k'_z \sigma^2} \tag{3.12}$$

Furthermore, a part of the incident beam is transmitted instead of reflected. Parratt developed a recursion formalism, which relates the reflected R_j and transmitted amplitude T_j to the reflection coefficient of the interface j.[122] Furthermore, the roughness of the interface can be included:

$$X_j = \frac{R_j}{T_j} = e^{-2k_{z,j}k_{z,j+1}+\sigma^2_{j,j+1}} \frac{r_{j,j+1} + X_{j+1}e^{2ik_{z,j}z_j}}{1 + r_{j,j+1}X_{j+1}e^{2ik_{z,j}z_j}} \tag{3.13}$$

For multilayer systems this formula can become pretty complex and is usually solved by a iterative fitting routine.

3.5.2 Experimental Setup for X-Ray and Neutron Reflectometry

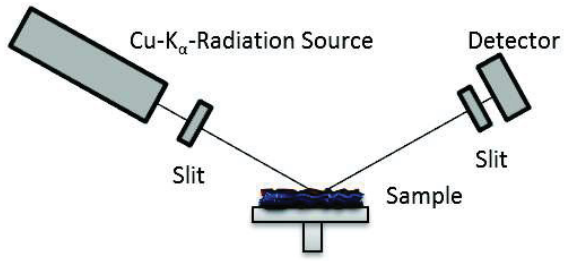

Figure 3.5: Schematic setup of an x-ray reflectometer. X-rays with a wavelength of $\lambda = 1.545$ Å passes an absorber and a slit and are reflected at the samples surface. After the reflection, the x-rays pass again a slit and incident the detector. Usually, the angle of the detector and x-ray source are changed during the measurement while the sample is fixed. The Setup for a neutron reflectometer is similar; the neutrons are generated by a nuclear reactor and guided to the neutron reflectometer. Because of the immobility of the neutron source during the measurement angle of detector and sample are changed.

The standard setup for reflectometry is shown in figure 3.5. For the x-ray reflectometry measurements a commercial reflectometer, D8 Discoverer (Bruker, Billerica

USA), with a Cu-K_α radiation ($\lambda = 1.545$ Å) was used. Neutron Reflectometry measurements were carried out at the V6 at Helmholtz institute (chapter 6 and 7) and the NREX at FRM II (chapter 5). At the V6 a neutron wavelength of 4.66 Å is selected by a graphite monochromator (PG(002)), with a wavelength variance of $\Delta\lambda/\lambda = 0.02$. The monochromatisation results from bragg reflection at the graphite grid. The resolution is dependent on the slit position. At small $Q_z \leq 0.05$ Å the reflected intensity is rather high and the slits can be set to 0.5 mm, which correlates with a resolution of $\delta Q = 0.001$. For $Q_z \geq 0.05$ the slits are set to 1 mm which correlates with a resolution for $\delta Q = 0.002$. The neutron intensity was monitored by ^{3}He detector tubes. ^{3}He detectors use the reaction of neutrons with ^{3}He. The generated energy can be monitored as ionization process.

At NREX a beryllium monochromator selects neutrons with a wavelength of $\lambda = 4.28$ Å and a variance of $\Delta\lambda/\lambda = 0.02$. At small $Q_z \leq 0.02$ Å the reflected intensity is rather high and the slits can be set to 0.5 mm, which correlates with a resolution of $\delta Q = 0.0005$. For $Q_z \geq 0.02$ the slits are set to 1 mm which correlates with a resolution for $\delta Q = 0.001$. The intensity is monitored by a 2D position sensitive ^{3}He wire chamber with an active area of 200 x 200 mm^2.

Controlled Humidity Measurements under controlled humidity were performed in a self-made humidity cell. The cell is hermetic isolated and can only be opened at the top. The top is sealed by a Plexiglas window. At the window, the gas in and outtake for humid nitrogen and the humidity and temperature sensor (Hygropalm- HP22-A with HC2-P05 Sensor, Rotronic AG, Bassersdorf, Switzerland) is attached. The sensor is placed right above the center of the sample. X-rays can pass the cell through windows covered by Capton foil. Capton foil has the lowest possible adsorption coefficient for x-rays. For neutron reflectometry the capton foil is exchanged by aluminum. The humidity can be controlled either by a stream of gas or due to saturated salt solutions. Salt changes the chemical potential of an aqueous solution. Thus, the difference of chemical potential between water vapor and the solution decreases. Therefore, the necessary amount of vaporized water to reach a state of equilibrium decreases. Thus, the air above the salt solution is in equilibrium at lower water vapor concentrations than above pure water. To achieve 1% RH the air was dried by silica gel and the humidity monitored by a humidity sensor (Hygropalm-HP22-A with HC2-P05 Sensor, Rotronic AG, Bassersdorf, Switzerland). The samples were equilibrated for 1 h.

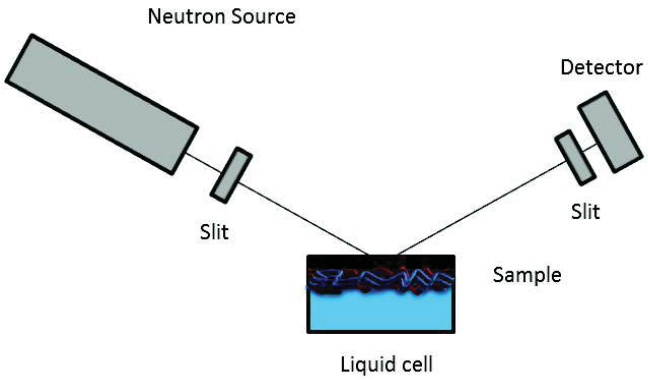

Figure 3.6: NR setup in water. The sample is positioned the up-site down. The Neutron beam passes the silicon block and is reflected at the PEM/water surface.

Neutron Reflectometry in Water Measurements in water are not possible with XRR due to the strong scattering of x-rays in water. For NR a special liquid cell was constructed. The central part of the cell is the teflon trough (72 x 42 x 3 mm^3) with stainless steel tubes for water inlet and outlets. The teflon trough is fixed at the silicon block by two aluminum blocks, which are mounted on both sides of the silicon block and screwed together. The aluminum blocks have in- and outlets to install a thermostat.

For measurements at the liquid PEM interface the liquid cell is installed the up-side down (fig. 3.6). Because neutrons strongly scatter in water and D_2O the neutron beam incidents the PEM/liquid interface by passing first the silicon block, which is much better penetrable for neutrons.

Data Treatment The data treatment for XRR and NR data is similar. First the raw data is normalized to the maximum intensity. Then a footprint correcting is necessary. At low angles the footprint of the beam is much bigger than the sample. Therefore, only a part of the beam is reflected. With increasing angle the ratio between sample size and footprint decreases, the reflected intensity increases linearly until the footprint becomes smaller than the sample. This linear increase is corrected. Further, for NR the background radiation is subtracted from the curve. This is not necessary for XRR because of the much higher intensity of the x-ray beam.

From the measured reflectivity curves the SLD profile across the PEM can be extracted by using a least mean-squares fitting routine. The data were fitted using the Motofit Package for Igor Pro.[123] The algorithm splits the measured PEM into boxes of constant SLD and thickness with a Gaussian roughness between each box. For XRR

Layer	d [nm]	SLD [10^{-6} Å^{-2}]	iSLD [10^{-6} Å^{-2}]
Air	infinite	0	0.000
PEM	fit	fit	0.065
SiOx	1.5	18.91	0.245
Si	infinite	20.15	0.459

Table 3.2: Layer model for XRR. Air and silicon are the surrounding media (infinite thickness). Thickness (d) and the scattering length density (SLD) of the PEM and are the fitting parameters. Thickness of the SiOx layer after etching was determined by XRR.

data, an one-box model for the PEM was assumed (table 3.2), the continuum media were silicon (SLD = 20.1 Å^{-6}) and air (SLD = 0.0 Å^{-6}), the parameter of the silicon oxide layer were fixed at SLD = 18.9 Å^{-6}, d = 1.5 nm ± 0.2 nm; σ = 0.3 nm ± 0.1 nm. The average thickness and roughness of the SiO_x layer was determined by measuring five individual Si wafers with ellipsometry and x-ray reflectometry after etching in H_2O_2/H_2SO_4. As fitting parameter the thickness, roughness and the SLD of the PEMs were chosen.

For NR data of PEMs with a deuterated inner block and a non-deuterated outer block a n-box model was chosen. To prevent artifacts in the SLD profile it is important that the roughness of one box does not exceed 1/3 of the box thickness. This is not an issue for the interface between the outermost non-deuterated block and the environment but for the interface between deuterated block and non-deuterated block. Therefore, the deuterated part and the transition region between deuterated and non-deuterated block were split into a varied number of boxes with a fixed thickness of 2 nm and a roughness of zero between the boxes. As additional constraint, the SLD decreases monotonically towards the outer interface of the PEM. The continuum media were silicon (SLD = 2.07 × 10^{-6}Å^{-2}) and air (SLD = 0.0 × 10^{-6}Å^{-2}) or D_2O (SLD = 6.36 × 10^{-6}Å^{-2}); the silicon oxide layer was fixed at SLD = 3.47 × 10^{-6}Å^{-2} , d = 1.5 nm ± 0.2 nm; σ = 0.3 nm ± 0.1 nm. From the SLD profiles the overall thickness was extracted by summarizing the thickness of all boxes. The average SLD was calculated by the area under the SLD profiles divided through the overall thickness.

Chapter 4

The Relation Between Surface and Bulk Characteristics and Void Water *

Abstract In the present chapter, the influence of the outermost layer and the number of layers on the amount of void water and swelling water inside polyelectrolyte multilayers was investigated. For that purpose PSS/PDADMAC polyelectrolyte multilayers were studied in air with 1% RH, 30% RH , 95% RH and in liquid water by ellipsometry, atomic force microscopy and x-ray reflectometry. The total amount of water uptake in swollen PEMs is divided into two fractions, the void water and the swelling water. Therefore, it is necessary to separate both fractions correctly. In order to allow measuring samples over a larger thickness regime the investigation of a larger amount of samples is required. Therefore, the concept of separating void water from swelling water using neutron reflectometry was for the first time transferred to ellipsometry. The subsequent analysis of swelling water, void water and roughness revealed the existence of two types of odd-even effects: an odd-even effect which addresses only the surface of the PEM (surface-odd-even effect) and an odd-even effect which addresses also the bulk of the PEM (bulk-odd-even effect). The appearance of both effects is dependent on the environment; the surface-odd-even effect is only detectable in humid air while the bulk-odd-even effect is only detectable in liquid water. The bulk-odd-even effect is related to the osmotic pressure between the PEM and the surrounding water. A correlation between the amount of void water and both odd-even effects is not found. The amount of void water is independent of the terminated layer and the thickness of PEMs.

*Similar content was published in Zerball, M.; Laschewsky, A.; von Klitzing, R. Swelling of Polyelectrolyte Multilayers: The Relation Between Surface and Bulk Characteristics. J. Phys. Chem. B, 2015, 119(35), 11879-11886

4.1 Introduction

In this chapter, the swelling behavior of PEMs is investigated over a large thickness regime. Three effects are known to influence the swelling behavior of PEMs, irrespective of the choice of the polyanions and polycations. First, PEMs swell inhomogeneously due to substrate effects.[29,37,124] Therefore, the swelling behavior depends on the number of layers and the absolute thickness of the PEM. Second, the swelling behavior depends on the outermost layer (odd-even effect).[29,33,35,80,96] Third, the high interdigitation during preparation favors the formation of voids inside the PEM, which influences the swelling behavior.[22,30,93] Filling of the voids with water during the swelling process would only affect the optical properties. These three phenomena, the local gradient in swelling[29,37,124], the odd-even effect[29,35,80] and amount of void water[22,30,93], have been investigated separately in previous studies. However, investigations about their mutual influence are missing.

The chapter addresses the mutual effect of odd-even effect at PEM surface and of the PEM bulk. The local swelling gradient and the void properties are assumed to be strongly related to the odd-even effect. Since, the existence of voids is assumed as a result of the preparation process, i.e. the interdigitation of the PEs, it is important to know how the void volume changes at different number of deposited layers. This demands a high number of samples to be investigated. Usually, neutron reflectivity is the appropriate method to investigate the amount of void water. Unfortunately, the capability for using neutron reflectometry is limited. Therefore, the technique to separate void water from swelling water implemented by means of neutron reflectometry is transferred for the first time to ellipsometry data. Similar to the scattering length density in neutron reflectometry the refractive index of ellipsometric measurements is used to investigate the water amount within the swollen PEM in comparison to the increase in thickness. Although ellipsometry is less precise than neutron reflectometry, it will be shown in the present study that ellipsometry can be used as a versatile and fast method to study the swelling of polymer coatings, at least for the purpose to separate void water and swelling water. The better understanding of the origin of voids will help to understand also the odd-even effect and the effect of PEM thickness. Therefore, the calculated void water of PEMs in dependence of the number of layers will be discussed concerning correlations to type of growth and odd-even effect of PEMs.

4.2 Results

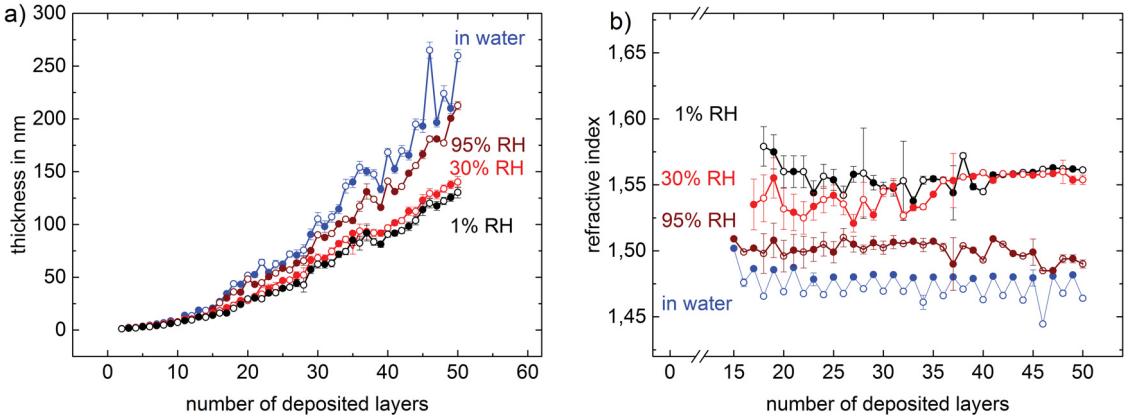

Figure 4.1: (a) Thickness and (b) refractive index of PSS/PDADMAC PEMs in dependence of the number of layers measured by ellipsometry in air at 1% RH, 30% RH, 95% RH and in water. Open symbols represent PDADMAC-terminated PEMs, filled symbols represent PSS-terminated PEMs.

4.2.1 Thickness of PSS/PDADMAC PEMs at Different RH and in Water

Figure 4.1 shows the thickness and refractive index of PSS/PDADMAC PEMs measured by ellipsometry in dependence of the number of deposited layers (N). The measurements were carried out in air with 1% RH, 30% RH, 95% RH and in liquid water. Every data point represents a unique sample, since an intermediate drying in order to measure the sample would influence the adsorbed amount of following adsorption steps.[125] The refractive index is only shown for PEMs > 20 nm (ca. 15 layers) for thinner PEMs it is not possible to calculate thickness and refractive index independently.

At 1% RH no specific effect of the outermost layer (PSS or PDADMAC) on the PEM thickness can be detected. Up to 22 layers the thickness increment increases. The PEMs grow non-linearly. After 22 layers, the thickness increment becomes constant, accompanied with a transition from non-linear to linear growth. This growth behavior was often described in literature.[68,126] Because of the low ionic strength (0.1 M NaCl) during preparation the non-linear growing regime is small in terms of thickness. The thickness increment grows from 1.0 nm to 4.0 nm at the end of the non-linear growing regime. The refractive index at 1% RH is constant with increasing layer number with

a value of n = 1.56. After increasing the RH from 1% to 30% the thickness increases independent of the terminated layer. The refractive index increases for N $<$ 26 and reaches a constant value of 1.56 for N $\geq$ 26, similar to the refractive index at 1% RH Increasing the RH to 95% RH causes a further increase in thickness independent of the terminated layer. In addition, the refractive index decreases to a constant value of 1.50. The strongest increase in thickness is detectable in water. In addition, an odd-even effect occurs in thickness and refractive index between PSS- and PDADMAC-terminated PEMs. The thickness of PDADMAC-terminated PEMs increases stronger than the thickness of PSS-terminated PEMs. This result agrees with the finding for the refractive index, which shows a zig-zag pattern with an average value of 1.48 for PSS-terminated PEMs and 1.46 for PDADMC-terminated PEMs. The individual values for PSS- and PDADMAC-terminated PEMs are independent of the number of layers.

4.2.2 Roughness of PSS/PDADMAC PEMs in Air at Different RH and in Water

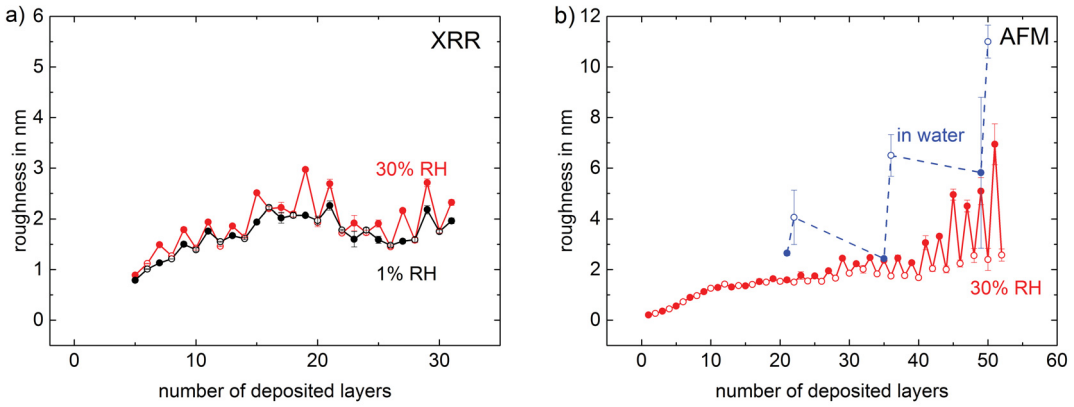

Figure 4.2: The roughness of PSS/PDADMAC PEMs in dependence of the number of layers measured with (a) XRR in air at 1% RH, 30% RH and with (b) AFM in air at 30% RH and in water. Open symbols represent PDADMAC-terminated PEMs, filled symbols represent PSS-terminated PEMs.

In order to get reliable values for the roughness both AFM and x-ray data were analyzed. The drawback of the analysis of x-ray data is that the roughness is only a model roughness, which depends on the chosen model for data analysis, while AFM measures the roughness directly. However, the direct interaction can influence the samples surface. Although the AFM measurements were done at the highest possible

set point and integral gain, it can not be excluded that the tapping of the AFM tip on the PEM surface influenced the PEM topography during the measurement. Beyond 30 layers the PEM becomes too thick for XRR analysis, while roughness determination by AFM is independent of PEM thickness.

Figure 4.2a shows the roughness calculated from XRR data, measured at 1% and 30% RH as a function of the number of deposited layers. The reflectivity curves and the corresponding fit are shown in appendix (figures A.2 and A.3). At 1% RH the roughness increases until the 14^{th} layer is reached, beyond 14 layers no odd-even effect is detectable. At 30% RH an odd-even effect beyond 14 layers is detected. The PSS-terminated PEMs increases in roughness while PDADMAC-terminated PEMs remains at the value for 1% RH. Figure 4.2b shows the roughness determined from AFM images at 30% RH and in water. In air with 30% RH the roughness increases until the 14^{th} layer and remains then constant until the 26^{th} layer. Beyond 26 layers only the roughness of PSS-terminated PEMs increases, the odd-even effect starts, i.e. at much higher number of deposited layers in comparison to XRR. Presumably, the tapping of the AFM tip on the PEM surface is responsible for this difference between XRR and AFM. With increasing number of layers the PSS-terminated PEMs become rougher while the roughness of PDADMAC-terminated PEMs is constant. In water the odd-even effect turn around, the PDADMAC-terminated PEMs are rougher than the PSS-terminated PEMs.

4.2.3 Calculation of Swelling Water and Void Water

The main focus of this study is the swelling behavior of PEMs. To discuss the swelling behavior of PEMs it is important to calculate their water content correctly. The typical approach to do that is to assume that the incorporated water induces a constant change in thickness. With this assumption the water content of the water swollen PEMs can be described in the following way:

$$\phi_{swell} = \frac{d_{swollen} - d_{dry}}{d_{swollen}} \tag{4.1}$$

where ϕ_{swell} is the water content $d_{swollen}$, the thickness in water and d_{dry} the thickness of the dried PEM. The water content can also be calculated by the change of optical properties of the PEM. If a material is diluted by another material, the refractive index of the composition is in between the refractive indices of both materials. Garnet showed this by investigating metallic melts and formulated the Garnet equation.[127] In ref. 29 the Garnet equation was transferred to PEM against water:

$$n_{swollen} = n_{water}\sqrt{1 + \frac{3(1-\phi_{swell})}{\left(\frac{n_{dry}^2+2n_{water}^2}{n_{dry}^2-n_{water}^2}\right) - (1-\phi_{swell})}} \tag{4.2}$$

where $n_{swollen}$ is the resulting refractive index in water, n_{dry} the refractive index of the dried PEM and n_{water} the refractive index of water. The garnet describes the swelling of PEMs exactly. Nevertheless, for the system of a PEM diluted by water the correlation between refractive index and water content can be assumed as linear, because of the small differences of refractive index between water and polymer (see appendix A.1). In this case the calculation of water content can be simplified in the following manner:

$$\phi'_{swell} = \frac{n_{swollen} - n_{dry}}{n_{water} - n_{dry}} \tag{4.3}$$

The comparison between water content calculated by refractive index (eq. 4.3) and from the thickness (eq. 4.1) shows a discrepancy between both values. A similar behavior was found in neutron reflectometry measurements and was explained by the existence of voids inside the PEM.[22,93] Because of the presence of voids inside the PEM the former assumptions becomes obsolete. In dry state the PEM is already diluted by air, which reduces the refractive index of the dry PEM. During the swelling process air is substituted by water, simultaneously polymer is diluted by water. The problem can be solved in analogy to the considerations in neutron reflectometry measurements.[22] To calculate the water content and also the void water correctly the SLD is replaced by refractive index. This equation describes the dried state and how the void volume affects the refractive index:

$$n_{dry} = xn_{Polymer} + (1-x)n_{air} \tag{4.4}$$

where x is the polymer fraction. In swollen state the PEM can be treated as sum of a water fraction and a polymer fraction. The polymer fraction can be described in the same manner as in dried state with the exception that the voids are filled with water. The next equation describes the swollen states and how the filling of voids and the water uptake influences the refractive index:

$$n_{swollen} = \phi_{swell}n_{water} + (1-\phi_{swell})[xn_{Polymer} + (1-x)n_{water}] \tag{4.5}$$

by inserting equation 4.4 into equation 4.5 the unknown polymer fraction x can be calculated:

$$= \phi_{swell} n_{water} + (1 - \phi_{swell})[n_{dry} - (1 - x)n_{air} + (1 - x)n_{water}] \tag{4.6}$$

$$x = \frac{n_{dry}}{n_{water} - n_{air}} - \frac{n_{swollen} - \phi_{swell} n_{water}}{(1 - \phi_{swell})(n_{water} - n_{air})} + 1 \tag{4.7}$$

If x is known the different types of containing water can be calculated by:

$$\phi_{total} = \phi_{void} + \phi_{swell} \tag{4.8}$$

$$\phi_{total} = (1 - \phi_{swell})(1 - x) + \phi_{swell} \tag{4.9}$$

Figure 4.3 shows the different contributions to the water content calculated from the measurements carried out against air with 95% RH and in liquid water. The analysis of error propagation for the void water can be found in the supporting information. The accuracy of the calculated data increases with increasing layer number because of increasing accuracy of the measured refractive indices and thicknesses. The average absolute error for the void water is ± 0.03 between 20 and 30 layers and decreases to < ± 0.01 for PEMs exceeding layer numbers of 40. The error of the amount of void water is mainly influenced by the error of the amount of swelling water, which depends on the error in thickness. As lower the difference between d_{dry} and $d_{swollen}$ as higher the error of the swelling water. Therefore, the void water is not calculated for PEMs swollen in 30% RH, the error is too high. In summary, this method to calculate the amount of void water should be used for samples with a thickness < 80 nm (the thickness of a 35 layers thick dried PEM) for smaller samples neutron reflectivity is still more accurate.

The data show that the water content is constant irrespective of the PEM thickness. Therefore, it is more convenient to discuss the average values. Table 4.1 and 4.2 shows the average ϕ_{total}, ϕ_{swell} and ϕ_{void} for PSS- and PDADMAC-terminated PEMs, which were either swollen in air with 95% RH or in water. There is no difference in the amount of void water between the measurement in liquid water and against air with 95% RH. Further, the void water is not affected by the terminated layer and shows an average value of 0.04. Dodoo et al.[22] measured with neutron reflectometry a value of 0.06 for a PEM with 12 layers prepared at the same conditions. Against air with 95% RH the swelling water is independent of the terminated layer with an average value of 0.3 while in liquid water, the swelling water depends on the terminating layer and shows a value of 0.39 for PSS-terminated PEMs and of 0.46 for PDADMAC-terminated

PEMs.

terminated layer	average ϕ_{total}	average ϕ_{swell}	average ϕ_{void}
PSS	0.349	0.306	0.047
PDADMAC	0.351	0.314	0.036

Table 4.1: Average values of ϕ_{total}, ϕ_{swell} and ϕ_{void} for PSS- and PDADMAC-terminated PEMs calculated from PEMs swollen in air with 95% RH.

terminated layer	average ϕ_{total}	average ϕ_{swell}	average ϕ_{void}
PSS	0.430	0.391	0.039
PDADMAC	0.503	0.462	0.041

Table 4.2: Average values of ϕ_{total}, ϕ_{swell} and ϕ_{void} for PSS- and PDADMAC-terminated PEMs calculated from PEMs swollen in liquid water.

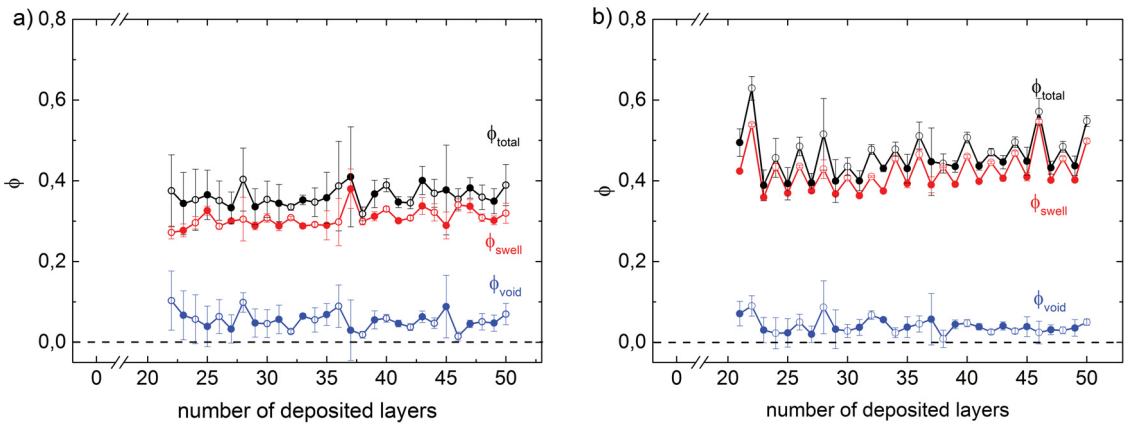

Figure 4.3: ϕ_{total}, ϕ_{swell} and ϕ_{void} in dependence of the number of layers of PEMs swollen in a) air with 95% RH and b) in water. Open symbols represent PDADMAC-terminated PEMs, filled symbols represent PSS-terminated PEMs.

4.2.4 The Swelling Behavior in 0.1 M NaCl

So far, the measurements against liquid were carried out against pure water. In order to study the effect of electrolytes on the swelling including the odd-even effect, 0.1 M NaCl was added to the water.

Table 4.3 shows the swelling water, void water and roughness of selected samples measured in liquid water and 0.1 M aqueous NaCl solution. While in liquid water the swelling water and the roughness is higher for PDADMAC-terminated PEMs in 0.1 M NaCl the differences between PSS- and PDADMAC-terminated PEMs are less

pronounced, the odd-even effect vanishes nearly completely. The void volume is not affected by the presence of NaCl.

number of layer	terminated layer	ϕ_{swell} in water	ϕ_{swell} in 0.1 M NaCl	ϕ_{voids} in water	ϕ_{voids} in 0.1 M NaCl	σ_{AFM} in water [nm]	σ_{AFM} in 0.1 M NaCl [nm]
35	PSS	0.39	0.37	0.04	0.04	2.43	1.91
36	PDADMAC	0.47	0.41	0.05	0.06	6.50	2.78
49	PSS	0.40	0.37	0.05	0.02	5.82	3.67
50	PDADMAC	0.50	0.36	0.04	0.04	11.00	4.55

Table 4.3: ϕ_{swell}, ϕ_{void} and σ_{AFM} (roughness measured by AFM) of selected samples in water and in 0.1 M NaCl.

4.3 Discussion

4.3.1 The Type of Growth of PSS/PDADMAC PEMs

PSS/PDADMAC PEMs show a non-linear growth with a transition to a linear growth at 22 layers, i.e. the thickness increment per added layer increases up to 22 layers and is constant after that. In literature two models are discussed to describe the exponential growth.[38,72] The common approach is the diffusion model.[68] It assumes that one of the polyelectrolytes is able to diffuse into the PEM during the preparation and remains there. The remaining PE diffuses back to the surface during the adsorption of the oppositely charged PE. At the surface, the PEs form complexes which give an additional contribution to the thickness increment. The transition from non-linear to linear growth takes place when no longer all PDADMAC diffuses back to the PEM/liquid interface.

An alternative model is the roughness model.[71,72] The roughness model assumes the formation of islands during the adsorption of the initial layers, i.e. the substrate is not completely covered by the PEM but by a high number of small PEM islands. These islands grow with increasing layer number until the islands begin to conglomerate.[38,67,72] The reasons for the transition from non-linear to linear growth regime are extensively discussed in ref. 38.

The recent work of Ghostine et al.[35] evidenced the diffusion model for PSS/PDADMAC PEMs by measuring the amount of extrinsic binding sites provided

by excess PDADMAC inside PDADMAC-terminated PEMs. The present work confirms the diffusion model, too. The mentioned island model would suggest an increasing roughness up to the transition point. Indeed, the roughness increases for the first layers. Nevertheless, the roughness becomes constant after 14 layers, while the transition to linear growth regime is at 22 layers. Further, the distinctive odd-even effect in water is the result of the extrinsic binding sites provided by the excess PDADMAC.

4.3.2 Swelling of PEMs in Air with 95% RH and in Water

At 1% RH PSS-terminated and PDADMAC-terminated PEMs show neither differences in thickness increment and refractive index nor in roughness. In air with 95% RH when the PEMs are strongly swollen, there is still no odd-even effect detectable in thickness and refractive index. PEMs swollen in liquid water show an odd-even effect. PDADMAC-terminated PEMs take up more water than PSS-terminated PEMs. Therefore, the thickness and roughness of PDADMAC- terminated PEMs increases stronger while the refractive index decreases stronger in comparison to PSS-terminated PEMs. The higher water uptake is caused by the higher amount of extrinsic binding sites inside PDADMAC-terminated PEMs.[35] The counter ions of the extrinsic binding sites induce an osmotic pressure which forces the PEM to uptake water.

That an odd-even effect in thickness is detectable in liquid water but not in air with 95% RH is astonishing. Because of the same chemical potential of air with 100% RH and water it is expected that the swelling behavior is the same. Indeed, the measurements were carried out against air with 95% RH. Consequently, also the chemical potential is slightly lower than the chemical potential of water. Therefore, a weaker odd-even effect is expected. The missing of the odd-even effect indicates a fundamental difference in swelling behavior between swelling in humid air and in liquid water. Apparently, the contribution of the extrinsic binding sites to the water uptake comes not into account if the surrounding medium is not liquid water.

That the extrinsic binding sites are responsible for the odd-even effect in water is also confirmed by the measurements in salt solution. In 0.1 M NaCl aqueous solution the water content and roughness of PDADMAC-terminated PEMs decreases compared to the values measured in water. The osmotic pressure vanishes, due to the similar ion concentration inside the PEM and the environmental liquid.

4.3.3 The Different Types of Odd-Even Effects

The investigated PSS/PDADMAC PEMs show different swelling behavior in humid air and in liquid water. Therefore, it is more convenient to differ between two types of odd-even effects; a surface-odd-even effect and a bulk-odd-even effect.

The surface-odd-even effect only influences the roughness, i.e. the surface of the PEM and is detectable only during swelling in humid air. PSS-terminated PEMs are stiffer than PDADMAC-terminated PEMs[94] since the PE chains are mainly intrinsically bonded. If a stiff and an elastic PEM take up the same amount of water and consequently also the change in thickness is similar, the surface of the stiffer PEM wrinkles more due to swelling.

The bulk-odd-even effect only occurs if PSS/PDADMAC PEMs are swollen in liquid water. Then PDADMAC-terminated PEMs take up more water than PSS-terminated PEMs. Therefore, the thickness and roughness of PDADMAC-terminated PEMs increases stronger as of PSS-terminated PEMs while the refractive index decreases stronger. The reason is the high amount of extrinsic binding sites inside PDADMAC-terminated PEMs.

It is assumed that the bulk-odd-even effect is driven by extrinsic charges. PEM systems prepared from weak PE are an excellent object to examine that. Because of the used weak polyelectrolytes, extrinsic charges are found in both the negatively-terminated PEM and the positively-terminated PEM. Tanchak et al.[128] investigated the swelling behavior and the contribution of ions of the weak PEM system PAA/PAH. the PAH-terminated PEMs showed higher concentration of counter ions at the PEM/liquid interface, which indicates a higher amount of charges on the surface and outermost part. However, the higher amount of charges close to the PEM/liquid interface has only a minor effect on the swelling. A bulk-odd-even effect with high differences in swelling water between PAH-terminated and PAA-terminated PEMs was not found. Apparently, the merely existence of extrinsic charges does not induce a strong bulk-odd-even effect, the amount of extrinsic binding sites have to differ significantly. In summary, extrinsic binding sites in PEMs are the necessary condition for a bulk-odd-even effect. In addition as the sufficient condition the amount of extrinsic binding sites have to be higher for one termination.

The odd-even effect of the more rigid and linear growing PEM system PSS/PAH[29] shares some characteristics of the surface- and bulk-odd-even effect but also shows some unique features. It is characterized due to a higher water uptake of PSS-terminated PEMs. Involved in the odd-even effect is a constant outermost part, neither only the

surface nor the entire bulk of the PEM. Because only a constant outermost part is affected the relative strength of the odd-even effect decreases with increasing number of deposited layers. Further, the odd-even effect of PSS/PAH is detectable in humid air [29] and in liquid water [33]. The reason for the odd-even effect of PSS/PAH PEMs is a higher hydrophilicity of PSS-terminated PEMs. Table 4.4 compares the characteristics of surface- and bulk-odd-even effects with the characteristics of the odd-even effect of PSS/PAH PEMs.

	surface-odd-even effect	bulk-odd-even effect	odd-even effect (PSS/PAH)
environment	humid air	liquid water	humid air and liquid water
region	surface	bulk	outermost region
thickness	none	increases	constant
refractive index	none	constant	decreases
roughness	constant	increases	not investigated
void water	none	none	not investigated

Table 4.4: Comparison of the characteristics of the different types of odd-even effects.

4.3.4 Void Water in PEMs

The separation between swelling water and void water showed that only the swelling water depends on the terminated layer, the amount of void water is constant at 4% irrespective of PEM thickness or terminated layer. Further, the amount of void water is similar in air with 95% RH and in liquid water. The voids are a result of the preparation process; the interdigitation of the PEM during the adsorption generates the voids inside the PEM. Dodoo et al. [22] show that the type and concentration of salt which is added to the preparation solution influences the amount of void water inside a PEM. The amount of void water decreases with increasing ionic strength and ionic radius. The density of a PEM is affected in the same way by the ionic strength and radius, which suggests that the amount of void water decreases with the density of PEMs.

The measurements in 0.1 M NaCl show that the amount of void water is unaffected by the ionic strength of the surrounding liquid, while the bulk-odd-even effect is weakened by increasing the ionic strength of the surrounding liquid. This indicates that there is no relation between the bulk-odd-even effect and the amount of void water.

While in air at 1% RH and in water the refractive index is independent of the number of layers at 30% RH, the refractive index increases up to 26 layers and is constant after that. The data only give information about the total volume of void water. In water is assumed that the voids are completely filled. Therefore, the amount of void water equals the void volume. It is not known if at 30% RH the voids are empty, filled or partly filled. The increase of refractive index with increasing number of layers at 30% RH indicates a change in void filling with increasing relative humidity.

4.4 Conclusion

To investigate the relation between the odd-even effects and the amount of void water, the concept of separating void water and swelling water was transferred from neutron reflectometry to ellipsometry. Thereby, ellipsometry became a versatile and fast tool to investigate the void water and swelling water of polyelectrolyte multilayers in water and water vapor. Through the possibility to use ellipsometry to calculate amount of void water it was possible to investigate a high number of samples. Hence, it was possible to investigate the correlation between number of deposited layers and the amount of void water. The amount of void water is independent of the terminated layer and the thickness of PEMs.

The amount of swelling water in PSS/PDADMAC PEMs depends on the outermost layer. This behavior is known as odd-even effect. The odd-even effect of PSS/PDADMAC PEMs can be divided into two types of odd-even effect named after their area of influence: the surface-odd-even effect and the bulk-odd-even effect. The bulk-odd-even effect is induced by an excess of charges inside PDADMAC-terminated PEMs and leads to an odd-even effect in thickness. The stronger swelling induces a decrease in refractive index and an increase in roughness. The bulk-odd-even effect only occurs in liquid water not in humid air. The surface-odd-even effect addresses only the roughness of the PEM and is only detectable in humid air.

The more rigid PEM system PSS/PAH with a linear growth behavior shows a rather different odd-even effect, which acts at the outer region of the PEM, while for PSS/PDADMAC the bulk-odd-even effect acts across the entire PEM and the surface-odd-even effect influences the PEM only at the surface.

Chapter 5

The Amount of Void Water at Low Relative Humidity

Abstract The change of void water and swelling water was studied more in detail. While the amount of swelling water increases continuously in dependence of the RH, the amount of void water does not change above 30% RH. Therefore, the RH region between 1% and 30% was investigated. The PEMs were measured at 1% RH, 6% RH, 12% RH and 23% RH, adjusted with respective salt solutions. In addition, the PEMs were measured in liquid D_2O to measure the maximum amount of void water and swelling water. The results showed that void water and swelling water increases paralelly. At 6% RH the voids were 60% filled. At 23% RH the amount of void water was nearly the same as in liquid D_2O. In this context measuring the amount of void water in dependence of the RH can be considered as an adsorption isotherm. The qualitative analysis of this adsorption isotherm indicates that, if the voids are considered as holes or pores, the void size should be about 0.3-0.9 nm.

5.1 Introduction

In the previous chapter the difference between swelling water and void water was investigated. The amount of swelling water inside PEMs increases continuously, while the amount of void water increases only between 1% RH and 30% RH. The region between 1% RH and 30% RH is investigated more in detail in this chapter.

For a long time only the swelling water, i.e. the water fraction which causes a change in PEM thickness, was considered in PEM swelling studies. The reason for this is that the most lab methods are only capable to determine changes in PEM thickness

caused by swelling.[93] NR measurements in liquid water allowed identifying a fraction of water which does not changes the thickness of PEMs.[22] With NR the change in thickness and SLD can be determined simultaneously. The SLD changes because the PEM is diluted by the surrounding water during the swelling process. Therefore, a mixed SLD is measured, which can be converted into water content. Usually, the amount of water determined by the SLD is higher as the amount calculated by the thickness.[93] This discrepancy is caused by the void water. For example, PSS/PAH PEMs build up in 0.1 M NaCl show about 12% void water, PSS/PDADMAC PEMs build up in 0.1 M NaCl about 5%.[22] The amount of void water depends on the density of the PEM, denser PEMs have more void water.

The concept of voids is rather theoretical; it is simply not known what voids really are. However, in the first instance it is reasonable to consider voids as pores. Then, PEMs can be treated as porous materials. In porous materials, usually the pore size is measured by recording the adsorption isotherm of a gas. In this context measuring the amount of void water in dependence of the RH can be considered as an adsorption isotherm. Löhman et al.[129] showed that the amount of void water increases only between 1% RH and 30% RH. Therefore, this region is most important to complete an adsorption isotherm for the amount of void water. For such low RH adjusting of RH by mixing streams of dry and humid nitrogen is not suitable anymore, because of the error margin about 2%-5% RH. Therefore, the RH is adjusted by the usage of saturated salt solutions; this method is less flexible but more accurate. The solved salt increases the chemical potential of the solution, i.e. it decreases the difference in chemical potential between water vapor and the solution. Therefore, equilibrium between water vapor and solution is achieved at lower water vapor pressure, i.e. a RH lower than 100% RH.

To measure the amount of void water at low RH, one PSS-terminated and one PDADMAC-terminated PEM are investigated by NR at 1% RH, 6% RH, 12% RH and 23% RH and in liquid D_2O. The RH is adjusted by saturated aqueous (D_2O) solutions of LiCl (6% RH), KCl (12% RH) and potassium acetate (23% RH).

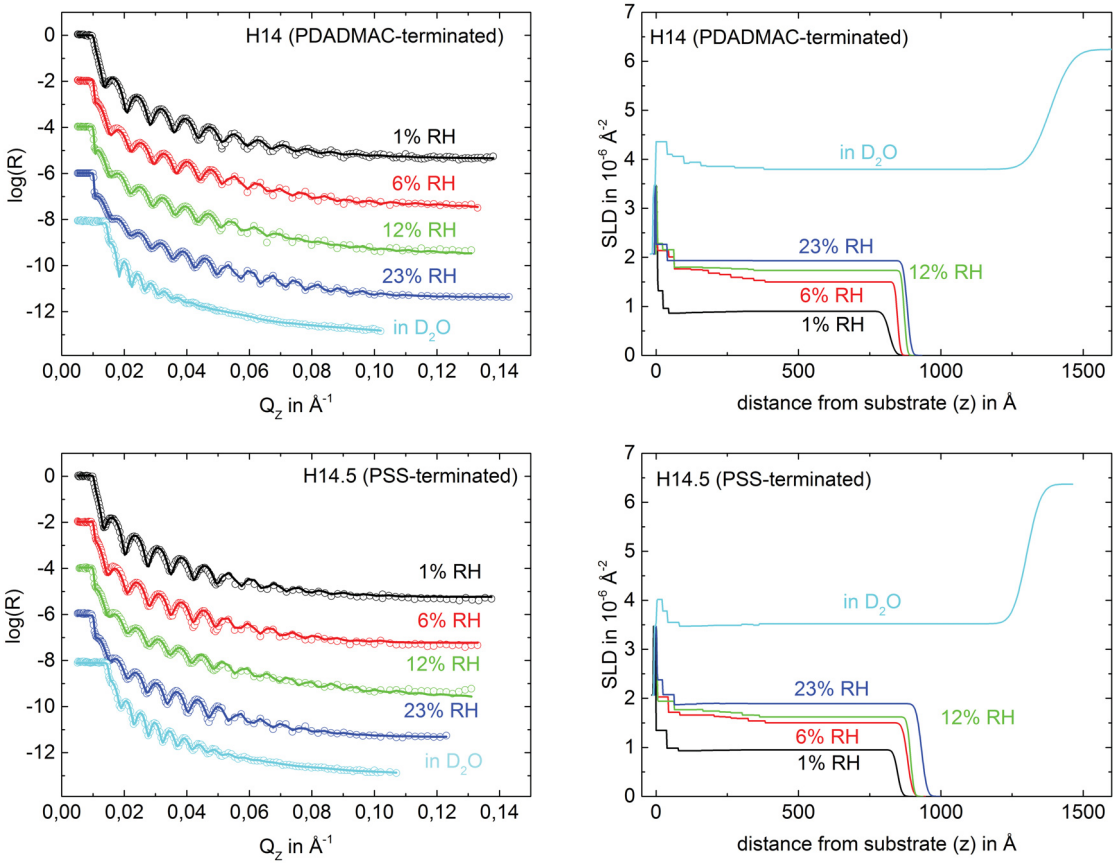

Figure 5.1: Neutron data (left) and SLD profile (right) of the samples H14 (left) and H14.5 (right) measured in 1% RH, 6% RH, 12% RH, 23% RH and in D_2O. The circles represent the measured data while the solid lines correspond to the data fit. For sake of clarity the reflectivity data were shifted by a value of -2 (log(0.01)), -4, -6 and -8.

5.2 Results

The PDADMAC-terminated PEM with 14 non-deuterated bilayers (H14)* and the PSS-terminated PEM with H14.5 were investigated by neutron reflectometry. To take density variations close to the substrate into account, an n-box model was chosen for the modeling of the data of the samples H14 and H14.5. Figure 5.1 shows the neutron reflectivity data and the corresponding fit of the data from the samples measured in humid air with 1% RH 6% RH 12% RH 23% RH and in liquid D_2O. The data fit is in good agreement with the measured data. Figure 5.1 shows the SLD profile

*In the following chapters partially deuterated PEMs are investigated. Therefore, the neutron reflectivity samples are named by the number of deuterated bilayers (Dx) and protonated bilayers (Hy), while half numbers indicate an additional layer of PSS on top (see chapter 3.2). For sake of uniformity the samples in this chapter are named by the same nomenclature.

corresponding to the fitted data. With increasing RH the thickness of the PEMs increases. The increase in thickness is rather small because of the small increase of RH. The SLD increases stronger between 1% RH and 6% RH, than between 6% RH and 12% RH and between 12% RH and 23% RH. The stronger increase in SLD between 1% RH and 6% RH indicates that the amount of void water increases stronger.

The calculation of swelling water and void water from neutron data is described in chapter 2.3.4 and briefly summarized in the following: The swelling water is calculated by:

$$\phi_{swell} = \frac{d_{swollen} - d_{dry}}{d_{swollen}} \tag{5.1}$$

where $d_{swollen}$ is the thickness at the respective RH (6% RH, 12% RH or 23% RH) or in D_2O and d_{dry} the thickness of the dried PEM (1% RH). For the amount of void water the polymer fraction x of the dried PEM have to be calculated according to:

$$x = \frac{SLD_{dry}}{SLD_{D_2O}} - \frac{SLD_{swollen} - \phi_{swell} SLD_{D_2O}}{(1 - \phi_{swell})(SLD_{D_2O})} + 1 \tag{5.2}$$

where SLD_{dry} is the SLD of the dried PEM (1% RH), $SLD_{swollen}$ is the SLD of the swollen PEM at 6% RH, 12% RH, 23% RH or in D_2O and SLD_{D_2O} the SLD of D_2O (6.36×10^{-6} Å^{-2}). By knowing the polymer fraction x the void water is calculated according to:

$$\phi_{void} = (1 - \phi_{swell})(1 - x) \tag{5.3}$$

The calculated amounts of void water and swelling water are summarized in figure 5.2. The amount of swelling water increases with increasing RH accordingly to the PEM swelling. Usually, the increase of swelling water in dependence of the RH can be divided into three regimes. Up to 40% RH the amount of swelling water increases strongly; between 40% RH and 60% RH the increase in swelling water flattens; above 60% RH the swelling water increases again strongly. The samples in this study were swollen up to 23% RH, therefore only the first regime with a strong swelling is detectable. A dependency between swelling water and the nature of the outermost layer is not detectable in humid air, but it is present in liquid D_2O. In liquid D_2O the PDADMAC-terminated PEM takes up 43% water, while the PSS-terminated PEM takes up 34% water. The amount of void water increases with the RH. It increases strongly between 1% RH and 6% RH. The increase in void water becomes weaker between 6% RH and 12% RH and 12% RH and 23% RH. At 23% RH the amount of

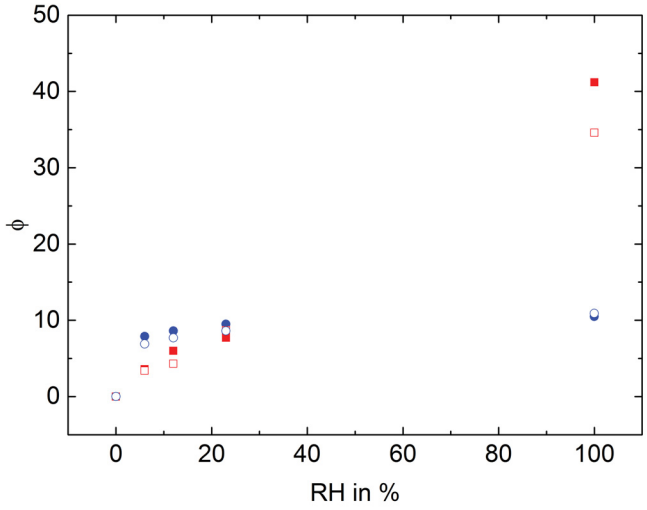

Figure 5.2: Squares represent the amount of swelling water (ϕ_{swell}) and circles the amount void water (ϕ_{voids}) in dependence of the RH and in liquid D_2O. Closed symbols represent the sample H14 (PDADMAC-terminated) Open symbols represent the sample H14.5 (PSS-terminated).

void water is nearly the same as in liquid D_2O.

5.3 Discussion

The void model was introduced to describe the discrepancy between the amount of water which causes an increase of PEM volume (swelling water) and the part of the absorbed water which does not causes a change in PEM thickness (void water). Anyway, in the first instance a comparison between PEMs with voids and porous materials is reasonable. Porous materials absorb water until the surface of the pores is completely covered with water molecules. At that point the pores are not completely filled with water. If the RH increased more, multilayers of water molecules are formed. An adsorption behavior like this can be described by either a BET or a Freundlich isotherm. Typical for such an isotherm is a fast increase in the beginning of the adsorption curve. The amount of absorbed water increases until a plateau is reached; this is the point when a monolayer is created. After that point the amount of absorbed water increases again. This transition can happen continuously (BET) or in a discontinuously way (Freundlich).

The adsorption of void water does not show such a behavior. The voids are filled quickly and a second increase after a plateau is not detected. This is typical for a simple

Langmuir-like isotherm, which not consider the possibility of forming a multilayer, i.e. inside the voids only a monolayer of water exists. Thus, the void size should not be bigger than the size of 1-3 water molecules. A pore covered with a monolayer of water is at least two water molecules thick, one water molecule on every side of the pore. Additionally, there is possible not with water filled "free space", which must be smaller than one water molecule. A pore size of 1-3 water molecules would be around 0.3-0.9 nm ($r_{H_2O} \approx 0.15$ nm) in diameter.[130] This size agrees with other studies. Jin et al. found pore sizes of 0.82 nm for PEM membranes consistent of PSS/PDADMAC and a pore size of 0.67 nm for membranes consistent of PSS/PAH. Vaca Chávez and Schönhoff determined with NMR a pore size of 1 nm for PSS/PAH PEMs.[131]

5.4 Conclusion

The amount of void water and swelling water at low RH was investigated. For this purpose a PSS-terminated PEM and a PDADMAC-terminated PEM was investigated at 1% RH 6% RH, 12% RH, 23% RH and in liquid D_2O with neutron reflectometry. The amount of void water and swelling water increases parallel with increasing RH. The amount of void water at 6% RH was already 60% of the maximum amount of void water. At 23% RH, the voids inside the PEM are nearly completely filled. The filling of the voids with increasing RH can be considered as an adsorption isotherm. From the adsorption isotherm a void size of around 0.3-0.9 nm is assumed. This small size indicates a distribution of void water over the entire PEM.

Chapter 6

Water Distribution inside Polyelectrolyte Multilayers

Abstract The uniformity of PEM swelling was investigated. For this purpose it was necessary to probe the internal structure of PEMs. In order to get insight into the internal structure, PEMs with a deuterated inner block close to the substrate and a non-deuterated outer block were prepared and investigated by neutron reflectometry (NR). The PEMs were measured in dried state, at 30% RH (D_2O vapor), 70% RH (D_2O vapor) and in liquid D_2O. Thus, it was possible to monitor the swelling behavior of the entire PEM, as well as the swelling behavior of the inner and outermost region. The analysis of the entire PEMs confirms the results of the measurements from chapter 4. An odd-even effect occurs. The PDADMAC-terminated PEM take up more water than the PSS-terminated PEM but only in liquid water. In humid air the odd-even effect is not detectable. Further, the amount of void water is constant above 30% RH and in liquid D_2O. From the scattering length density profiles a water distribution was calculated. The water distribution shows that in humid air the PEM swells uniformly, while in liquid D_2O the PEMs are most hydrated in the middle of the PEM. The effect is more pronounced for PDADMAC-terminated PEMs. Apparently, the non-uniform swelling in liquid water is related to the odd-even effect. The odd-even effect is caused by different amount of extrinsic binding sites inside PSS-terminated and PDADMAC-terminated PEMs. Therefore, it is possible that the non-uniform water distribution inside PEMs swollen in liquid water is related to the distributions of extrinsic binding sites inside the PEM. The extrinsic binding sites cause in liquid water an osmotic pressure which forces the PEM to uptake more water. This does not happen in humid air. Reasons for these differences in humid air and in liquid water are discussed.

6.1 Introduction

In the previous chapters the importance of the swelling behavior of PEMs was discussed. It was mentioned that three phenomena affect the swelling behavior: the uniformity of the swelling, the odd-even effect and the voids. The last chapter examined the role of voids inside PEMs and how they related to the odd-even effect. In this chapter the uniformity of the swelling is investigated. Especially, how the distribution of swelling water inside the PEM influences the odd-even effect and the amount of void water

The water distribution inside PSS/PDADMAC PEMs is unknown. In the past the majority of swelling studies addressed the average amount of water without any spatial resolution. However, some studies found hints for non-uniform swelling behavior. For example, PAH/PAA PEMs show a non-uniform water distribution.[36] De Vos et al.[37] found differences in the water distributions inside PSS/PAH PEMs under confining pressure. Furthermore, in PSS/PDADMAC PEMs hints for non-uniform contributions of extrinsic binding sites were found.[35] The amount of extrinsic binding sites strongly influences the amount of absorbed water. They induce an osmotic pressure which is balanced out by the PEM due to absorption of more water. There are also theoretical indications for a non-uniform swelling behavior. According to the three zone model[68] (see section 2.1.2) PEMs have a non-uniform structure. Consequently, a non-uniform water distribution is very likely. Additionally, the influence of the substrate on the PEM is obvious but not understood yet and could influence the swelling behavior.

Probing the water distribution inside PEMs is not trivial. While the investigations of the average structural changes of PEMs are possible with a high variety of methods (ellipsometry, QCM-D, x-ray reflectometry, etc.), the access to internal properties is rather difficult. The most powerful technique to probe internal properties of nanometer thick PEMs is Neutron Reflectometry.[36,73,97,99,132] NR determines the scattering length density profile across the PEM. In order to get information about the internal structure of the film, one can change the contrast by controlled deuteration of specific regions. In general there are two approaches to use deuteration. First, the fabrication of a super lattice structure due to periodic substitution of non-deuterated layers by deuterated layers.[37,97] If the distance between particular deuterated layers is constant, a bragg peak is detectable. Position and width of the peak give information about the uniformity of the PEM. The second method is the deuteration of an entire PEM block.[98,99] Especially, the properties of the interface between deuterated and non-deuterated block is of interest, but also changes in block sizes during swelling.

In this chapter the uniformity of PEM swelling behavior is investigated. For this purpose, two-block PEMs with an inner deuterated and an outermost non-deuterated part were investigated by neutron reflectometry. The deuterated and non-deuterated part is differently affected by swelling in 1% RH 30% RH 70% RH and in liquid D_2O. Additionally, the influence of the outermost layer is investigated, by using PEMs with different termination (either PSS- or PDADMAC-terminated PEMs). Thus, it is possible to investigate differences in swelling uniformity due to the odd-even effect.

6.2 Results

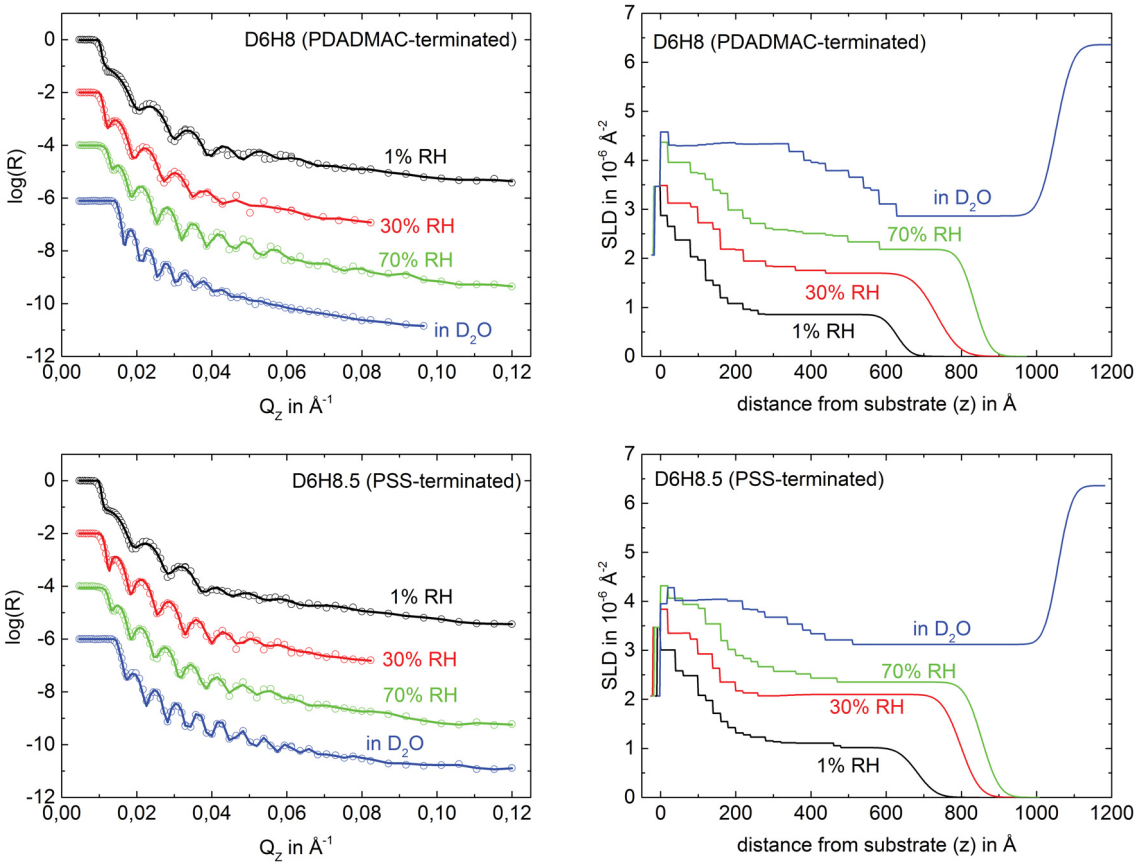

Figure 6.1: Reflectivity data (left) and SLD profile (right) of the PDADMAC-terminated PEM D6H8 (top) and the PSS-terminated PEM D6H8.5 (bottom) measured in 1% RH, 30% RH, 70% RH and in liquid D_2O. For sake of clarity the reflectivity data were shifted by a value of -2 (log(0.01)), -4 and -6.

The PDADMAC-terminated PEM with 6 deuterated bilayers and 8 non-deuterated bilayers (D6H8) and the PSS-terminated PEM with 6 deuterated bilayers and 8 non-

conditions	D6H8			
	$d_{NR}[nm]$	SLD [10^{-6} Å^{-2}]	ϕ_{swell}	ϕ_{void}
1%	63.8 ± 1	1.19 ± 0.03		
30%	73.5 ± 3	2.06 ± 0.1	0.13 ± 0.02	0.03 ± 0.01
70%	83.7 ± 1	2.70 ± 0.02	0.24 ± 0.03	0.04 ± 0.01
D_2O	121.0 ± 2	4.13 ± 0.1	0.47 ± 0.05	0.08 ± 0.02
conditions	D6H8.5			
	$d_{NR}[nm]$	SLD [10^{-6} Å^{-2}]	ϕ_{swell}	ϕ_{void}
1%	68.3 ± 1	1.42 ± 0.03		
30%	80.1 ± 3	2.32 ± 0.1	0.15 ± 0.02	0.03 ± 0.01
70%	85.6 ± 1	2.75 ± 0.02	0.20 ± 0.03	0.05 ± 0.01
D_2O	105.1 ± 2	3.42 ± 0.1	0.30 ± 0.05	0.04 ± 0.01

Table 6.1: Thickness (d_{NR}) and scattering length density (SLD), amount of swelling water (ϕ_{swell}) and void water (ϕ_{void}) of the samples D6H8 and D6H8.5 measured by neutron reflectometry. The samples were measured in nitrogen with 1% RH, 30% RH, 70% RH and in liquid D_2O.

deuterated bilayers (D6H8.5) were investigated by neutron reflectometry. The left hand site of figure 6.1 shows the neutron reflectivity data and the corresponding fit of the data for the samples D6H8 and D6H8.5 measured in humid air with 1% RH 30% RH 70% RH and in liquid D_2O. The different RH are produced by mixing dry nitrogen, with nitrogen which is bubbled through D_2O. The data fit is in good agreement with the measured data. The right hand site of figure 6.1 shows the SLD profile corresponding to the fitted data. In addition table 6.1 shows the thickness and average SLD of the entire PEM extracted from the SLD profiles. The thickness is calculated by adding the thickness of all boxes. The average SLD is determined by calculating the area under the SLD curve divided by the PEM thickness. From the extracted values for thickness and average SLD the amount of swelling water and void water according to eq. 2.5 and 2.6 (see chapter 5.2 or chapter 2.3.4) is calculated and also summarized in table 6.1.

The average structure of the PEMs The PSS-terminated sample D6H8.5 is in dry state (1% RH) slightly thicker than the PDADMAC-terminated samples D6H8 because of the additional layer. The average SLD of the PSS-terminated sample is slightly higher than the average SLD of the PDADMAC-terminated sample; this is because of a slightly higher PSS/PDADMAC ratio of the PSS-terminated sample and the fact that the SLD of PSS (SLD $\approx 2\times10^{-6}$ Å^{-2}) is higher than the SLD of PDADMAC (SLD $\approx 0.5\times10^{-6}$ Å^{-2}).

With increasing RH the thickness and the SLD of the PEMs increases. The reason is the incorporation of D_2O into the PEM due to the swelling process. For measurements carried out in humid air (30% RH and 70% RH) the increase of SLD and thickness does not differ significantly between the PSS-terminated and the PDADMAC-terminated sample. Furthermore, the amount of swelling water is the same within the error margin inside PSS- and PDADMAC-terminated PEMs, i.e. no odd-even effect is observable in humid air.

In liquid D_2O the thickness and SLD of the PDADMAC-terminated PEM increase stronger than the thickness and SLD of the PSS-terminated PEM. In addition, the amount of swelling water is higher inside the PDADMAC-terminated PEM. In opposite to the measurements in humid air, an odd-even effect is detectable in liquid D_2O.

The amount of void water is constant inside the error margin for all conditions and both samples, which is consistent with the results form chapter 4 and 5.

The shape of SLD profiles and the water distribution The measurements carried out in humid air (1% RH 30% RH and 70% RH) show SLD profiles with similar shape. The SLD decreases for 20-50 nm until the SLD reaches a constant value. With increasing RH, the absolute SLD increases but the shape of the profile does not change. In liquid D_2O the SLD profile changes. The inner block and outer block are well pronounced with an Gaussian-like roughness profile between both blocks. The inner block of the sample D6H8 is about 50 nm thick while the inner block of the sample D6H8.5 is about 30 nm thick. From the SLD profiles a roughly water distribution can be calculated. For this purpose the SLD profiles are normalized to the total thickness. Afterwards, the water profile is calculated by subtracting the normalized SLD profile of the dried PEM (1% RH) from the normalized SLD of the in 30% RH, 70% RH or D_2O swollen PEM. The left hand side of figure 6.2 shows the normalized SLD profiles of the samples D6H8 and D6H8.5. The right hand side of figure 6.2 presents the relative water profiles of the PEMs. The water profiles of PEMs swollen in humid air show a constant amount of water over the entire thickness of the PEM. The water is equally distributed.

The water profiles of PEMs swollen in D_2O show a non-uniform distribution. Close to the substrate the amount of water is low. The amount of water inside the PEM increases with increasing distance away from the substrate until a maximum value is reached. This maximum appears at about 30% of the normalized PEM thickness, for both the PSS- and the PDADMAC-terminated PEM. After the maximum, the amount of water decreases until a constant value is reached. This happens at 50% of

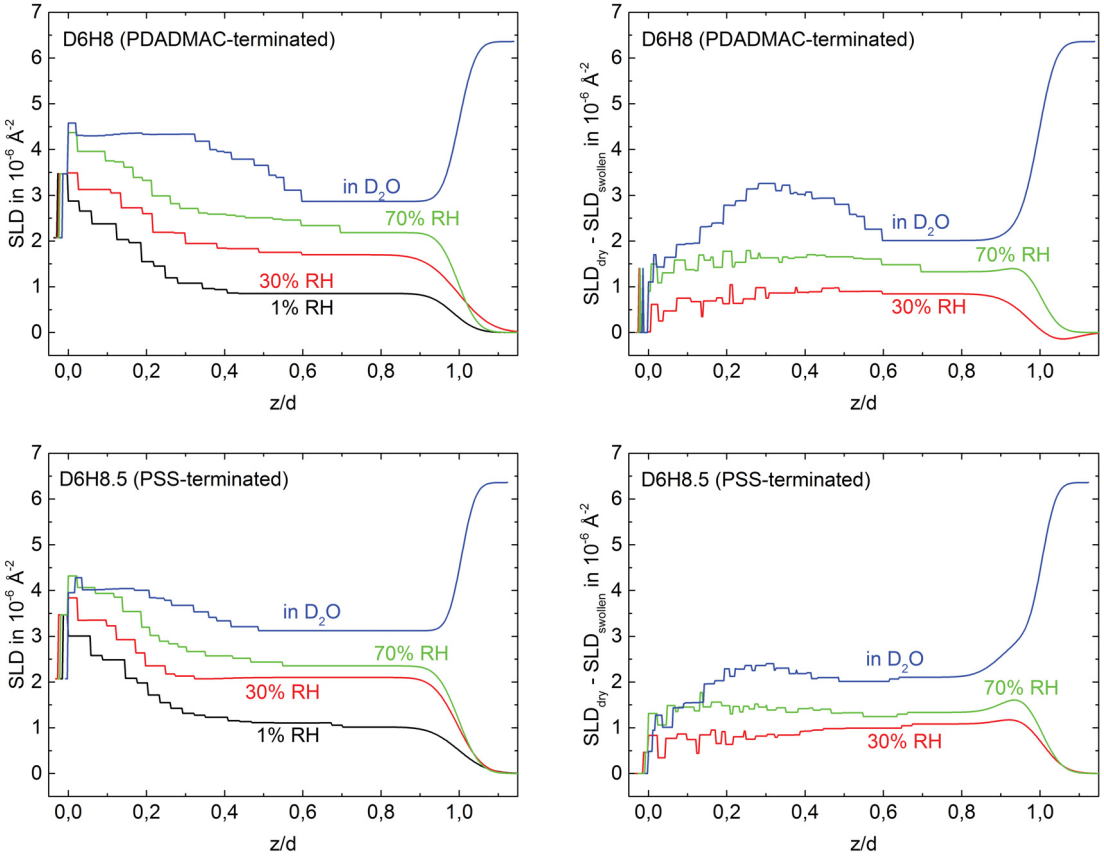

Figure 6.2: SLD profiles normalized to the total thickness d (left) and water profile calculated by subtracting the normalized SLD profile of the dried PEM (1% RH) from the SLD of the in 30% RH, 70%RH or D_2O swollen PEM of the samples D6H8 (top) and D6H8.5(bottom)

the PEM thickness for the PSS-terminated PEM and at 60% of the PEM thickness for the PDADMAC-terminated PEM. The shape of the water distribution is equally for the PSS- and the PDADMAC-terminated PEM but the relative amount of water inside the PDADMAC-terminated PEM is higher.

6.3 Discussion

The values of the average SLD and the PEM thickness are in agreement with the results of chapter 4. PSS/PDADMAC PEMs show an odd-even effect in liquid water but not in humid air. The results show that the PDADMAC-terminated PEM takes up more water than the PSS-terminated PEM in liquid water. For 30% RH and 70% RH no odd-even effect is detectable. The odd-even effect appears because of an excess

of PDADMAC inside PDADMAC-terminated PEM.[35] Due to the excess PDADMAC there is an additional amount of extrinsic binding sites. The extrinsic binding sites dissociate in water and induce an osmotic pressure, which is balanced out by a higher amount of absorbed water.

The maximum value of ϕ_{void} is reached at 30% RH at higher RH the amount of void water does not increase anymore. Further, ϕ_{void} is independent of the chemical nature of the outermost layer. This was also shown by Löhmann et al.[129]. They showed in ellipsometry measurements that the voids are completely filled at relative humidities higher than 30%.

The most prominent result of the NR measurements is the different shape in SLD profiles between PEMs measured in humid air and in liquid D_2O and the resulting differences in water distribution inside the PEMs. In humid air the PEM swells uniformly. The distribution of water inside the PEM is equally at 30% RH and at 70% RH.

The water distribution changes in liquid D_2O. The most water was present in the middle of the PEM. Close to the substrate the fewest amount of water was located. In the outer part of the PEM an intermediate amount of water was found. The differences in water distribution could be related to the density profile of the PEM. The region close to the substrate is assumed to be denser than the rest of the PEM. The reason is a restructuring of the polyelectrolyte chains during the preparation process.[68] A non-uniform water distribution could result from differences in PEM density. Anyway, this hypothesis is not valid in this case. A higher density close to the substrate should also affect the swelling behavior in humid air, which is not the case. However, the restructuring of the polyelectrolyte chains could have another consequence. Volodkin et al.[38] suggested that the PE-chains in the restructured zone are mainly intrinsically connected, while the outer diffusion zone has a high amount of extrinsic binding sites. As mentioned in the discussion about the odd-even effect (chapter 4.3) the presence of extrinsic binding sites increases the amount of absorbed water, but only in liquid water, not in humid air. Probably, just as the higher amount of extrinsic binding sites inside PDADMAC-terminated PEMs increases the amount of absorbed water in PDADMAC-terminated PEMs, the distribution of extrinsic binding sites inside the PEM could cause the non-uniform swelling observed in liquid D_2O. Thus, a lower amount of extrinsic binding sites inside the inner part of the PEM would cause the detected lower amount of water in this region. Further, the maximum amount of extrinsic binding sites must be located in the middle of the PEM, because in the middle of the PEM the amount of water is the highest. In the outer region of the

PEM must be less extrinsic binding sites than in the middle part but more than close to the substrate.

The question which arises is why the extrinsic binding sites have no influence in humid air. Extrinsic binding sites are compensated by small counter ions. The counter ions induce an osmotic pressure, which sucks in more water with increasing amount of extrinsic binding sites inside the PEM. Somehow, the osmotic pressure is only present when the PEM is immersed in water. The osmotic pressure correlates with the chemical potential, which is the same for liquid water and 100 % RH, i.e. there is no physical reason for the difference between PEM in 100% RH or immersed into liquid water. Thus, the chemical mechanism must be different. Apparently, in liquid water the PEM act like a separating membrane, the counter ions of extrinsic binding sites dissociate and can move at least partially through the PEM, but cannot leave the PEM, which induces the osmotic pressure. Probably, the dissociation of counter ions happens only if the PEM is immersed in liquid water, i.e. the properties of the water incorporated into the PEM somehow differ in humid air and in liquid water. A reason could be that the water absorbed in humid air is tightly bound and *immobile* like in hydrates. Thus, ions cannot dissolve in this tightly bound immobile water. If the PEM is immersed in liquid water there occur reservoirs of not bounded *mobile* water, counter ions close to these reservoirs can dissociate and are hydrated by the mobile water. The counter ions induce the mentioned osmotic pressure which causes the odd-even effect and the non-uniform water distribution.

Though, is the existence of chemically different types of water realistic? The chemical environment of both types of water should be different; the immobile water must be bound to the polymer while the mobile water is surrounded by other water molecules. Therefore, NMR measurements can distinguish between immobile water and mobile water in PEMs. Schwarz et al.[33] showed that the amount of *immobile* water inside PSS/PDADMAC PEMs is independent of the outermost layer. McCormic et al.[96] showed that the amount of *mobile* water inside PDADMAC-terminated PEMs is much higher than in PSS-terminated PEMs. Thus, PSS/PDADMAC PEMs swollen in liquid water show both, mobile and immobile water, but only the mobile water fraction is related to the odd-even effect in PSS/PDADMAC PEM, i.e. the osmotic pressure due to extrinsic binding sites is only induced if mobile water is present.

The assumption, that mobile and immobile water inside PEMs have an influence on the odd-even effect is supported by the findings of PSS/PAH PEM. The odd-even effect in PSS/PAH PEMs is visible both in humid air[29] and in liquid water[37]. Further, PSS/PAH PEMs are mainly intrinsically charge compensated. Thus, the

odd-even effect of PSS/PAH PEMs is not caused by extrinsic binding sites. NMR shows that the amount of immobile water differs strongly between PSS-terminated and PAH-terminated PEM.[33] Apparently, the odd-even effect of PSS/PAH PEMs is induced by immobile water. Therefore it is also detectable in humid air.

Differences in mobile water cause an odd-even effect only in liquid water, while differences in immobile water cause also an odd-even effect in humid air. The final question is, why show PSS/PAH PEMs differences in immobile water, while PSS/PDADMAC PEMs does not. One reason could be the differences in surface hydrophilicity. The differences in contact angle in dependence of the outermost layer are much higher in PSS/PAH PEMs than in PSS/PDADMAC PEMs. The contact angle of PSS/PDADMAC PEMs oscillate between 20° (PSS-terminated) and 30° (PDADMAC-terminated), while the contact angle of PSS/PAH PEMs oscillates between 20° (PSS-terminated) and 50° (PDADMAC-terminated).[74]

6.4 Conclusion

The effect of swelling on the internal and average structure of PEMs was investigated. Thereby, the result of the entire structure confirmed the results of the ellipsometry measurements from chapter 4. An odd-even effect occurs: the PDADMAC-terminated PEM take up more water than the PSS-terminated PEM but only in liquid water, the odd-even effect is not observable in humid air. In addition, the results of Löhman et al. could be confirmed. The amount of void water does not increase anymore after 30% RH.

The analysis of the internal structure reveals that in humid air the PEM swells uniformly. In liquid D_2O the water distribution changes completely. The most water is in the middle of the PEM. Close to the substrate less water is located. In the outermost zone an intermediate amount of water is located. The differences between swelling in humid air and in liquid water are assumed to be related to the mobility of the water. In humid air the absorbed water is strongly bound and immobile, while in liquid water additionally to the immobile water a fraction of mobile water is absorbed. Apparently, the amount of absorbed mobile water strongly correlates with the amount of extrinsic binding sites.

With regard of practical application it is important to know that swelling behavior significant differs between PEMs swollen in humid air and in liquid water. Because of the same chemical potential of liquid water and with water saturated air it is usually assumed that the swelling behavior should be the same. This is obviously not the case

Chapter 7

The Effect of Temperature Treatment on the Swelling Behavior of Polyelectrolyte Multilayers *

Abstract This chapter addresses the effect of thermal treatment on the internal structure of polyelectrolyte multilayers. Especially, on the swelling behavior in general and the water distribution, odd-even effect and void water in particular. In order to get insight into the internal structure of PEMs neutron reflectometry was used. PEMs with a deuterated inner block towards the substrate and a non-deuterated outer block were prepared and measured in 1% RH and in D_2O before and after a thermal treatment. Complementarily, PEMs with the same number of layers but completely non-deuterated were investigated by ellipsometry. The analysis of the overall thickness, the average scattering length density and the refractive index indicate a degradation of the PEM. The loss in material is independent of the number of layers, i.e. only a constant part of the PEM is affected by degradation. The analysis of the internal structure revealed a more complex influence of thermal treatment on PEM structure. Only the outermost part of the PEM degenerates, while the inner part becomes denser during the thermal treatment. Also the swelling behavior of PEMs is influenced by the thermal treatment. The untreated PEM shows a well pronounced odd-even effect, i.e. PDADMAC-terminated PEMs take up more water than PSS-terminated PEMs. After the thermal treatment the odd-even effect becomes much weaker.

*Similar content was published in Zerball, M.; Laschewsky, A.; Köhler R.; von Klitzing, R. The Effect of Temperature Treatment on the Structure of Polyelectrolyte Multilayers. Polymers 2016, 8(4), 120

7.1 Introduction

The previous chapters showed how water distribution, odd-even effect and void water affect the swelling behavior of PEMs and each other. In this chapter the effect of a thermal treatment on the swelling behavior is investigated. The properties of PEMs can be affected by temperature treatment during[19,20,64,80,133] or after[26,27,106,107] the PEM preparation. In general, an increased temperature during PEM preparation increases the thickness increment per PE layer and extends the non-linear growing phase of non-linearly growing PEMs.[20,80] In addition, linearly growing PEM systems can be forced to a non-linear growth. The increase in temperature changes the balance between polyion-polyion and polyion-counterion interaction and increases the probability of polymer transport to the surface. The effect of thermal treatment after preparation is interesting for possible PEM containing devices, e.g., for devices designed for high operation temperatures. Furthermore, the understanding of the reaction of PEMs on thermal stress helps to better understand their nature.

The effect of temperature on PEMs was intensively investigated for microcapsules.[26,27,28] During the heating of PSS/PDADMAC microcapsules to temperatures over 65°C PSS-terminated capsules shrink, while PDADMAC-terminated capsules swell until they rupture. The different behavior of PSS-terminated and PDADMAC-terminated capsules was attributed to the different ratio of positive and negative charges inside the PEM capsules. The PDADMAC-terminated PEM capsules take up more water during heating to increase the distance between charges, while the more charge balanced PSS-terminated PEM capsules minimize the polymer water surface. Unfortunately, the behavior of PEM microcapsules can not be transferred readily to PEMs attached on a solid substrate. Due to the fixation on the substrate, the PEMs are less flexible, provide a smaller surface and are sterically hindered. Microcapsules can respond with changes in wall thickness and changes in capsule diameter, while a PEM attached on a solid substrate can only react by changes in thickness. Furthermore, the influence of the substrate itself on the PEM is obvious but not understood yet. QCM-D measurements show an increasing swelling of PEMs with increasing temperature, but a rupturing was not reported.[106] For non-linearly growing PSS/PDADMAC PEMs (prepared at ionic strength >0.1 mol/L) a glass transition temperature at about 50°C was determined. Linearly growing PSS/PDADMAC PEMs (prepared without salt) did not show any transition up to 110°C.[106] Neutron reflectometry measurements after a thermal treatment revealed annealing effects related to a loss in swelling, which was detectable by a decrease in roughness and scattering length density.[107]

Temperature studies indicate a restructuring of the PEM.[26,27,28,107,134,135,136] The question arises whether the structure across the PEM perpendicular to the PEM surface changes during thermal treatment. While investigation of the average structure of PEMs is well established with a high variety of methods (ellipsometry, QCM-D, X-ray reflectometry, etc.), the access to internal properties is rather difficult. One powerful technique to probe internal properties is Neutron Reflectometry.[36,97] NR determines the scattering length density profile across the PEM. In order to get information about the internal structure of the film, one can change the contrast by controlled deuteration of the specific region, i.e., a specific block.[37,39,99,132,133] Hence, different contrasts inside PEMs can be achieved without changing their chemical behavior. Thus, the effect of a thermal treatment on the internal structure can be traced by measuring the changes in thickness, SLD and roughness of the deuterated and non-deuterated block.

Complementary to neutron reflectometry, ellipsometry was used to investigate effects on thickness and refractive index before, after and during the temperature treatment. Non-linearly growing PSS/PDADMAC PEMs of two different thicknesses are studied. In this context, thin refers to PEMs with 20 and 21 single layers while thick refers to PEMs with 36 and 37 single layers. In addition, the effect of thermal treatment is studied in dependence of polyion type (PSS or PDADMAC) of the outermost layer.

7.2 Results

7.2.1 The Effect of Thermal Treatment on the Average Structure of PEMs

Table 7.1 shows the results of ellipsometric and neutron reflectometric measurements. The PEMs were measured in dried nitrogen (1% RH) and in water (H_2O for ellipsometry and D_2O for NR), before (b.t.) and after (a.t.) the thermal treatment. The neutron reflectivity curves are discussed in detail in the next section. Although ellipsometry and neutron reflectometry were carried out with different samples, the measured thicknesses are in good agreement within the expected error. At 1% RH, the thick PEMs (36/37 layers) are thicker than the thin PEMs (20/21 layers). Furthermore, the PSS-terminated samples are slightly thicker than the PDADMAC-terminated ones because of the additional layer. The refractive index of all samples is the same, which indicates a similar density of all samples. The average SLD of the PSS-terminated samples is slightly higher than the average SLD of the PDADMAC-terminated samples; this

conditions	20 layers			
	d_{elli} [nm]	n_{elli}	$d_{NR}[nm]$	SLD_{NR} [10^{-6} Å^2]
1 % b.t.	31 ± 1	1.54 ± 0.01	32.8 ± 0.7	1.55 ± 0.03
water b.t.	55 ± 3	1.468 ± 0.005	56.6 ± 0.9	3.6 ± 0.1
1 % a.t.	29 ± 1	1.52 ± 0.01	24.9 ± 0.5	1.13 ± 0.02
water a.t.	53 ± 2	1.462 ± 0.004	54.1 ± 0.8	3.9 ± 0.1
conditions	21 layers			
	d_{elli} [nm]	n_{elli}	$d_{NR}[nm]$	SLD_{NR} [10^{-6} Å^2]
1 % b.t.	37 ± 1	1.55 ± 0.01	40.0 ± 0.8	1.71 ± 0.04
water b.t.	60 ± 3	1.488 ± 0.004	59.8 ± 0.9	3.3 ± 0.1
1 % a.t.	34 ± 1	1.52 ± 0.01	31.2 ± 0.6	1.12 ± 0.02
water a.t.	59 ± 3	1.472 ± 0.003	60.6 ± 0.9	3.7 ± 0.1
conditions	36 layers			
	d_{elli} [nm]	n_{elli}	$d_{NR}[nm]$	SLD_{NR} [10^{-6} Å^2]
1 % b.t.	92 ± 4	1.553 ± 0.003	90 ± 2	1.11 ± 0.02
water b.t.	164 ± 6	1.470 ± 0.002	174 ± 4	4.02 ± 0.07
1 % a.t.	89 ± 4	1.544 ± 0.003	79 ± 2	0.97 ± 0.02
water a.t.	142 ± 5	1.486 ± 0.002	136 ± 3	3.47 ± 0.08
conditions	37 layers			
	d_{elli} [nm]	n_{elli}	$d_{NR}[nm]$	SLD_{NR} [10^{-6} Å^2]
1 % b.t.	94 ± 3	1.559 ± 0.002	105 ± 3	1.21 ± 0.02
water b.t.	154 ± 4	1.483 ± 0.001	165 ± 5	3.3 ± 0.1
1 % a.t.	91 ± 3	1.553 ± 0.001	94 ± 2	1.06 ± 0.02
water a.t.	147 ± 4	1.488 ± 0.001	162 ± 5	3.2 ± 0.1

Table 7.1: Thickness (d), refractive index (n) and scattering length density (SLD) of the samples measured by ellipsometry and neutron reflectometry. The samples were measured in dried nitrogen (1% RH) and in water (H_2O for ellipsometry and D_2O for NR) before (b.t.) and after (a.t.) the temperature treatment.

is because of a slightly higher PSS/PDADMAC ratio of the PSS-terminated samples and the fact that the SLD of PSS (SLD $\approx 2\times10^{-6}$ Å^{-2}) is higher than the SLD of PDADMAC (SLD $\approx 0.5\times10^{-6}$ Å^{-2}). The average SLD of the thin PEMs is higher than the one of the thick PEMs because of the relative larger amount of deuterated layers.

After the thermal treatment, thickness, refractive index and SLD of all samples decrease in 1% RH. A decrease in SLD and refractive index is typical for a decreased density. If accompanied with a decreased thickness, a decreased density indicates a loss of material. The absolute decrease in thickness caused by the thermal treatment is the same for all samples, i.e., irrespective of the type of outermost layer and the number of layers. According to the NR data, the absolute loss in thickness is about 9 nm for all

samples. The ellipsometric data also show constant though lower decreased thickness of about 3 nm after the thermal treatment. Obviously, the thermal treatment affects only a constant outermost part of the PEM.

Complementary to the measurements at 1% RH, the PEMs were investigated in water (H_2O for ellipsometry and D_2O for NR) before and after the thermal treatment. Before the thermal treatment, the PEMs swell as shown in the last chapters. The thickness of the PDADMAC-terminated PEMs increases more as the thickness of the PSS-terminated PEMs, the refractive index behaves oppositely, i.e., the PDADMAC-terminated PEMs takes up more water than the PSS-terminated PEMs. This phenomenon is called odd-even effect, and it is intensively discussed in literature.[29,33,35,96,137] The values for thickness and refractive index in dried and swollen state are in good agreement with the results from chapter 4.

The discussion about the swollen PEMs after the thermal treatment has to be distinguished between thin (20/21 layers) and thick (36/37 layers) PEMs. The swollen thin PEMs show after the thermal treatment a slightly lower thickness than before the thermal treatment. The average SLD of the thin samples measured in D_2O is higher after the thermal treatment than before, while the refractive index behaves the opposite. Both indicate a higher water uptake and consequently lower density of the PEM. The lower density together with the slightly lower thickness indicate a loss of material, which is in agreement with the results from the measurement in 1% RH.

The swollen thick PEMs exhibit a lower thickness after thermal treatment. In opposition to the thin samples, the average SLD of the swollen thick PEMs decreases after the thermal treatment, while the refractive index increases. The decreased thickness together with the decrease of the average SLD, and the increase of the refractive index indicate an increased density. The change in average SLD and refractive index is much more pronounced for the thick PDADMAC-terminated sample. In contrast, dried PEMs behave oppositely, the change in thickness, SLD and refractive index indicate decreases in density during the thermal treatment.

For a better understanding of the swelling process, a more detailed examination of the swelling behavior before and after the thermal treatment is necessary. The total amount of water, which is absorbed by a PEM during the swelling process is separated into swelling water and void water. Swelling water increases the thickness of the PEM, void water does not influence the thickness but the SLD of the PEM. The neutron data are used to calculate the swelling water and void water of the PEMs in the following manner:

The swelling water is calculated by:

conditions	20 layers		21 layers	
	ϕ_{swell}	ϕ_{void}	ϕ_{swell}	ϕ_{void}
D_2O b.t.	0.42 ± 0.04	0.02 ± 0.01	0.33 ± 0.04	0.03 ± 0.01
D_2O a.t.	0.54 ± 0.05	0.00 ± 0.01	0.48 ± 0.04	0.01 ± 0.01
conditions	36 layers		37 layers	
	ϕ_{swell}	ϕ_{void}	ϕ_{swell}	ϕ_{void}
D_2O b.t.	0.48 ± 0.04	0.06 ± 0.01	0.38 ± 0.04	0.03 ± 0.01
D_2O a.t.	0.42 ± 0.05	0.03 ± 0.01	0.42 ± 0.04	0.00 ± 0.01

Table 7.2: The swelling water (ϕ_{swell}) and void water (ϕ_{swell}) before (b.t.) and after (a.t.) thermal treatment, calculated from d_{NR} and SLD.

$$\phi_{swell} = \frac{d_{swollen} - d_{dry}}{d_{swollen}} \tag{7.1}$$

where $d_{swollen}$ is the thickness in D_2O and d_{dry} the thickness of the dried PEM. According to previous publications[22,93,137,138], the amount of void water depends on the polymer fraction x of the dried PEM, which is calculated in the following manner:

$$x = \frac{SLD_{dry}}{SLD_{D_2O}} - \frac{SLD_{swollen} - \phi_{swell} SLD_{D_2O}}{(1 - \phi_{swell})(SLD_{D_2O})} + 1 \tag{7.2}$$

where SLD_{dry} is the SLD of the dried PEM, $SLD_{swollen}$ is the SLD of the swollen PEM and SLD_{D_2O} the SLD of D_2O (6.36×10^{-6} Å^{-2}). The model assumes that the dry PEM has a volume ratio of voids $(1 - x)$ which is filled with vacuum. Due to the fact that the PEM swells by ϕ_{swell}, the volume ratio of the voids ϕ_{void} decreases by factor $(1 - \phi_{swell})$. Hence, the amount of void water inside the swollen PEM is calculated by:

$$\phi_{void} = (1 - \phi_{swell})(1 - x) \tag{7.3}$$

The role of void water inside PEMs was recently reviewed.[93] Furthermore, a method to calculate the amount of void water from ellipsometry data was recently reported.[137] Because of the low number of individual samples and the lower accuracy of void water calculated from ellipsometry data, void water and swelling water are only calculated from NR data in this study.

Table 7.2 shows the swelling water and void water of the investigated PEMs calculated from NR data. As already mentioned, the water content in PDADMAC-terminated PEMs is higher as in PSS-terminated PEMs. The amount of void water before the thermal treatment agrees with previous studies.[22,137] After the thermal

treatment the water content of the thin samples increases strongly in comparison to the water content before the thermal treatment. Furthermore, the amount of void water decreases, but the difference is within the error margin. The strong increase in absorbed water indicates a lower density of the PEMs. Furthermore, the difference in swelling water between the thin PDADMAC-terminated PEM and the PSS-terminated PEM decreases from 9% before the thermal treatment to 5% after the thermal treatment, which indicates a weaker odd-even effect between the thin PDADMAC-terminated and PSS-terminated PEMs. The effect of the thermal treatment on the amount of swelling water inside the thick PEMs is less pronounced than for the thin PEMs. The water content of the thick PSS-terminated PEM is constant within the error margin, while the water content of the thick PDADMAC-terminated PEM decreases after the thermal treatment. The amount of void water decreases for both the PSS-terminated and the PDADMAC-terminated PEM. In addition, the differences in swelling water between the thick PDADMAC-terminated PEM and the PSS-terminated PEM decreases to zero, which indicates a vanishing of the odd-even effect between the thick PDADMAC-terminated and PSS-terminated PEMs. The effect of the thermal treatment on the odd-even effect is discussed later in detail.

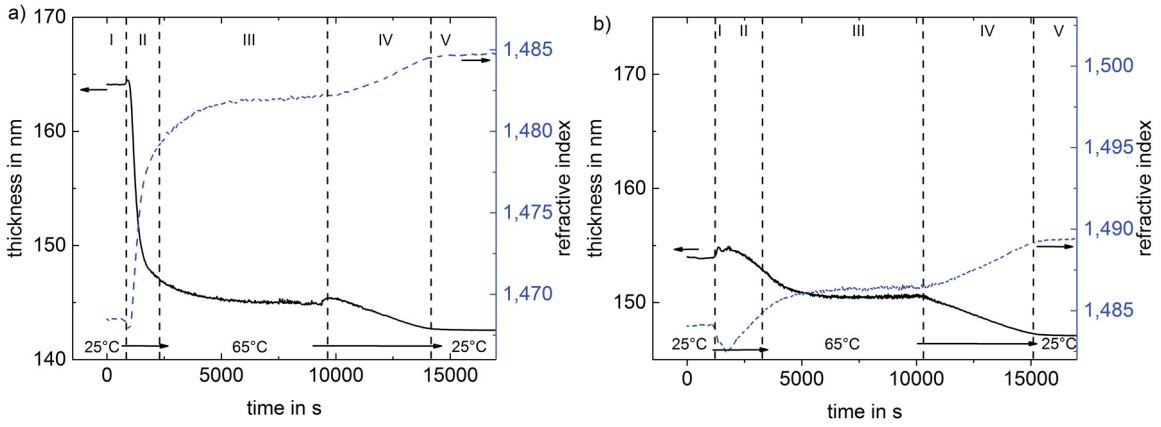

Figure 7.1: Change of thickness and refractive index over time during the temperature treatment measured by ellipsometrie of samples with a) 36 layers and b) 37 layers. The measurement began at 25°C then the temperature was increased to 65°C where it persists for 2h. Then the temperature was decreased back to 25°C

Due to the speed of a single ellipsometry measurement, it is possible to carry out kinetic measurements of PEMs during the temperature treatment. Figure 7.1 shows exemplary the change of thickness and refractive index over time during the temperature treatment of the two thick samples swollen in water. The measurements are divided into five phases: (I) starting phase at 25°C; (II) heating phase with increasing

temperature up to 65°C; (III) constant temperature phase for 2 h at 65°C; (IV) cooling phase with decreasing temperature down to 25°C; (V) final phase with constant 25°C.

For each constant temperature regime (phase I, III, V), a plateau value for both thickness and refractive index is reached. From 25°C to 65°C, the refractive index increases and the thickness decreases. After cooling down to 25°C, the thickness further decreases and the refractive index increases. The described changes in thickness and refractive index due to thermal treatment are independent of the outermost layer. Nevertheless, the change is more pronounced for the PDADMAC-terminated PEM. Therefore, the difference in swelling water between PSS-terminated and PDADMAC-terminated PEMs is after the temperature treatment less than before. The changes in thickness and refractive index are monotonous during cooling, while they are non-monotonous during heating. The over/undershoot of thickness and refractive index indicate a short term swelling of the PEM after starting to heat, which is more pronounced for the 37 layers thick PEM.

In summary, the measurements of the average structure of the PEMs show that both thickness and refractive index of dried samples is decreased after thermal treatment, what indicates degradation. Obviously, the degradation affects only a constant outermost part of the PEM. Therefore, the thin PEMs are more strongly affected from the relative loss of thickness by the thermal treatment, which is detectable by a stronger relative decrease in thickness, refractive index and SLD. Furthermore, the amount of swelling water strongly increases the thermal treatment. The thick samples are relatively less affected by the degradation. Furthermore, the thick samples show hints of a PEM densification. In the swollen state, the refractive index increases and SLD decreases. An additional hint for densification of the samples is given by the decreased amount of void water after the thermal treatment. Obviously, both loss in material and densification takes place during thermal treatment, and the whole process of thermal treatment is more complex as previously studies described.[26,107] It is assumed that densification and degradation take place in different regions of the PEM.

7.2.2 The Effect of Thermal Treatment on the Internal Structure of PEMs

Figure 7.2 shows the NR data fitted by an n-box model (between 20 and 40 boxes) of the thin samples D6H4, D6H4.5 and of the thick samples D6H12 and D6H12.5 measured at 1% RH and in D_2O before and after thermal treatment. Figure 7.3 shows the resulting SLD profiles of the measured samples. For better comparability to the

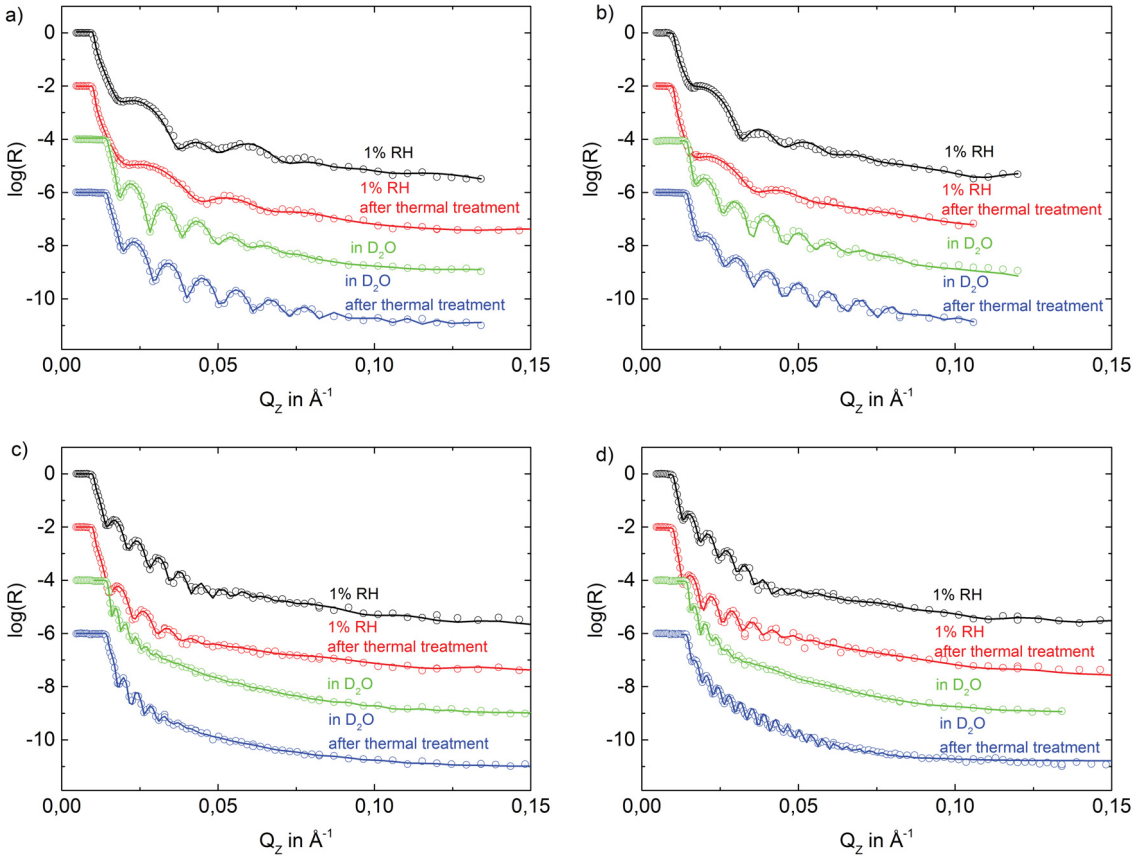

Figure 7.2: Neutron data of a) D6H4, b) D6H4.5 c) D6H12 and d) D6H12.5. The circles represent the measured data while the solid lines correspond to data fit. For sake of clarity the data were shifted by a value of -2 (log(0.01)), -4 and -6.

ellipsometric data, the SiO_x/PEM interface is defined as $z = 0$. The measurements carried out in 1% RH show the expected SLD profile, with a higher SLD of the inner block and a lower SLD of the outermost block. Furthermore, the PEMs show nearly the same roughness in dried nitrogen, i.e., there is no roughness odd-even effect as recently observed.[137] After the thermal treatment, the samples D6H12 and D6H12.5 show in 1% RH nearly the same roughness as before the treatment. In contrast, the samples D6H4 and D6H4.5 show after the thermal treatment a higher roughness than before the thermal treatment. The samples D6H4 and D6H4.5 are also the more degraded samples. Apparently, the strong degradation increases the roughness of dried PEMs. The measurements in D_2O show that before the thermal treatment, the roughness of the PEMs increases due to the swelling. More water is absorbed by the PDADMAC-terminated PEMs than by the PSS-terminated PEMs. Consequently, the roughness of PDADMAC-terminated PEMs also increases more strongly during swelling. After the

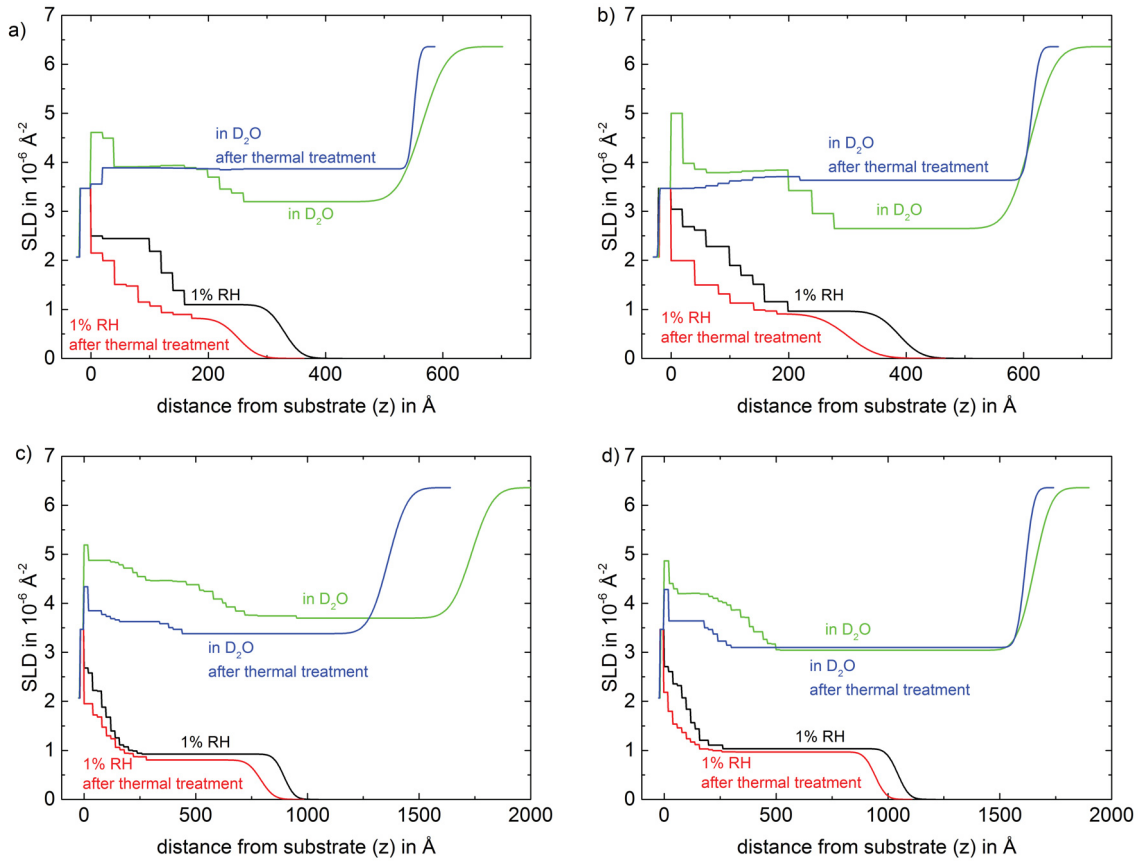

Figure 7.3: SLD profiles of a) D6H4, b) D6H4.5 c) D6H12 and d) D6H12.5 according to the fitted reflectivity data shown in figure 7.2.

thermal treatment, the roughness measured in D_2O decreases for all samples i.e., the thermal treatment causes a smoothening of the surface. A smoothening of the surface is an indication for a densification of the PEMs.

For easier comparison of the different blocks, the distance z from substrate was normalized to the total thickness of the respective PEM d (Figure 7.4), which corresponds to the total PEM thickness shown in Table 7.1. After the thermal treatment of all PEMs, the block structure is still observable in 1% RH, although less pronounced than before the thermal treatment. The effect is more pronounced for the thin PEMs D6H4 and D6H4.5 than for the thick PEMs D6H12 and D6H12.5. Apparently, the deuterated part of the PEM mixes with the non-deuterated part of the PEM at least partially. Furthermore, the average SLD decreases, which suggests a loss of material.

The discussion of the effect of thermal treatment on swollen PEMs has to distinguish between thin and thick PEMs. Surprisingly, the block structure of thin PEMs is not observable after the thermal treatment. In comparison to the measurement

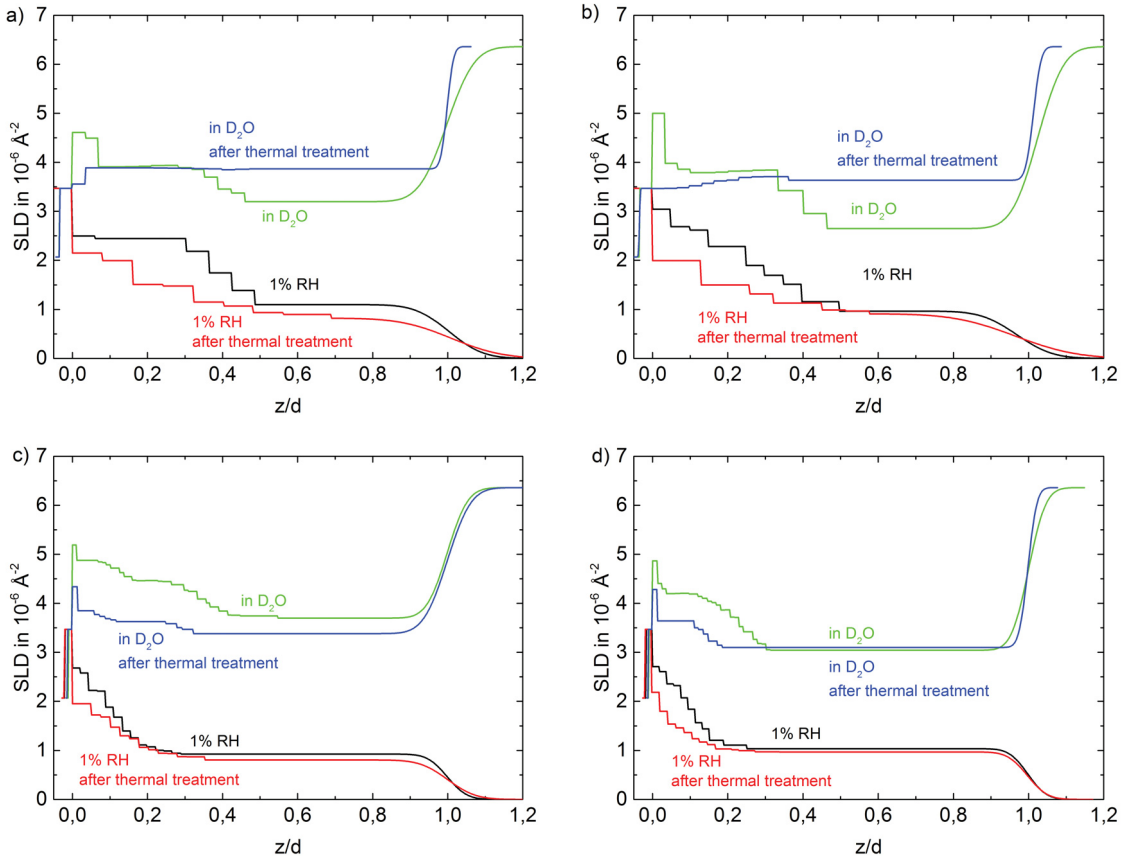

Figure 7.4: SLD profiles normalized to the total thickness d of a) D6H4, b) D6H4.5 c) D6H12 and d) D6H12.5

in D_2O before the thermal treatment, the average SLD of the inner block decreases slightly while the SLD of the outer block increases. In respect to the dried PEMs, the increase in SLD due to swelling increases of the outermost block but decreases of the innermost block after the thermal treatment, i.e., the inner block swells less than the outermost block. Consequently, it is assumed that the temperature affects the inner and outermost part differently, whereas the term "part" is used in a general case and does not necessarily match our block size. The treatment increases the density of the inner part, while the density of outer part decreases due to degradation.

The swollen thick PEMs preserve the block structure after the thermal treatment but much less pronounced than before the thermal treatment. The outermost block of the PSS-terminated PEM shows after the thermal treatment a slightly higher SLD than before the thermal treatment, while the SLD of the inner block decreases after the thermal treatment. The outermost block of the PDADMAC-terminated PEM shows, after the thermal treatment, a slightly lower SLD than before the thermal treatment,

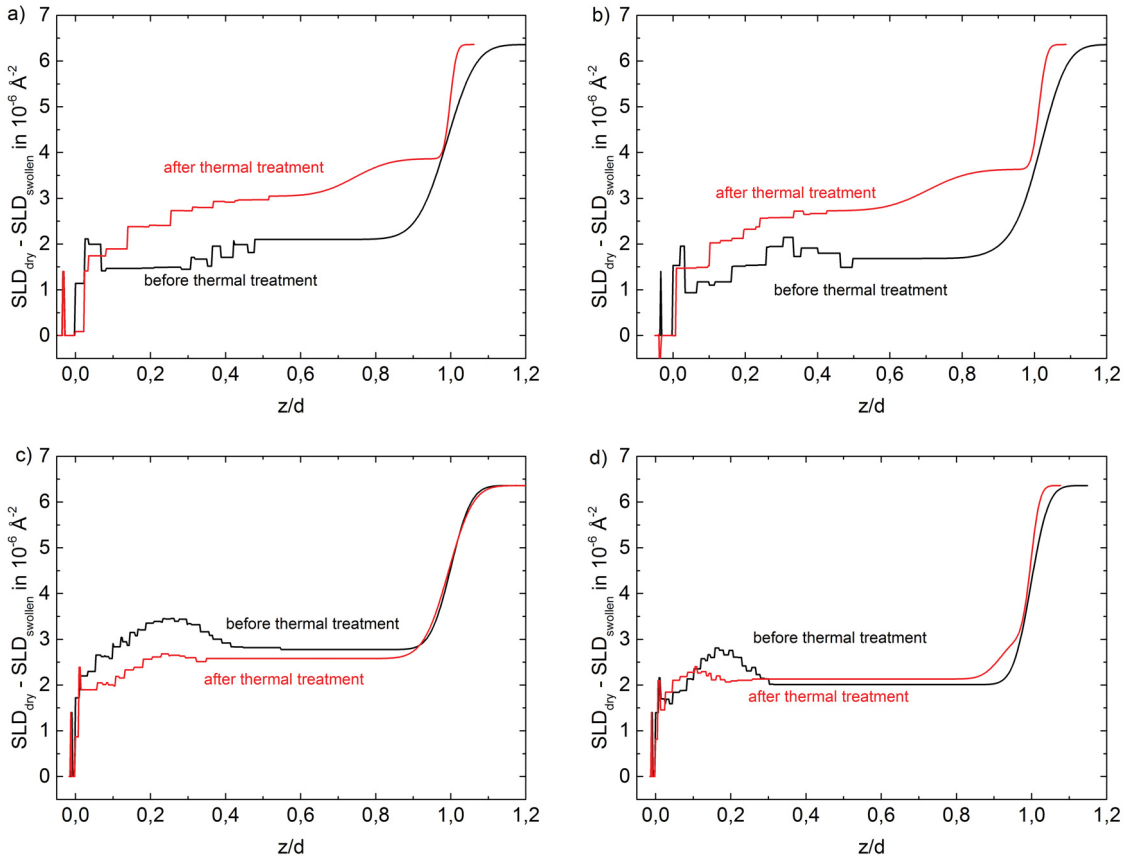

Figure 7.5: Water profile calculated by subtracting the normalized SLD profile of the dried PEM (1%RH) from the SLD of in D_2O swollen PEMs of the samples a) D6H4, b) D6H45, c) D6H12, d) D6H12.5

while the SLD of the innermost block decreases strongly due to the thermal treatment. In both cases, the SLD difference between the inner and outer block decreases in comparison to the measurement in D_2O of the non-treated PEMs. This is also because of densification of the inner part and degradation of the outermost part of the PEMs.

Figure 7.5 shows the water profile of the samples calculated by subtracting the normalized SLD profile of the dried PEMs from the normalized SLD profile of in D_2O swollen PEMs, for the measurements before the thermal treatment and after the thermal treatment. Before the thermal treatment, the thin samples show less water close to the substrate. The amount of water increases until a constant value is reached. In opposite to the thicker samples discussed in chapter 6 (D6H8 and D6H8.5) the samples D6H4 and D6H4.5 does not show the most water in the middle of the PEM. After the thermal treatment the amount of water inside the thin samples increases. This indicates a less compact PEM structure due to the degradation of the PEM.

The thick samples D6H12 and D6H12.5 show before the thermal treatment the most water in the middle of the PEM, and the least water close to the substrate. This is similar to the samples D6H8 and D6H8.5 from chapter 6. After the thermal treatment both samples show a more equal water distribution. There is still less water close to the substrate but in the middle of the PEM is no additional water. The reason for the change in water distribution could be a change in the amount and distribution of extrinsic binding sites inside the PEM.

7.3 Discussion

7.3.1 Destruction and Densification of the PEMs

The analysis of the average PEM structure indicates that two processes affect the PEMs during temperature treatment, degradation and densification. The analysis of the internal PEM structure indicates a partial degradation of the outermost part of the PEM and densification of the inner part.

The degradation of the PEM is indicated by the fact that the average SLD, refractive index and thickness of the PEMs measured in dried state decrease after the thermal treatment. Furthermore, it was concluded that the degradation affects only the outermost part of the PEM, which is detectable by two observations. First, the absolute loss in thickness is about 9 nm for all samples independent of the number of layers and the type of the outermost layer. Furthermore, the refractive index decreases at the same time, which is a clear hint for material loss. Kinetic ellipsometry measurements show that the thickness and refractive index of the PEMs reach a constant value during the constant temperature regime of 65°C, i.e., the equilibrium is reached. Second, the neutron data show that mainly the outermost block of the partially deuterated PEMs is affected by degradation. The analysis of the SLD shows that thermal treatment causes a stronger swelling of the outer block than of the inner block. To summarize, these results indicate a degradation of the outer zone of all PEM.

The densification is indicated by a decrease of SLD and an increase of refractive index of the thick swollen PEMs after the thermal treatment, which indicates a lower amount of absorbed water and consequently a higher density. It is concluded for all samples that the densification affects mainly the inner part of the PEMs, which is detectable by a stronger swelling of the outer block in comparison to the inner block after the thermal treatment. In addition, the partial mixing of the deuterated and

non-deuterated block provides an indirect indication for densification. Densification presupposes an increased mobility of PE chains so that the PE chains can arrange into a more compact conformation. In addition, earlier studies reported densification of PEMs.[107] Steitz et al. heated PSS/PDADMAC PEMs up to 40°C. The PEMs showed lower SLD in D_2O and a decreased roughness but no degradation of the PEM took place. Apparently, degradation of the PEM only appears above a critical temperature, while densification always takes place. In the present study, the PEMs were heated up to 65°C, which is obviously high enough to cause degradation. An effect of the temperature on the amount of absorbed water was also detected for PLL/case in PEMs.[139]

The degradation of a constant outermost part suggests a correlation with the type of growth. Most of the PEMs initially grow non-linear until a transition point is reached where the growth changes to a linear one. In addition, the investigated PEMs show an initial non-linear growth. The non-linear to linear growth transition is at about 20 layers.[35,137] Consequently, the thin samples are close to the transition point while the thick samples are clearly in the linear growing regime. The currently most favored approach to describe the non-linear to linear growth transition is to assume that the PEM as divided into an outermost less compact diffusion zone and a denser buried restructured zone.[68] The diffusion zone initially grows non-linearly until a critical thickness is reached, where the diffusion zone does not grow anymore. If the diffusion zone reaches its maximal thickness, the deepest buried layers begin to form the restructured zone, which grows linear. Apparently, the thermal treatment affects mainly the diffusion zone. The outer part of the diffusion zone is degenerated by the thermal treatment, while the inner part restructures and increases the size of the restructured zone. In a recent review, Volodkin et al.[38] suggest that the charges in the diffusion zone are mainly extrinsically compensated, while the charges in the restricted zone are intrinsically compensated. In the restructured zone, the polyelectrolyte chains are maximal crosslinked because of direct polyion-polyion interaction. In the diffusion zone, the amount of polyions-polyion bindings is lower. Instead, the charges are extrinsically compensated due to polyion-counterion interaction. Therefore, in this region, the PEM is softer, and less stable. An increase in temperature changes the balance between polyion-polyion interaction and polyion-counterion interaction towards the polyion-counterion interaction. Therefore, in the diffusion zone the number of polyion-polyion connections decreases and a dissolving of polyelectrolytes become more likely. Ghostine et al.[35] showed that PSS/PDADMAC PEMs contain extrinsic binding sites . The amount of negative binding sites is constant and indepen-

dent of the outermost layer after 16 single layers (for PEMs prepared with 0.1 mol/L NaCl), while the amount of positive extrinsic binding sites depends on the layer number and the chemical nature of the outermost layer. The amount of positive extrinsic binding sites increases in a zig-zag shape, PDADMAC-terminated PEMs contain more positive extrinsic binding sites, than PSS-terminated PEMs. The latter shows only positive extrinsic binding sites after about 20 layers. Because the degradation appears in a constant part of the PEM, it is obvious that, for the degradation process, only the existence of extrinsic charge compensation is essential, and the amount of extrinsic binding sites has no effect on the total amount of lost material.

The block structure of the PEMs after the thermal treatment is less pronounced than before the thermal treatment but still present, i.e. either only a part of the material inside the PEM is capable to freely move through the polymer matrix, or the restructuring process is not finished after 2 h (in opposite to the degradation process). The kinetic ellipsometry measurements show that the densification process is finished within the time of the temperature treatment. The refractive index and thickness show a constant value at the end of the constant temperature regime at 65°C. Therefore, the assumption of a higher mobility of only a part of the PEM seems more appropriate. Furthermore, this assumption is in agreement with the theory that the restructured zone grows due to the thermal treatment. The incorporation of non-deuterated material into the deuterated block would decrease the average SLD even if the material becomes denser. In summary, the restructured zone grows due to thermal treatment, while the diffusion zone degenerates.

7.3.2 The Weakened Odd-Even Effect

PSS/PDADMAC PEMs show an odd-even effect. PDADMAC-terminated PEMs take up more water than PSS-terminated PEMs. The odd-even effect is caused by the higher amount of positive extrinsic binding sites inside PDADMAC-terminated PEMs.[35] Surprisingly, the odd-even effect appears only if the PEM is immersed into liquid water, but not at high RH.[137] The reason for this difference could be that, only in water, the ions in the polyion-counterion binding dissociate, thus inducing an osmotic pressure. The osmotic pressure is compensated by a higher water uptake.

The odd-even effect can also be created during the PEM build-up, especially if at least one of the polyelectrolytes is a weak one,[61,102,140] for short chain polyelectrolytes,[141] at high salt concentration or if large ions are added.[23] In these studies, it could be shown that the complexation between the adsorbing polyelectrolyte and the

formerly adsorbed polyelectrolyte is stronger than their adsorption to the PEM surface. In the present study, both polyanions and polycations are strong, and the PEMs are prepared at intermediate salt concentrations (0.1 mol/L NaCl). This system does not show any degradation in presence of one of the polyelectrolyte solutions.[141] The odd-even effect can not be explained by long-range interactions with the substrate due to two reasons: (1) Branched PEI was used as the first layer, which overcompensates for the charge immediately and levels off all substrate effects as potential and roughness etc.; (2) Even in the case that the surface potential of the substrate would be partially present, the interaction is strongly screened due to the low dielectric permittivity (ϵ_r about 20–30) of the PEM[142,143] and the presence of counter ions. The Debye length is quite short (in the range of nanometers). Here, the odd-even effect is a water swelling effect.

The results indicate a weakening of the odd-even effect due to the thermal treatment. For the thick samples, the weakening of the odd-even effect is obvious. The amount of absorbed water of the PDADMAC-terminated PEM decreases strongly after the thermal treatment, while the amount of absorbed water of the PSS-terminated PEM does not change. Before the thermal treatment, the PDADMAC-terminated PEM absorbs 10% more water than the PSS-terminated PEM. After the thermal treatment, the difference is close to zero. For the thin PEMs, the weakening of the odd-even effect is less obvious because the amount of swelling water increases for both PEMs. Nevertheless, the difference decreases. Before the thermal treatment the difference in water uptake between the PDADMAC-terminated and the PSS-terminated PEM is 9%, after the thermal treatment the difference is only 5%, i.e., the odd-even effect becomes weaker. Furthermore, the relative degradation of the 20 layers thick PEM is stronger than the relative degradation of the 21 layers thick sample (25% for 20 layers 21% for 21 layers). Because the degradation also causes a lower density of the PEM, a more degraded PEM also absorbs more water, i.e., the reduced water uptake caused by a weakened odd-even effect is partly counteracted by a stronger water uptake caused by a stronger relative degradation of the PDADMAC-terminated PEM in comparison to the PSS-terminated PEM. Furthermore, the change of water distribution inside the PEMs indicate a decrease of extrinsic binding sites inside the PEM due to the thermal treatment.

The question which arises is why is the odd-even effect weakened. The most obvious answer would be that the amount of positive extrinsic binding sites decreases. The excess of positive binding sites is due to an excess of PDADMAC inside PDADMAC-terminated PEMs. Therefore, a probable explanation for the weakened odd-even effect

could be simply the release of excess PDADMAC. When the amount of excess PDADMAC is lowered, the odd-even effect should become weaker. However, a higher release of material in comparison to the PSS-terminated sample during the thermal treatment should amplify the decrease of SLD and refractive index, which was not observed. The decrease in SLD and refractive index is the same for all samples. The only way to assume a weakening of the odd-even effect due to exposure of excess PDADMAC is to assume that the excess of PDADMAC is mainly located on the surface of the PEM. If the excess PDADMAC were located on the surface of the PEM, the average SLD and refractive index of the PEM would not be influenced by a release of the PDADMAC.

7.4 Conclusion

The thermally induced structural changes of polyelectrolyte multilayer in dependence of the outermost layer were investigated by neutron reflectivity and ellipsometry. Thereby, the inner and outer parts were observed independently due to partial deuteration of the PEM. The inner block of the PEMs was deuterated while the outermost block was non-deuterated. The thermal treatment causes a partial intermixing of the block structure. Furthermore, the PEMs are affected by two processes simultaneously; a densification and a degradation of the PEM.

The absolute decrease in thickness due to the thermal treatment is similar for all investigated PEMs, which indicates that only a constant outermost part degenerates. It is assumed that the degradation process only influences the diffusion zone of the PEM. The inner part of the PEM densifies due to thermal treatment. The densification mainly affects the restructured zone of the PEM.

In addition, the thermal treatment also influences the swelling behavior of the PEMs. While before the thermal treatment the PDADMAC-terminated PEMs contain much more swelling water than the PSS-terminated PEMs, after the thermal treatment, the differences in swelling water between PSS-terminated and PDADMAC-terminated PEMs decrease slightly for the thin PEMs and vanishes completely for the thick PEMs. Apparently, the odd-even effect becomes weaker due to the thermal treatment. The odd-even effect is caused by excess PDADMAC which can be found in PDADMAC-terminated PEMs. The reason might be that the excess PDADMAC is expelled due to the thermal treatment.

Chapter 8

Summary and Outlook

8.1 Summary and Conclusion

The response of PEMs on external stimuli is from greatest interest for fundamental research and applicable use. In this thesis different aspects of the swelling behavior of PSS/PDADMAC PEMs were investigated: the distribution of water inside the PEM, the amount of void water inside the PEM and the odd-even effect, i.e. the dependence between swelling behavior and chemical nature of the outermost layer.

The first part of the thesis (chapter 4 and 5) was focused on the interaction between swelling water and void water. First the influence of the outermost layer and the number of layers on the amount of void water and swelling water inside polyelectrolyte multilayers was investigated. For that purpose PSS/PDADMAC PEMs were studied in air with 1% RH, 30% RH , 95% RH and in liquid water by ellipsometry, atomic force microscopy and x-ray reflectometry. The total amount of absorbed water in swollen PEMs is divided into two fractions, the void water and the swelling water. Therefore, it is necessary to separate both fractions correctly. In order to allow measuring samples over a larger thickness regime the investigation of a larger amount of samples is required. Therefore, the concept of separating void water from swelling water using neutron reflectometry was transferred to ellipsometry. The subsequent analysis of swelling water and void water revealed that the amount of void water is independent of the number of deposited layers and the chemical nature of the outermost layer. On the other hand, the swelling water depends on the chemical nature of the outermost layer; an odd-even effect is detectable. PDADMAC-terminated PEMs take up more water than PSS-terminated PEMs. Further, the odd-even effect is dependent on the surrounding medium. It only appears in liquid water not in humid air (95%

RH). The odd-even effect is related to the osmotic pressure between the PEM and the surrounding water.

Then the change of void water and swelling water at low relative humidity was studied more in detail. While the amount of swelling water in dependence of the RH increases continuously up to 100% RH, the amount of void water does not change above 30% RH. Therefore, the RH region between 1% and 30% was investigated. The PEMs were measured at 1% RH, 6% RH, 12% RH and 23% RH, adjusted with respective salt solutions. In addition, the PEMs were measured in liquid D_2O to measure the maximum amount of void water and swelling water. The amount of void water and swelling water increases parallel with increasing RH. The amount of void water at 6% RH was already 60% of the maximum amount of void water. At 23% RH, the voids inside the PEM are nearly completely filled. The filling of the voids with increasing RH can be considered as an adsorption isotherm. From the adsorption isotherm a void size of around 0.3-0.9 nanometer is assumed. Which is in accordance with the pore size found in previous studies, which is about 0.8 nm for PSS/PDADMAC PEMs and 0.7-1.0 nm for PSS/PAH PEMs. This small size indicates a distribution of void water over the entire PEM.

The second part of the thesis (chapter 6) focused on the contribution of water inside PEMs. For this purpose it is necessary to probe the internal structure of PEMs. In order to get insight into the internal structure, PEMs with a deuterated inner block close to the substrate and a non-deuterated outer block were prepared and investigated by neutron reflectometry (NR). The PEMs were measured in dried state, at 30% RH, 70% RH and in liquid D_2O. Thus, it was possible to monitor the swelling behavior of the entire PEM, as well as the swelling behavior of the inner and outermost region. The analysis of the entire PEM structure confirms the results from the first part of the theses. An odd-even effect occurs but only in liquid water. In humid air an odd-even effect is not detectable. Further, the amount of void water is constant above 30% RH and in liquid D_2O. The most prominent result is the different shape in SLD profiles between PEMs measured in humid air and in liquid D_2O and the resulting differences in water distribution inside the PEMs. In humid air the PEMs swells uniformly. In liquid D_2O the most water was found in the middle of the PEM, while the least water was located close to the substrate. The effect is more pronounced for PDADMAC-terminated PEMs. Apparently, the non-uniform swelling in liquid water is related to the odd-even effect. The odd-even effect is caused by different amount of extrinsic binding sites inside PSS-terminated and PDADMAC-terminated PEMs. Therefore, it is possible that the non-uniform water distribution inside PEMs swollen in liquid

water is related to the distributions of extrinsic binding sites inside the PEM. That the contribution of the extrinsic binding sites to the amount of absorbed water is only detectable in liquid water is assumed to be related to the mobility of the water. In humid air, the absorbed water is strongly bound and *immobile*, while in liquid water additionally to the immobile water a fraction of *mobile* water is absorbed. Apparently, the amount of adsorbed mobile water strongly correlates with the amount of extrinsic binding sites. In this context the difference between the odd-even effect of PSS/PAH PEMs and the odd-even effect in PSS/PDADMAC PEMs is more comprehensible. NMR measurements show in PSS/PDADMAC PEMs differences in mobile water but no differences in immobile water between PSS- and PDADMAC-terminated PEMs. For PSS/PAH PEMs differences in immobile water between PSS-terminated and PAH-terminated PEMs were found. Therefore, it can be concluded that the odd-even effect in PSS/PDADMAC PEMs (which only appears in liquid water) is driven by mobile water, while the odd-even effect in PSS/PAH PEMs is driven by immobile water.

The last chapter addresses the effect of thermal treatment on the internal structure of polyelectrolyte multilayers. Especially, on the swelling behavior in general and the water distribution, odd-even effect and void water in particular. In order to get access to the internal properties of the PEMs the same approach as in chapter 6 were used. PEMs with a deuterated inner block towards the substrate and a non-deuterated outer block were investigated by neutron reflectivity. The PEMs were measured in 1% RH and in D_2O before and after a thermal treatment. Complementarily, PEMs with the same number of layers but completely non-deuterated were investigated by ellipsometry. The analysis for the overall thickness, the average scattering length density and the refractive index indicate a degradation of the PEM. The loss in material is independent of the number of layers, i.e. only a constant part of the PEM is affected by degradation. The analysis of the internal structure revealed a more complex influence of thermal treatment on PEM structure. Only the outermost part of the PEM degenerates, while the inner part becomes denser during the thermal treatment. Also the swelling behavior of PEMs is influenced by the thermal treatment. The untreated PEM shows a well pronounced odd-even effect, i.e. PDADMAC-terminated PEMs take up more water than PSS-terminated PEMs. After the thermal treatment the odd-even effect becomes much weaker.

The most important contributions to the swelling behavior, the odd-even effect, the void water and the water distribution affect each other in different ways. On one hand, the amount of void water and the filling of voids are independent of the water distribution inside the PEM further it is not influenced by the chemical nature of

the outermost layer. On the other hand, the odd-even effect and the distribution of water inside the PEM are strongly connected. Both are affected by the amount and distribution of extrinsic binding sites inside the PEM. However the most prominent result of the thesis is the difference between PEMs swollen in humid air and in liquid water. Only in liquid water the odd-even effect appears and only in liquid water a non-uniform water distribution was detected. With regard of practical application it is important to know that swelling behavior significant differs between PEMs swollen in humid air and in liquid water. Because of the same chemical potential of liquid water and with water saturated air it is usually assumed that the swelling behavior should be the same. This is obviously not the case.

8.2 Outlook

The present thesis showed the importance of internal properties for the understanding of water distribution, odd-even effect and amount of void water inside PEMs. However, an interesting approach to get more information about the water distribution is the investigation of partially deuterated PEMs in zero-water, i.e. a mixture of H_2O and D_2O (92:8) with an SLD of zero. The SLD profile of a PEM swollen in zero-water shows all structural changes of the PEM. Subtracting the SLD profiles of a PEM measured in D_2O from a PEM measured in zero-water equates to the water distribution inside the PEM.

Also the distribution of extrinsic binding sites inside PEMs could be probed by NR. Extrinsic binding sites are compensated by small counter ions. The small counter ions can be exchanged by ions which strongly interact with neutrons, e.g. small deuterated organic ions, like deuterated acetate. The ions would increase the SLD in the region where the PEM shows a high number of extrinsic binding sites.

Further, the temperature treated PEMs could be investigated more in detail. The structural changes during temperature treatment are composed from three different effects, the densification of the inner part, the degeneration of the outer part, and the partial intermixing of the deuterated and non-deuterated block. It was not possible to determine the exact quantity of every contribution. Especially the intermixing was problematic; this process could not be separated from the densification and degeneration. Nestler et al.[144] showed a way to limit diffusion inside a PEM by a layer of branched PEI in the middle of the PEM. Temperature treated PEMs with a deuterated and non-deuterated block should only show densification and degeneration but no intermixing.

PEMs are interesting candidates for several applications. Therefore, the response of PEMs to external stimuli is important to know. Thus, a device with a PEM as central part has also to work in different environments. This thesis shows, how PEM parameters, like thickness, roughness and optical properties changes reversibly and irreversibly due to changes of the environmental humidity and temperature. These variations have to be considered for the construction of PEM containing devices.

Bibliography

[1] G. Decher, J.D. Hong, and J. Schmitt. Buildup of Ultrathin Multilayer Films by a Self-Assembly Process: III. Consecutively Alternating Adsorption of Anionic and Cationic Polyelectrolytes on Charged Surfaces. *Thin Solid Films*, 210-211:831–835, 1992.

[2] K. Ariga, Y. Yamauchi, G. Rydzek, Q. Ji, Y Yonamine, K. C.-W. Wu, and J. P. Hill. Layer-by-layer Nanoarchitectonics: Invention, Innovation, and Evolution. *Chem. Lett.*, 43(1):36–68, 2014.

[3] J. Borges and J. F. Mano. Molecular Interactions Driving the Layer-by-Layer Assembly of Multilayers. *Chem. Rev.*, 114(18):8883–8942, 2014.

[4] J. J. Richardson, M. Bjornmalm, and F. Caruso. Technology-driven layer-by-layer assembly of nanofilms. *Science*, 348(6233):aaa2491, 2015.

[5] F. Caruso, K. Niikura, D. N. Furlong, and Y. Okahata. 2. Assembly of Alternating Polyelectrolyte and Protein Multilayer Films for Immunosensing. *Langmuir*, 13(13):3427–3433, 1997.

[6] P. K. Deshmukh, K. P. Ramani, S. S. Singh, A. R. Tekade, V. K. Chatap, G. B. Patil, and S. B. Bari. Stimuli-Sensitive Layer-by-Layer (LbL) Self-Assembly Systems: Targeting and Biosensory Applications. *J. Controlled Release*, 166(3):294–306, 2013.

[7] B. G. De Geest, N. N. Sanders, G. B. Sukhorukov, J. Demeester, and S. C. De Smedt. Release Mechanisms for Polyelectrolyte Capsules. *Chem. Soc. Rev.*, 36(4):636–649, 2007.

[8] S. Pavlukhina and S. Sukhishvili. Polymer Assemblies for Controlled Delivery of Bioactive Molecules from Surfaces. *Adv. Drug Deliv. Rev.*, 63(9):822–836, 2011.

[9] M. Vargas, C. Pastor, A. Chiralt, D J. McClements, and C. González-Martínez. Recent Advances in Edible Coatings for Fresh and Minimally Processed Fruits. *Crit. Rev. Food Sci. Nutr.*, 48(6):496–511, 2008.

[10] D. Guzey and D. J. McClements. Formation, Stability and Properties of Multilayer Emulsions for Application in the Food Industry. *Adv. Colloid Interface Sci.*, 128-130(2006):227–248, 2006.

[11] L. Ouyang, D. M. Dotzauer, S. R. Hogg, J. Macanás, J.-F. Lahitte, and M. L. Bruening. Catalytic Hollow Fiber Membranes Prepared using Layer-by-Layer Adsorption of Polyelectrolytes and Metal Nanoparticles. *Catal. Today*, 156(3-4):100–106, 2010.

[12] F. Caruso and C. Schüler. Enzyme Multilayers on Colloid Particles: Assembly, Stability, and Enzymatic Activity. *Langmuir*, 16(24):9595–9603, 2000.

[13] F. Xiao. Layer-by-Layer Self-Assembly Construction of Highly Ordered Metal-TiO 2 Nanotube Arrays Heterostructures (M / TNTs , M = Au , Ag , Pt) with Tunable Catalytic Activities. *J. Phys. Chem. C*, 116:16487–16498, 2012.

[14] A. K. Sarker and J.-D. Hong. Layer-by-Layer Self-Assembled Multilayer Films Composed of Graphene/Polyaniline Bilayers: High-Energy Electrode Materials for Supercapacitors. *Langmuir*, 28(34):12637–12646, 2012.

[15] L. Shao, J. W. Jeon, and J. L. Lutkenhaus. Polyaniline/Vanadium Pentoxide Layer-by-Layer Electrodes for Energy Storage. *Chem. Mater.*, 24(1):181–189, 2012.

[16] X. Dong, L. Wang, D. Wang, C. Li, and J. Jin. Layer-by-Layer Engineered Co-Al Hydroxide Nanosheets/Graphene Multilayer Films as Flexible Electrode for Supercapacitor. *Langmuir*, 28(1):293–298, 2012.

[17] P. Bertrand, A. Jonas, A. Laschewsky, and R. Legras. Ultrathin Polymer Coatings by Complexation of Polyelectrolytes at Interfaces: Suitable Materials, Structure and Properties. *Macromol. Rapid Commun.*, 21(7):319–348, 2000.

[18] R. Advincula, E. Aust, W. Meyer, and W. Knoll. In Situ Investigations of Polymer Self-Assembly Solution Adsorption by Surface Plasmon Spectroscopy. *Langmuir*, 7463(6):3536–3540, 1996.

[19] H. L. Tan, M. J. Mcmurdo, G. Pan, and P. G. van Patten. Temperature Dependence of Polyelectrolyte Multilayer Assembly. *Langmuir*, 19:9311–9314, 2003.

[20] M. Salomäki, I. A. Vinokurov, and J. Kankare. Effect of Temperature on the Buildup of Polyelectrolyte Multilayers. *Langmuir*, 21(24):11232–11240, 2005.

[21] M. Salomäki, P. Tervasmäki, S. Areva, and J. Kankare. The Hofmeister Anion Effect and the Growth of Polyelectrolyte Multilayers. *Langmuir*, 20(9):3679–3683, 2004.

[22] S. Dodoo, R. Steitz, A. Laschewsky, and R. von Klitzing. Effect of Ionic Strength and Type of Ions on the Structure of Water Swollen Polyelectrolyte Multilayers. *Phys. Chem. Chem. Phys.*, 13(21):10318–10325, 2011.

[23] J. E. Wong, H. Zastrow, W. Jaeger, and R. von Klitzing. Specific Ion versus Electrostatic Effects on the Construction of Polyelectrolyte Multilayers. *Langmuir*, 25(24):14061–14070, 2009.

[24] S. T. Dubas and J. B. Schlenoff. Factors Controlling the Growth of Polyelectrolyte Multilayers. *Macromolecules*, 32(24):8153–8160, 1999.

[25] R. A. McAloney, M. Sinyor, V. Dudnik, and M. C. Goh. Atomic Force Microscopy Studies of Salt Effects on Polyelectrolyte Multilayer Film Morphology. *Langmuir*, 17(21):6655–6663, 2001.

[26] K. Köhler, D. G. Shchukin, H. Möhwald, and G. B. Sukhorukov. Thermal Behavior of Polyelectrolyte Multilayer Microcapsules. 1. The Effect of Odd and Even Layer Number. *J. Phys. Chem. B*, 109(39):18250–18259, 2005.

[27] K. Köhler, H. Möhewald, and G. B. Sukhorukow. Thermal Behavior of Polyelectrolyte Multilayer Microcapsules : 2 . Insight into Molecular Mechanisms for the PDADMAC / PSS System. *J. Phys. Chem. B*, 110:24002–24010, 2006.

[28] B.-S. Kim, T.-H. Fan, and O. I. Vinogradova. Thermal Softening of Superswollen Polyelectrolyte Microcapsules. *Soft Matter*, 7(6):2705–2708, 2011.

[29] J. E. Wong, F. Rehfeldt, P. Ha, M. Tanaka, and R. von Klitzing. Swelling Behavior of Polyelectrolyte Multilayers in Saturated Water Vapor. *Macromolecules*, 37:7285–7289, 2004.

[30] R. Köhler, I. Dönch, P. Ott, A. Laschewsky, A. Fery, and R. Krastev. Neutron Reflectometry Study of Swelling of Polyelectrolyte Multilayers in Water Vapors: Influence of Charge Density of the Polycation. *Langmuir*, 25(19):11576–11585, 2009.

[31] R. A. Ghostine, R. M. Jisr, A. Lehaf, and J. B. Schlenoff. Roughness and Salt Annealing in a Polyelectrolyte Multilayer. *Langmuir*, 29(37):11742–11750, 2013.

[32] S. E. Burke and C. J. Barrett. pH-Responsive Properties of Multilayered Poly(L-lysine)/Hyaluronic Acid Surfaces. *Biomacromolecules*, 4(6):1773–83, 2003.

[33] B. Schwarz and M. Schönhoff. Surface Potential Driven Swelling of Polyelectrolyte Multilayers. *Langmuir*, 250(12):2964–2966, 2002.

[34] J. J. Iturri Ramos, S. Stahl, R. P. Richter, and S. E. Moya. Water Content and Buildup of Poly(diallyldimethylammonium chloride)/Poly(sodium 4-styrenesulfonate) and Poly(allylamine hydrochloride)/Poly(sodium 4-styrenesulfonate) Polyelectrolyte Multilayers Studied by an in Situ Combination of a Quartz Crystal Microb. *Macromolecules*, 43(21):9063–9070, 2010.

[35] Ramy A Ghostine, Marie Z Markarian, and Joseph B Schlenoff. Asymmetric Growth in Polyelectrolyte Multilayers. *J. Am. Chem. Soc.*, 135:7636–7646, 2013.

[36] O. M. Tanchak, K. G. Yager, H. Fritzsche, T. Harroun, J. Katsaras, and C. J. Barrett. Water Distribution in Multilayers of Weak Polyelectrolytes. *Langmuir*, 22(11):5137–5143, 2006.

[37] W. M.. de Vos, L. L. E. Mears, R. M. Richardson, T. Cosgrove, R. Barker, and S. W. Prescott. Nonuniform Hydration and Odd-Even Effects in Polyelectrolyte Multilayers under a Confining Pressure. *Macromolecules*, 46(3):1027–1034, 2013.

[38] D. Volodkin and R. von Klitzing. Competing Mechanisms in Polyelectrolyte Multilayer Formation and Swelling: Polycation - Polyanion Pairing vs. Polyelectrolyte - Ion Pairing. *Curr. Opin. Colloid In.*, 19(1):25–31, 2014.

[39] G. Decher. Fuzzy Nanoassemblies: Toward Layered Polymeric Multicomposites. *Science*, 277(5330):1232–1237, 1997.

[40] A. D. Jenkins, P. Kratochvíl, R. F. T. Stepto, and U. W. Suter. Glossary of Basic Terms in Polymer Science (IUPAC Recommendations 1996). *Pure & Appl.Chem.*, 68(12):2287–2311, 1996.

[41] D. Rawtani and Y. K. Agrawal. Emerging Strategies and Applications of Layer-by-layer Self-Assembly. *Nanobiomedicine*, 1:8, 2014.

[42] C. C. Buron, C. Filiâtre, F. Membrey, C. Bainier, D. Charraut, and A. Foissy. Effect of Substrate on the Adsorption of Polyelectrolyte Multilayers: Study by Optical Fixed-Angle Reflectometry and AFM. *Colloids Surf. A.*, 305(1-3):105–111, 2007.

[43] A. Barrantes, O. Santos, J. Sotres, and T. Arnebrant. Influence of pH on the build-up of poly-L-lysine/heparin multilayers. *J. Colloid Interface Sci.*, 388(1):191–200, 2012.

[44] T. Cosgrove, T.M. Obey, and M. Taylor. Solvent Relaxation NMR: Bound Fraction Determination for Sodium Poly(styrene sulphonate) at the Solid/Solution Interface. *Colloids Surf.*, 64(3-4):311–316, 1992.

[45] K. Müller, J. F. Quinn, A. P. R. Johnston, M. Becker, A. Greiner, and F. Caruso. Polyelectrolyte Functionalization of Electrospun Fibers. *Chem. Mater.*, 18(9):2397–2403, 2006.

[46] Y. Yan, M. Björnmalm, and F. Caruso. Assembly of Layer-by-Layer Particles and their Interactions with Biological Systems. *Chem. Mater.*, 26(1):452–460, 2014.

[47] K. C. Krogman, J. L. Lowery, N. S. Zacharia, G. C. Rutledge, and P. T. Hammond. Spraying Asymmetry into Functional Membranes Layer-by-Layer. *Nat. Mater.*, 8(6):512–518, 2009.

[48] E. Donath, G. B. Sukhorukov, F. Caruso, S. A. Davis, and H. Möhwald. Novel Hollow Polymer Shells by Colloid-Templated Assembly of Polyelectrolytes. *Angew. Chem. Int. Ed.*, 37(16):2201–2205, 1998.

[49] K. M. Chen, X. Jiang, L. C. Kimerling, and P. T. Hammond. Selective Self-Organization of Colloids on Patterned Polyelectrolyte Templates. *Langmuir*, 16(20):7825–7834, 2000.

[50] N. G. Hoogeveen, M. A. C. Stuart, G. J. Fleer, and M. R. Bo. Formation and Stability of Multilayers of Polyelectrolytes. *Langmuir*, 7463(12):3675–3681, 1996.

[51] A. Izquierdo, S. S. Ono, J.-C. Voegel, P. Schaaf, and G. Decher. Dipping versus Spraying: Exploring the Deposition Conditions for Speeding Up Layer-by-Layer Assembly. *Langmuir*, 21(16):7558–7567, 2005.

[52] P. Schaaf, J.-C. Voegel, L. Jierry, and F. Boulmedais. Spray-Assisted Polyelectrolyte Multilayer Buildup: from Step-by-Step to Single-Step Polyelectrolyte Film Constructions. *Adv. Mater.*, 24(8):1001–1016, 2012.

[53] S.-S. Lee, J.-D. Hong, C. H. Kim, K. Kim, J. P. Koo, and K.-B. Lee. Layer-by-Layer Deposited Multilayer Assemblies of Ionene-Type Polyelectrolytes Based on the Spin-Coating Method. *Macromolecules*, 34(16):5358–5360, 2001.

[54] J. Cho, K. Char, J.-D. Hong, and K.-B. Lee. Fabrication of Highly Ordered Multilayer Films Using a Spin Self-Assembly Method. *Adv. Mater.*, 13(14):1076–1078, 2001.

[55] P. A. Patel, A. V. Dobrynin, and P. T. Mather. Combined Effect of Spin Speed and Ionic Strength on Polyelectrolyte Spin Assembly. *Langmuir*, 23(25):12589–12597, 2007.

[56] S. S. Shiratori, T. Ito, and T. Yamada. Automatic Film Formation System for Ultra-Thin Organic/Inorganic Hetero-Structure by Mass-Controlled Layer-by-Layer Sequential Adsorption Method with 'nm' Scale Accuracy. *Colloids Surf. A*, 198-200:415–423, 2002.

[57] S. S. Shiratori and M. Yamada. Nano-Scale Control of Composite Polymer Films by Mass-Controlled Layer-by-Layer Sequential Adsorption of Polyelectrolytes. *Polym. Adv. Technol.*, 11(8-12):810–814, 2000.

[58] S. L. Clark and P. T. Hammond. Engineering the Microfabrication of Layer-by-Layer Thin Films. *Adv. Mater.*, 10(18):1515–1519, 1998.

[59] N. Laugel, C. Betscha, M. Winterhalter, J.-C. Voegel, P. Schaaf, and V. Ball. Relationship between the Growth Regime of Polyelectrolyte Multilayers and the Polyanion/Polycation Complexation Enthalpy. *J. Phys. Chem. B*, 110(39):19443–19449, 2006.

[60] C. B. Bucur, Z. Sui, and J. B. Schlenoff. Ideal Mixing in Polyelectrolyte Complexes and Multilayers: Entropy Driven Assembly. *J. Am. Chem. Soc.*, 128(42):13690–1, 2006.

[61] R. von Klitzing. Internal Structure of Polyelectrolyte Multilayer Assemblies. *Phys. Chem. Chem. Phys.*, 8(43):5012–5033, 2006.

[62] R. Zahn, K. R. Bickel, T. Zambelli, J. Reichenbach, F. M. Kuhn, J. Vörös, and R. Schuster. The Entropy of Water in Swelling PGA/PAH Polyelectrolyte Multilayers. *Soft Matter*, 10(5):688–93, 2014.

[63] M. Lösche, J. Schmitt, G. Decher, W. G. Bouwman, and K. Kjaer. Detailed Structure of Molecularly Thin Polyelectrolyte Multilayer Films on Solid Substrates as Revealed by Neutron Reflectometry. *Macromolecules*, 31:8893–8906, 1998.

[64] K. Büscher, K. Graf, H. Ahrens, and C. A. Helm. Influence of Adsorption Conditions on the Structure of Polyelectrolyte Multilayers. *Langmuir*, 18(18):3585–3591, 2002.

[65] J. B. Schlenoff, H. Ly, and M. Li. Charge and Mass Balance in Polyelectrolyte Multilayers. *J. Am. Chem. Soc.*, 7863(13):7626–7634, 1998.

[66] G. Ladam, P. Schaad, J. C. Voegel, P. Schaaf, G. Decher, and F. Cuisinier. In Situ Determination of the Structural Properties of Initially Deposited Polyelectrolyte Multilayers. *Langmuir*, 31(6):1249–1255, 2000.

[67] C. Picart, Ph. Lavalle, P. Hubert, F. J. G. Cuisinier, and G. Decher. Buildup Mechanism for Poly (L -lysine)/ Hyaluronic Acid Films onto a Solid Surface. *Langmuir*, 17:7414–7424, 2001.

[68] C. Porcel, P. Lavalle, V. Ball, G. Decher, B. Senger, J.-C. Voegel, and P. Schaaf. From Exponential to Linear Growth in Polyelectrolyte Multilayers. *Langmuir*, 22(9):4376–4383, 2006.

[69] M. Salomäki and J. Kankare. Modeling the Growth Processes of Polyelectrolyte Multilayers Using a Quartz Crystal Resonator. *The Journal of Physical Chemistry B*, 111(29):8509–8519, 2007.

[70] C. Porcel, Ph. Lavalle, G. Decher, B. Senger, J.-C. Voegel, and P. Schaaf. Influence of the Polyelectrolyte Molecular Weight on Exponentially Growing Multilayer Films in the Linear Regime. *Langmuir*, 23(4):1898–1904, 2007.

[71] J. Ruths, F. Essler, G. Decher, and H. Riegler. Polyelectrolytes I : Polyanion / Polycation Multilayers at the Air / Monolayer / Water Interface as Elements for Quantitative Polymer Adsorption Studies and Preparation of Heterosuperlattices on Solid Surfaces. *Langmuir*, 37(4):8871–8878, 2000.

[72] D. T. Haynie, E. Cho, and P. Waduge. "In and Out Diffusion" Hypothesis of Exponential Multilayer Film Buildup Revisited. *Langmuir*, 27(9):5700–5704, 2011.

[73] R. Steitz, W. Jaeger, and R. von Klitzing. Influence of Charge Density and Ionic Strength on the Multilayer Formation of Strong Polyelectrolytes. *Langmuir*, 17:4471–4474, 2001.

[74] M. Elzbieciak, M. Kolasinska, and P. Warszynski. Characteristics of Polyelectrolyte Multilayers: The Effect of Polyion Charge on Thickness and Wetting Properties. *Colloids Surf. A.*, 321(1-3):258–261, 2008.

[75] J. J. Harris, P. M. DeRose, and M. L. Bruening. Synthesis of Passivating, Nylon-Like Coatings through Cross-Linking of Ultrathin Polyelectrolyte Films. *J. Am. Chem. Soc.*, 121(9):1978–1979, 1999.

[76] P. Schuetz and F. Caruso. Copper-Assisted Weak Polyelectrolyte Multilayer Formation on Microspheres and Subsequent Film Crosslinking. *Adv. Funct. Mater.*, 13(12):929–937, 2003.

[77] T. Boudou, T. Crouzier, R. Auzély-Velty, K. Glinel, and C. Picart. Internal Composition versus the Mechanical Properties of Polyelectrolyte Multilayer Films: The Influence of Chemical Cross-Linking. *Langmuir*, 25(24):13809–13819, 2009.

[78] D. Volodkin, Y. Arntz, P. Schaaf, H. Moehwald, J.-C. Voegel, and V. Ball. Composite Multilayered Biocompatible Polyelectrolyte Films with Intact Liposomes: Stability and Temperature Triggered Dye Release. *Soft Matter*, 4(1):122–130, 2008.

[79] P. Nazaran, V. Bosio, W. Jaeger, D. F. Anghel, and R. v. Klitzing. Lateral Mobility of Polyelectrolyte Chains in Multilayers. *J. Phys. Chem. B*, 111(29):8572–8581, 2007.

[80] P. Nestler, S. Block, and C. A. Helm. Temperature-Induced Transition from Odd-Even to Even-Odd Effect in Polyelectrolyte Multilayers due to Interpolyelectrolyte Interactions. *J. Phys. Chem. B*, 116(4):1234–1243, 2012.

[81] P. Ott, J. Gensel, S. Roesler, K. Trenkenschuh, D. Andreeva, A. Laschewsky, and A. Fery. Cross-Linkable Polyelectrolyte Multilayer Films of Tailored Charge Density. *Chem. Mater.*, 22(11):3323–3331, 2010.

[82] L. Richert, F. Boulmedais, P. Lavalle, J. Mutterer, E. Ferreux, G. Decher, P. Schaaf, J.-C. Voegel, and C. Picart. Improvement of Stability and Cell Adhesion Properties of Polyelectrolyte Multilayer Films by Chemical Cross-Linking. *Biomacromolecules*, 5(2):284–294, 2004.

[83] A. G. Skirtach, A. M. Yashchenok, and H. Möhwald. Encapsulation, Release and Applications of LbL Polyelectrolyte Multilayer Capsules. *Chem. Commun.*, 47(48):12736–46, 2011.

[84] W. Yuan, Z. Lu, and C. M. Li. Charged Drug Delivery by Ultrafast Exponentially Grown Weak Polyelectrolyte Multilayers: Amphoteric Properties, Ultrahigh Loading Capacity and pH-Responsiveness. *J. Mater. Chem.*, 22(18):9351, 2012.

[85] E. Leguen, A. Chassepot, G. Decher, P. Schaaf, J.-C. Voegel, and N. Jessel. Bioactive Coatings Based on Polyelectrolyte Multilayer Architectures Functionalized by Embedded Proteins, Peptides or Drugs. *Biomol. Eng.*, 24(1):33–41, 2007.

[86] B. Sun and D. M. Lynn. Release of DNA from Polyelectrolyte Multilayers Fabricated using 'Charge-Shifting' Cationic Polymers: Tunable Temporal Control and Sequential, Multi-Agent Release. *J. Controlled Release*, 148(1):91–100, 2010.

[87] E. Guzmán, H. Ritacco, J. E. F. Rubio, R. G. Rubio, and F. Ortega. Salt-Induced Changes in the Growth of Polyelectrolyte Layers of Üoly(diallyldimethylammonium chloride) and Poly(4-styrene sulfonate of sodium). *Soft Matter*, 5(10):2130, 2009.

[88] Y. Zhang and P. S. Cremer. Interactions between Macromolecules and Ions: The Hofmeister Series. *Curr. Opin. Chem. Biol.*, 10(6):658–63, 2006.

[89] F. Hofmeister. Zur Lehre von der Wirkung der Salze - Zweite Mittheilung. *Archiv für Experimentelle Pathologie und Pharmakologie*, 24(4-5):247–260, 1888.

[90] L. L. Del Mercato, M. M. Ferraro, F. Baldassarre, S. Mancarella, V. Greco, R. Rinaldi, and S. Leporatti. Biological Applications of LbL Multilayer Capsules: From Drug Delivery to Sensing. *Adv. Colloid. Interface*, 207(1):139–154, 2014.

[91] S. M. Oliveira, T. H. Silva, R. L. Reis, and J. F. Mano. Hierarchical Fibrillar Scaffolds Obtained by Non-conventional Layer-By-Layer Electrostatic Self-Assembly. *Adv. Healthcare Mater.*, 2(3):422–427, 2013.

[92] N. Joseph, P. Ahmadiannamini, R. Hoogenboom, and I. F. J. Vankelecom. Layer-by-Layer Preparation of Polyelectrolyte Multilayer Membranes for Separation. *Polym. Chem.*, 5(6):1817–1831, 2014.

[93] R. Köhler, R. Steitz, and R. von Klitzing. About Different Types of Water in Swollen Polyelectrolyte Multilayers. *Adv. Colloid Interface Sci.*, 207:325–31, 2014.

[94] A. M. Lehaf, H. H. Hariri, and J. B. Schlenoff. Homogeneity, Modulus, and Viscoelasticity of Polyelectrolyte Multilayers by Nanoindentation: Refining the Buildup Mechanism. *Langmuir*, 28(15):6348–6355, 2012.

[95] Jonathan B Gilbert, Michael F Rubner, and Robert E Cohen. Depth-Profiling X-ray Photoelectron Spectroscopy (XPS) Analysis of Interlayer Diffusion in Polyelectrolyte Multilayers. *PNAS*, 110(17):6651–6656, 2013.

[96] M. McCormick, R. N. Smith, R. Graf, C. J. Barrett, L. Reven, and H. W. Spiess. NMR Studies of the Effect of Adsorbed Water on Polyelectrolyte Multilayer Films in the Solid State. *Macromolecules*, 36(10):3616–3625, 2003.

[97] J. Schmitt, T. Gruenwald, G. Decher, P. S. Pershan, K. Kjaer, and M. Lösche. Internal Structure of Layer-byLayer Adsorbed Polyelectrolyte Films: A Neutron and X-Ray Reflectivity Study. *Macromolecules*, 26:7058–7063, 1993.

[98] O. Soltwedel, P. Nestler, H.-G. Neumann, M. Paßvogel, R. Köhler, and C. A Helm. Influence of Polycation (PDADMAC) Weight on Vertical Diffusion within Polyelectrolyte Multilayers during Film Formation and Postpreparation Treatment. *Macromolecules*, 45(19):7995–8004, 2012.

[99] O. Soltwedel, O. Ivanova, P. Nestler, M. Müller, R. Köhler, and C. A. Helm. Interdiffusion in Polyelectrolyte Multilayers. *Macromolecules*, 43(17):7288–7293, 2010.

[100] D. Carrière, R. Krastev, and M. Schönhoff. Oscillations in Solvent Fraction of Polyelectrolyte Multilayers Driven by the Charge of the Terminating Layer. *Langmuir*, 20(26):11465–11472, 2004.

[101] R. von Klitzing and H. Moehwald. Proton Concentration Profile in Ultrathin Polyelectrolyte Films. *Langmuir*, 11(9):3554–3559, sep 1995.

[102] D. Kovacevic, S. van der Burgh, A. de Keizer, and M. A. Cohen Stuart. Kinetics of Formation and Dissolution of Weak Polyelectrolyte Multilayers: Role of Salt and Free Polyions. *Langmuir*, 18(14):5607–5612, 2002.

[103] R. A. McAloney, V. Dudnik, and M. C. Goh. Kinetics of Salt-Induced Annealing of a Polyelectrolyte Multilayer Film Morphology. *Langmuir*, 19(9):3947–3952, 2003.

[104] H. Mjahed, G. Cado, F. Boulmedais, B. Senger, P. Schaaf, V. Ball, and J.-C. Voegel. Restructuring of Exponentially Growing Polyelectrolyte Multilayer Films Induced by Salt Concentration Variations after Film Deposition. *J. Mater. Chem.*, 21(23):8416, 2011.

[105] H. M. Fares, Y. E. Ghoussoub, R. L. Surmaitis, and J. B. Schlenoff. Toward Ion-Free Polyelectrolyte Multilayers: Cyclic Salt Annealing. *Langmuir*, 31(21):5787–5795, 2015.

[106] A. Vidyasagar, C. Sung, R. Gamble, and J. L. Lutkenhaus. Thermal Transitions in dry and Hydrated Layer-by-Layer Assemblies Exhibiting Linear and Exponential Growth. *ACS Nano*, 6(7):6174–6184, 2012.

[107] R. Steitz, V. Leiner, K. Tauer, V. Khrenov, and R. von Klitzing. Temperature-Induced Changes in Polyelectrolyte Films at the Solid - Liquid Interface. *Appl. Phys. A*, 521:519–521, 2002.

[108] H. Dautzenberg, E. Görnitz, and W. Jaeger. Synthesis and Characterization of Poly(diallyldimethylammonium chloride) in a Broad Range of Molecular Weight. *Macromol. Chem. Phys.*, 199(8):1561–1571, 1998.

[109] M. Kolasinska, R. Krastev, and P. Warszynski. Characteristics of Polyelectrolyte Multilayers: Effect of PEI Anchoring Layer and Posttreatment after Deposition. *J. Colloid Interface Sci.*, 305(1):46–56, 2007.

[110] H. G. Tompkins, E. A. Irene, C. Hill, and N. Carolina. *Handbook of Ellipsometry.* Springer Berlin Heidelberg, 2005.

[111] R. C. Jones. A New Calculus for the Treatment of Optical Systems: Description and Discussion of the Calculus. *J. Opt. Soc. Am.*, 31(7):488, 1941.

[112] W. Ogieglo, H. Wormeester, K.-J. Eichhorn, M. Wessling, and N. E. Benes. In Situ Ellipsometry Studies on Swelling of Thin Polymer Films: A Review. *Prog. Polym. Sci.*, 42:42–78, 2015.

[113] J.-W. Benjamins, B. Joensson, K. Thuresson, and T. Nylander. New Experimental Setup to Use Ellipsometry to Study Liquid-Liquid and Liquid-Solid Interfaces. *Langmuir*, 18:6437–6444, 2002.

[114] C. M. Herzinger, B. Johs, W. A. McGahan, J. A. Woollam, and W. Paulson. Ellipsometric Determination of Optical Constants for Silicon and Thermally Grown Silicon Dioxide via a Multi-Sample, Multi-Wavelength, Multi-Angle Investigation. *J. Appl. Phys.*, 83(6):3323–3336, 1998.

[115] G. Binning and C. F. Quate. Atomic Force Microscope. *Phys. Rev. Lett.*, 56(9):930–934, 1986.

[116] L. Gross, F. Mohn, N. Moll, P. Liljeroth, and G. Meyer. The Chemical Structure of a Molecule Resolved by Atomic Force Microscopy. *Science*, 325(5944):1110–1114, 2009.

[117] H. J. Butt, R. Berger, E. Bonaccurso, Y. Chen, and J. Wang. Impact of Atomic Force Microscopy on Interface and Colloid Science. *Adv. Colloid. Interface Sci.*, 133(2):91–104, 2007.

[118] E. Chason and T. M. Mayer. Thin Film and Surface Characterization by Specular X-Ray Reflectivity. *Crit. Rev. Solid State Mater. Sci.*, 22:1–67, 1997.

[119] H. Looyenga. Relation between Refractive Index and Density of Polymer Solutions. *J. Polymer Sci. A2*, 11(7):1331–1336, 1973.

[120] M. Tolan. *X-Ray Scattering from Soft-Matter Thin Films*, volume 148 of *Springer Tracts in Modern Physics*. Springer Berlin Heidelberg, Heidelberg, 1999.

[121] J. Daillant and A. Gibaud, editors. *X-Ray and Neutron Reflectivity*, volume 770 of *Lecture Notes in Physics*. Springer, Berlin, Heidelberg, 2009.

[122] L. G. Parratt. Surface Studies of Solids by Total Reflection of X-Rays. *Phys. Rev.*, 95(2):359–369, 1954.

[123] A. Nelson. Co-Refinement of Multiple-Contrast Neutron/X-Ray Reflectivity Data Using MOTOFIT. *J. Appl. Cryst.*, 39:273–276, 2006.

[124] M. Schönhoff, V. Ball, A. R. Bausch, C. Dejugnat, N. Delorme, K. Glinel, R. von Klitzing, and R. Steitz. Hydration and Internal Properties of Polyelectrolyte Multilayers. *Colloids Surf., A*, 303(1-2):14–29, 2007.

[125] Y. Lvov, K. Ariga, M. Onda, I. Ichinose, and T. Kunitake. A Careful Examination of the Adsorption Step in the Alternate Layer-by-Layer Assembly of Linear Polyanion and Polycation. *Colloids Surf., A*, 146:337–346, 1999.

[126] P. Nestler, M. Passvogel, and C. A Helm. Influence of Polymer Molecular Weight on the Parabolic and Linear Growth Regime of PDADMAC/PSS Multilayers. *Macromolecules*, 46:8–15, 2013.

[127] M. Garnett. Colours in Metal Glasses, in Metallic Films, and in Metallic Solutions. - II. *Philos. Trans. R. Soc. London, Ser. A*, 205:237–288, 1905.

[128] O. M. Tanchak, K. G. Yager, H. Fritzsche, T. Harroun, J. Katsaras, and C. J. Barrett. Ion Distribution in Multilayers of Weak Polyelectrolytes: A Neutron Reflectometry Study. *J. Chem. Phys.*, 129(8):084901, 2008.

[129] O. Löhmann, M. Zerball, and R. von Klitzing. Water Uptake of Polyelectrolyte Multilayers Including Water Condensation in Voids. *unpublished results*.

[130] W. Jin, A. Toutianoush, and B. Tieke. Size- and Charge-Selective Transport of Aromatic Compounds Across Polyelectrolyte Multilayer Membranes. *Applied Surface Science*, 246(4):444–450, 2005.

[131] F. Vaca Chávez and M. Schönhoff. Pore Size Distributions in Polyelectrolyte Multilayers Determined by Nuclear Magnetic Resonance Cryoporometry. *J. Chem. Phys.*, 126(10):104705, 2007.

[132] H. W. Jomaa and J. B. Schlenoff. Salt-Induced Polyelectrolyte Interdiffusion in Multilayered Films: A Neutron Reflectivity Study. *Macromolecules*, 38(20):8473–8480, 2005.

[133] M. Gopinadhan, H. Ahrens, J.-U. Gu, R. Steitz, and C. A. Helm. Approaching the Precipitation Temperature of the Deposition Solution and the Effects on the Internal Order of Polyelectrolyte Multilayers. *Macromolecules*, 38:5228–5235, 2005.

[134] J. Ma, S. Yang, Y. Li, X. Xu, and J. Xu. Effect of Temperature on the Build-Up and Post Hydrothermal Processing of Hydrogen-Bonded PVPON/PAA Film. *Soft Matter*, 7(19):9435–9443, 2011.

[135] A. Vidyasagar, C. Sung, K. Losensky, and J. L. Lutkenhaus. pH-Dependent Thermal Transitions in Hydrated Layer-by-Layer Assemblies Containing Weak Polyelectrolytes. *Macromolecules*, 45(22):9169–9176, 2012.

[136] Choonghyun Sung, Ajay Vidyasagar, Katelin Hearn, and Jodie L Lutkenhaus. Effect of Thickness on the Thermal Properties of Hydrogen-Bonded LbL Assemblies. *Langmuir*, 28(21):8100–8109, 2012.

[137] M. Zerball, A. Laschewsky, and R. von Klitzing. Swelling of Polyelectrolyte Multilayers: The Relation Between, Surface and Bulk Characteristics. *J. Phys. Chem. B*, 119:11879–11886, 2015.

[138] R. Köhler, C. Chevigny, and R. von Klitzing. Neutron Reflectometry at Polyelectrolyte Multilayers. In Gero Decher and Joseph B. Schlenoff, editors, *Multilayer Thin Films: Sequential Assembly of Nanocomposite Materials*, pages 219–268. Wiley-VCH Verlag GmbH & Co. KGaA: Weinheim, Germany, second edition, 2012.

[139] L. Szyk-Warszyńska, J. Piekoszewska, and P. Warszyński. Formation and Stability of Poly-L-Lysine/Casein Multilayers. *Adsorption*, 16(4-5):241–248, 2010.

[140] E. Kharlampieva and S. A. Sukhishvili. Polyelectrolyte Multilayers of Weak Polyacid and Cationic Copolymer: Competition of Hydrogen-Bonding and Electrostatic Interactions. *Macromolecules*, 36(26):9950–9956, 2003.

[141] S. Micciulla, S. Dodoo, C. Chevigny, A. Laschewsky, and R. von Klitzing. Short versus Long Chain Polyelectrolyte Multilayers: a Direct Comparison of Self-Assembly and Structural Properties. *Phys. Chem. Chem. Phys.*, 16(40):21988–21998, 2014.

[142] Petra A. Neff, A. Naji, C. Ecker, F. Nickel, R. von Klitzing, and A.R. Bausch. Electrical Detection of Self-Assembled Polyelectrolyte Multilayers by a Thin Film Resistor. *Macromolecules*, 39:463–466, 2006.

[143] P. A. Neff, B. K. Wunderlich, R. von Klitzing, and A. R. Bausch. Formation and Dielectric Properties of Polyelectrolyte Multilayers Studied by a Silicon-on-Insulator Based Thin Film Resistor. *Langmuir*, 23(7):4048–4052, 2007.

[144] P. Nestler, M. Paßvogel, H. Ahrens, O. Soltwedel, R. Köhler, and C. A. Helm. Branched Poly(ethylenimine) as Barrier Layer for Polyelectrolyte Diffusion in Multilayer Films. *Macromolecules*, 48(23):8546–8556, 2015.

Appendix A

Supporting Information

Comparison between Garnet-Equation and Linear Correlation

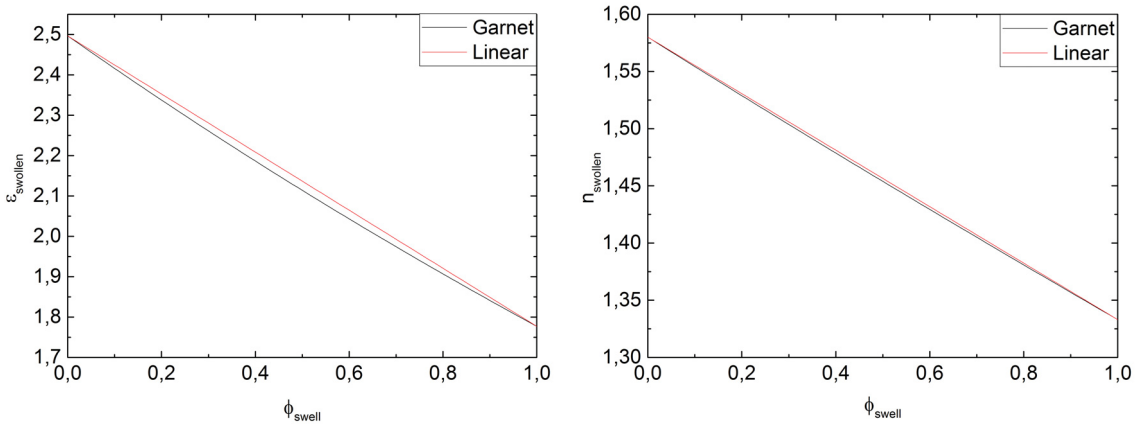

Figure A.1: Change of dielectric constant (ϵ) (a) and refractive index (b) in dependence on the water content calculated by the garnet equation and from the linear correlation.

Voids Error Propagation

To calculate the error propagation the formula has to be partially derivated for all measured values. For the error of the swelling water ϕ_{swell} have to be considered d_{dry} and $d_{swollen}$:

$$\phi_{swell} = \frac{d_{swollen} - d_{dry}}{d_{swollen}} \tag{A.1}$$

$$\Delta\phi_{swell} = \left|\frac{\partial\phi_{swell}}{\partial d_{dry}}\right| \Delta d_{dry} + \left|\frac{\partial\phi_{swell}}{\partial d_{swollen}}\right| \Delta d_{swollen} \tag{A.2}$$

$$\Delta\phi_{swell} = \left|\frac{-1}{d_{swell}}\right| \Delta d_{dry} + \left|\frac{d_{dry}}{{d_{swell}}^2}\right| \Delta d_{swell} \tag{A.3}$$

For calculating the error of polymer fraction Δx the swelling water $\phi_{swollen}$, the refractive index in dried state n_{dry} and the refractive index in swollen state $n_{swollen}$ have to be considered:

$$x = \frac{n_{dry}}{n_{water} - n_{air}} - \frac{n_{swollen} - \phi_{swell} n_{water}}{(1 - \phi_{swell})(n_{water} - n_{air})} + 1 \tag{A.4}$$

$$\Delta x = \left|\frac{\partial x}{\partial n_{swollen}}\right| \Delta n_{swollen} + \left|\frac{\partial x}{\partial n_{dry}}\right| \Delta n_{dry} + \left|\frac{\partial x}{\partial \phi_{swell}}\right| \Delta\phi_{swell} \tag{A.5}$$

$$\begin{aligned} \Delta x = &\left|\frac{-1}{(1 - \phi_{swell})(n_{water} - n_{air})}\right| \Delta n_{swollen} + \left|\frac{1}{n_{water} - n_{air}}\right| \Delta n_{dry} \\ &+ \left|\frac{-n_{water}\phi_{swell} - n_{water}(1 - \phi_{swell}) + n_{swollen}}{(n_{water} - n_{air})(1 - \phi_{swell})^2}\right| \Delta\phi_{swell} \end{aligned} \tag{A.6}$$

To find the error for the amount of void water $\Delta\phi_{void}$ the polymer fraction x and the swelling water ϕ_{swell} comes into account:

$$\phi_{void} = (1 - \phi_{swell})(1 - x) \tag{A.7}$$

$$\Delta\phi_{void} = \left|\frac{\partial\phi_{void}}{\partial\phi_{swell}}\right| \Delta\phi_{swell} + \left|\frac{\partial\phi_{void}}{\partial x}\right| \Delta x \tag{A.8}$$

$$\Delta\phi_{void} = |1 - x| \, \Delta\phi_{swell} + |1 - \phi_{swell}| \, \Delta x \tag{A.9}$$

X-Ray Reflectometry Data

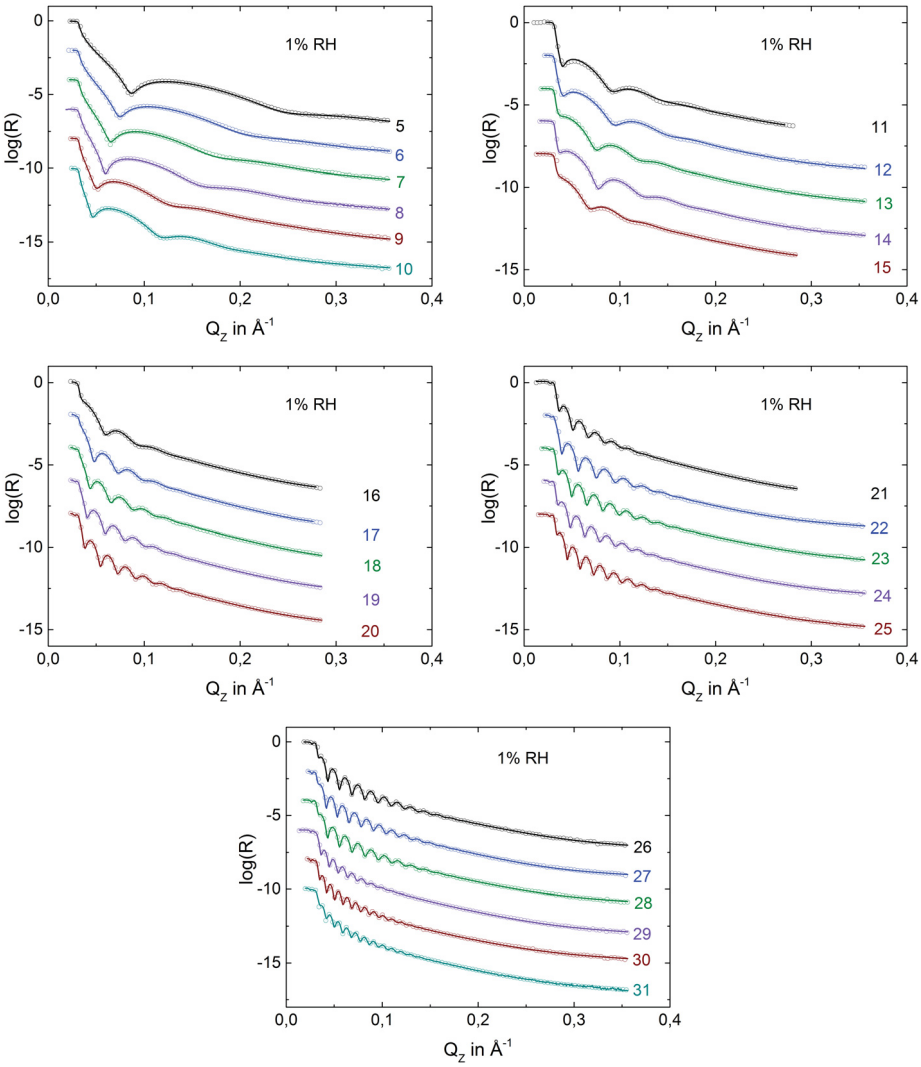

Figure A.2: XRR data and fit of PEMs with 5-31 deposited layers measured at 1% RH. For better visualization only every 5^{th} data point of measured data is shown in the diagram.

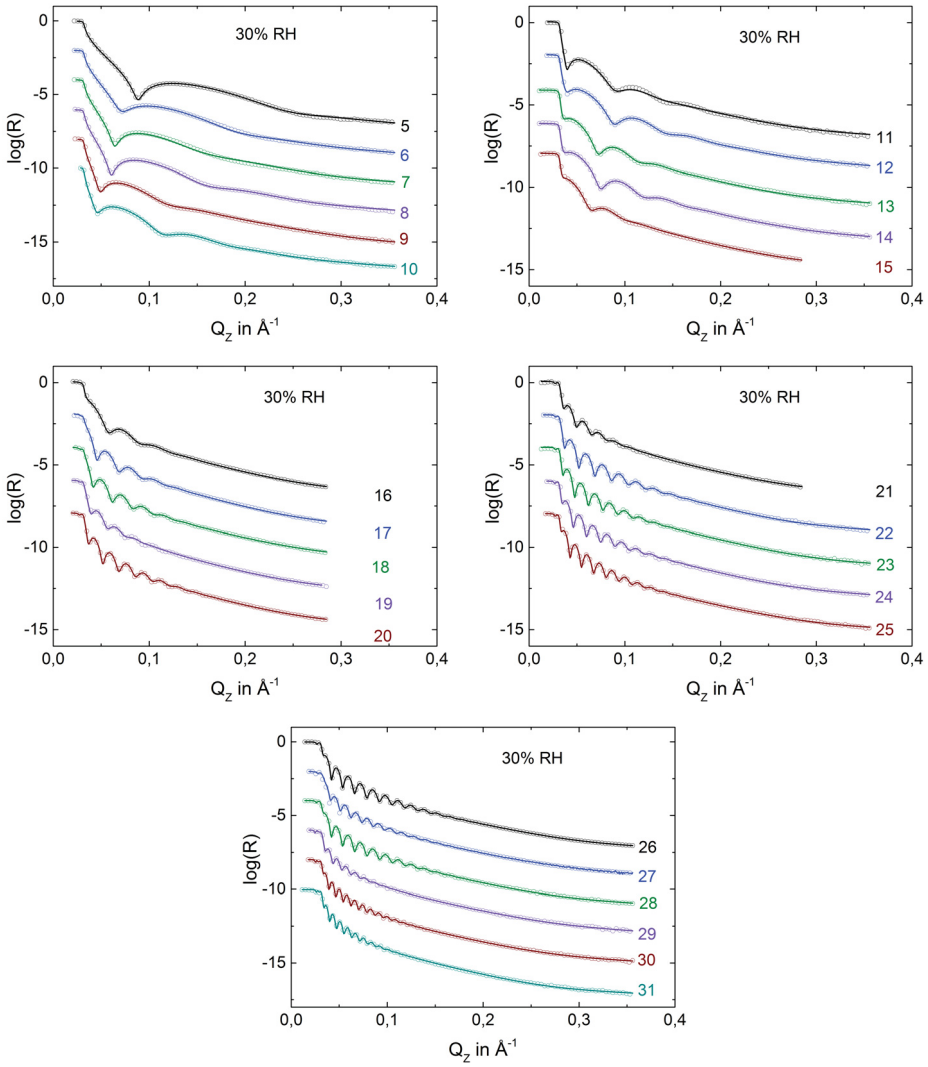

Figure A.3: XRR data and fit of PEMs with 5-31 deposited layers measured at 30% RH. For better visualization only every 5^{th} data point of measured data is shown in the diagram.